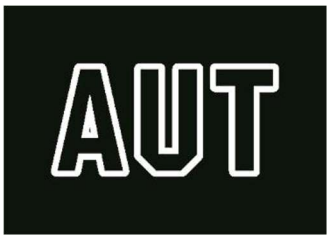

School of Science

Synthesis of MCR-1 inhibitors to overcome antibacterial resistance

Sabeena

A thesis submitted in fulfilment

of the requirements for the degree of

Master of Philosophy

Auckland University of Technology

March 2019

Abstract

This thesis describes the synthesis of a series of pyrazole and isoflavone analogues in order to find drug-like molecules which can act as an inhibitor of MCR-1 (mobilised colistin resistance). This enzyme causes resistance to the last resort antibiotic - colistin (polymyxin E) which has recently become a global concern due to its easily transmissible nature.

Two types of pyrazole analogues were prepared – disubstituted and trisubstituted pyrazole rings. For the synthesis of trisubstituted pyrazole analogues – a sequence involving a Friedel-Crafts acylation, a Kostanecki acylation and an aza-Michael addition was followed to form an alkyldiarylpyrazole ring. On the other hand, for the disubstituted pyrazoles – a sequence involving Suzuki coupling of an iodochromone and a boronic acid was used followed by an aza-Michael addition.

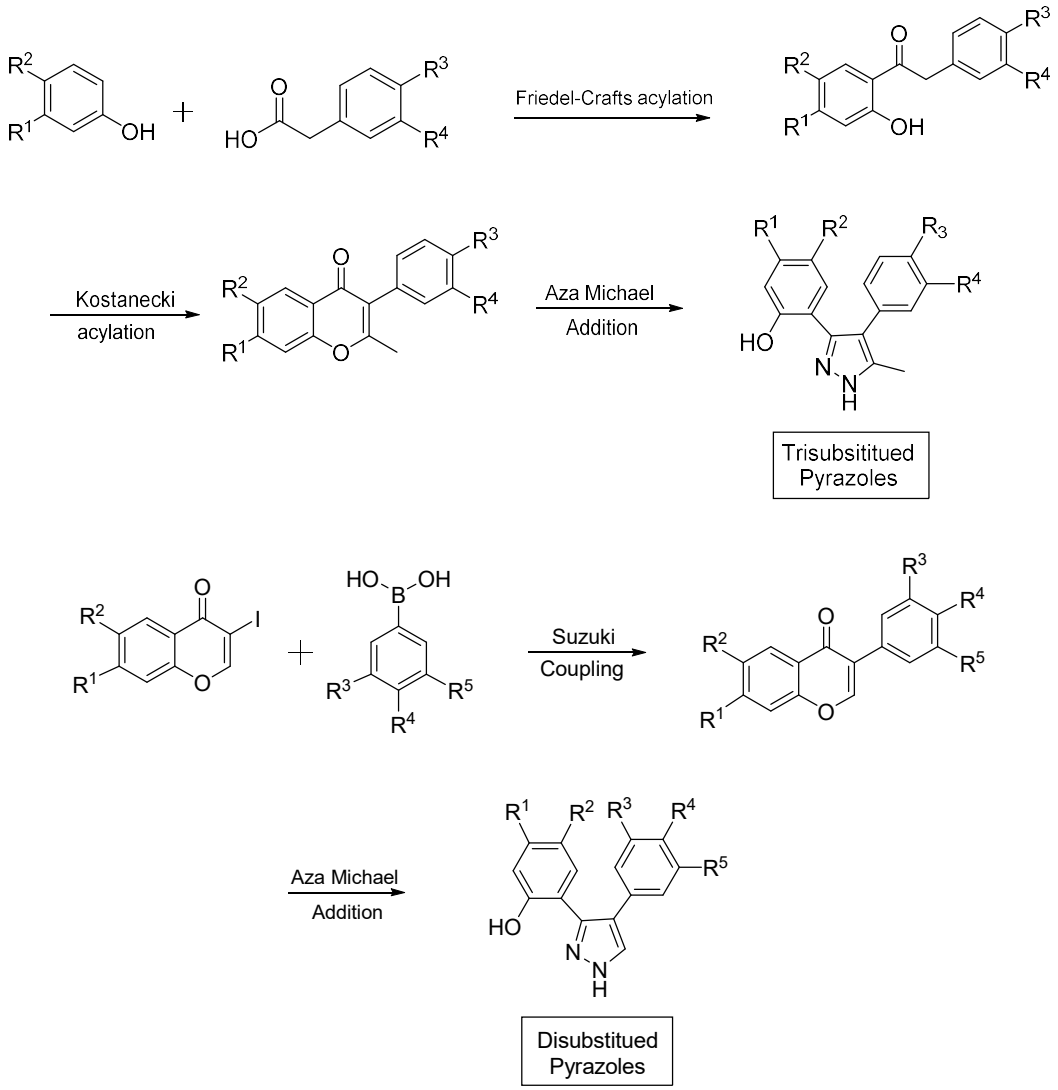

After the initial synthesis of two pyrazole analogues, testing of these compounds was performed using NMR techniques to examine the binding of these compounds with the MCR-1 protein. The results from these initial studies were positive and demonstrated that there was binding towards MCR-1 but the low solubility of several compounds was noted and became a major concern at that time. Analogues with a greater number of hydroxyl groups were therefore prepared to increase the water solubility. However, the higher number of hydroxyl groups present in the starting materials resulting in the formation of complex mixtures during the reaction sequence, causing difficult separations and low yields. At that point, following a discussion of potential side products, a transesterification step was introduced into the synthetic sequence, which managed to dramatically minimise the number of side products formed and greatly increased the yields achieved. In total, 10 pyrazoles and 11 isoflavones were synthesised and 7 pyrazoles and 5 isoflavones have been tested together with colistin against *E. coli* with mcr-1 resistance. Initial results are very positive, with 6 out of the 13 compounds tested found to decrease the minimum inhibitory concentration (MIC) of polymyxin towards *E. coli* with mcr-1 resistance. This research is ongoing, and we are currently synthesising more structural analogues, guided by the biological results as they are released. In the future, the aim is to be able to build a picture of the structure-activity-relationship required for MCR-1 inhibition.

TABLE OF CONTENTS

CHAPTER ONE: INTRODUCTION

CHAPTER TWO: RESULT AND DISCUSSION

CHAPTER THREE : EXPERIMENTAL

Abbreviations:

δ	chemical shift
β	beta
°C	degrees Celsius
AACs	chloramphenicol acetyltransferases
Ac	acetyl
AMEs	aminoglycoside modifying enzymes
BH	bridging helix
EtN	ethanolamine
DBU	1,8-diazabicyclo[5.4.0]undec-7-ene
DCC	dicyclohexylcarbodiimide
DCM	dichloromethane
dd	double of doublet
DFT	density functional theory
DMF	*N,N*-dimethylformamide
DMAP	*N,N*-dimethyl-4-aminopyridine
DMF-DMA	*N,N*-dimethylformamide dimethyl acetal
DNA	deoxyribonucleic acid
EDTA	ethylenediaminetetraacetic acid
ESBLs	plasmid-encoded β-lactamases
ESI	electrospray ionization
Et	ethyl
eq.	equivalent

FQ	fluoroquinolones
h	hour(s)
HRMS	high resolution mass spectroscopy
HSQC	heteronuclear single quantum correlation
Hz	hertz
IR	infra-red
LPS	lipopolysaccharides
J	coupling constant
m	multiplet
MDR	multi-drug resistance
mg	milligram(s)
MHz	megahertz
MIC	mininum inhibitory concentration
ml	millilitre
mmol	millimole(s)
m/z	mass to charge ratio
NMR	nuclear magnetic resonance
PEA	phosphoethanolamine
PE	phosphatidylethananolamine
PEtN	phosphoethananolamine
ppm	parts per million
q	quartet
R	unspecified alkyl group
r.t.	room temperature

RNA	ribonucleic acid
m-RNA	messenger ribonucleic acid
t-RNA	transfer ribonucleic acid
R_f	retention factor
s	singlet
SAR	structure -activity relationship
t	triplet
THF	tetrahydrofuran
TLC	thin layer chromatography
v	wavenumber (cm^{-1})
WHO	World Health Organization

List of Figures:

List of Tables:

Attestation of Authorship

"I hereby declare that this submission is my own work and that, to the best of my knowledge and belief, it contains no material previously published or written by another person (except where explicitly defined in the acknowledgements), nor material which to a substantial extent has been submitted for the award of any other degree or diploma of a university or other institution of higher learning."

Sabeena

4th March 2019

Acknowledgement

The time I spent in AUT as a MPhil student from March 2018 to February 2019 was a memorable one for me as it was rich in experience and helped me discover my potential. I have had so many rich experiences and opportunities that I personally believe will forever shape and influence my professional life while fostering potential growth and development.

First and foremost, I would like to express my sincere gratitude to my supervisor, Dr Jack Li-Yang Chen, AUT, whose encouragement, guidance and support from the beginning to the end has enabled me to develop a deep understanding of the subject. I am overwhelmed for his supervision, motivation and inspiration throughout the tenure of my project in spite of his hectic schedule, who truly remained a driving spirit in my project and helped me in clarifying abstruse concepts, requiring knowledge and perception, handling critical situations and in understanding the objective of the work. Thank you for always being there and for devoting many hours on this thesis.

I express my deepest thanks to Pablo, one of the group members, for giving me excellent training and making me eligible for working fearlessly in the lab. Despite being extraordinarily busy with his own work, he took time out to hear, guide and keep me on the correct path and allowed me to carry out my project.

Thanks to Chloe, for all your help with the NMR and column chromatography. I am thankful for the positive attitude she showed for my work, always allowing me to ask as many questions as I can and giving me prompt replies for my uncertainties in any step of the experiments especially in the work-up of the reactions. I am also thankful to Bhanu and Anau, for extending their friendship towards me and looking after my overnight reactions in my absence.

I am highly indebted to my friend, Navneet, for being my stress-buster. Despite being a Ph.D. student in a different group, I feel so lively and comfortable when she is around. I had extreme fun during our lunch breaks and even in the research lab. Thanks to Navneet, for your unconditional help in this one-year journey. Thanks to Sanjay Sir, Shrusti and Rashmeet for their advice and support.

To my parents, I would like to thank them for their consistent support and counselling in my daily life. And lastly, this project is dedicated to my husband and especially, to my brother who have never failed to give emotional and moral support. I am blessed for having them by my

side to guide me always, their prosperity and love for me. Without their guidance and persistent help this project would not have been possible.

CHAPTER ONE: INTRODUCTION

1.1 Antibiotics

Antibiotics are a group of drugs that are able to kill or hinder the growth of bacteria. They have been used by a number of societies for centuries, but the 'modern era' of antibiotics is attached with two names: Paul Ehrlich and Alexander Fleming.[1] Paul Ehrlich described the potential of using antibiotics as a "magic bullet." According to this idea, a compound could be synthesised that would selectively target the disease – causing the bacteria to die, but not the host. The principle of the idea was based on the observation that aniline and other synthetic dyes could stain some microbes but not others. He also developed a systematic approach to the screening of compounds for antibiotic activity, which has become an integral part of modern drug discovery.

In 1928, the discovery of penicillin by Alexander Fleming led to a boom in the field of medicine. Fleming's methods involving inhibition zones around wells within agar-medium petri dishes was much more cost-effective than animal testing and was widely adopted in subsequent antibacterial research. Fleming was also one of the first to warn the scientific community about the potential risks of antibacterial resistance.[1]

1.1.1 Modes of action of antibiotics:

Different classes of antibiotics have different mechanism to perform their action depending on their target site.[2] They generally achieve high levels of selectivity by targeting structures or enzymes which are present only in bacterial cells. The main mode of actions for antibiotics are:

- Inhibition of cell wall synthesis
- Inhibition of protein synthesis
- Hindrance in nucleic acid synthesis
- Retardation in folic acid metabolism
- Collapse in cell membrane structure

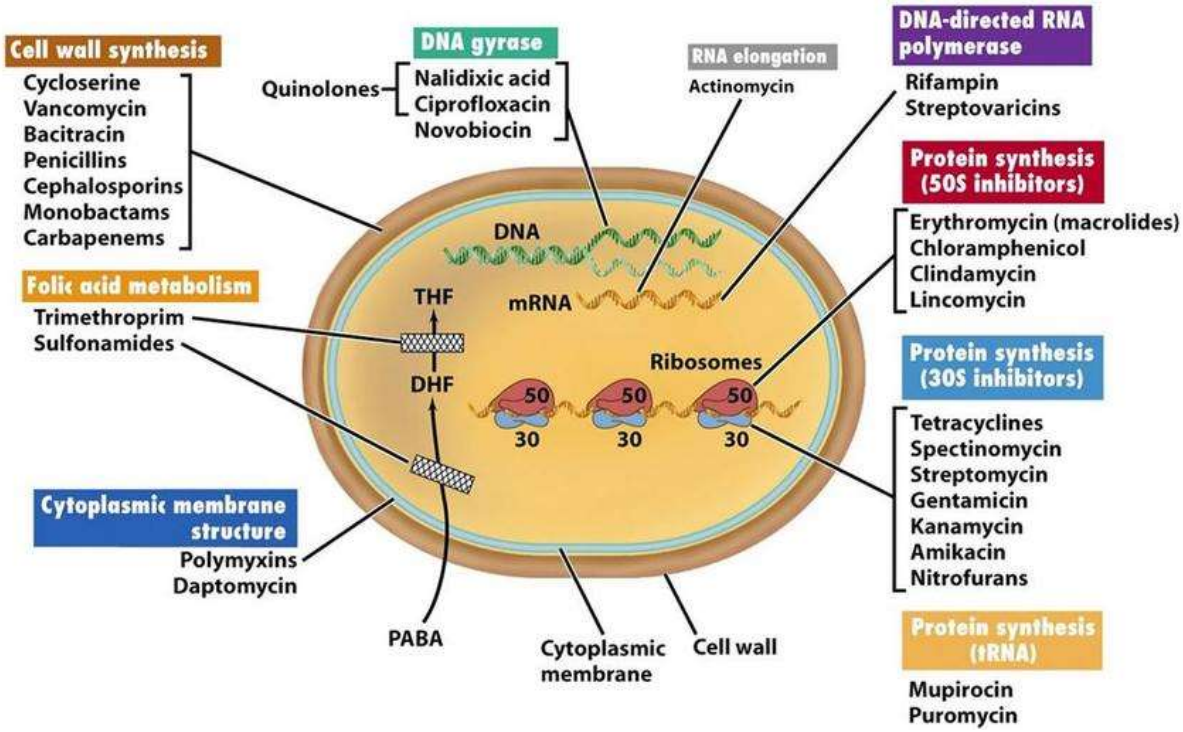

Figure 1. Mechanisms of antibacterial action

1) Inhibition of cell wall synthesis – the cell wall is present next to the cell membrane and is essential for structural growth and protection of the bacterial cell under the unfavourable conditions of survival. It is a hard layer, composed of a peptidoglycan structure. In order to produce the cell wall, synthesis of peptidoglycans is the first requirement. Peptidoglycans form by joining disaccharide pentapeptides to glycan strands (by enzymes called transglycosylases) and cross linking the glycan strands by the action of penicillin-binding proteins (transpeptidases). During the cross linking, the D-alanyl-alanine portion of the peptide chain is linked with another glycine strand. In this way, the peptidoglycan becomes cross-linked and the cell wall becomes stronger. Antibiotics such as the penicillins, carbapenems and cephalosporins, all target the cell wall by hindering the cross-linking of peptidoglycan, which inhibits the synthesis of the cell wall. In the absence of cell wall, bacteria cannot survive. For example, glycopeptides (vancomycin) attach to the D-alanyl-D-alanine unit of the peptide and suppress the binding of D-alanyl-alanine to transpeptidase. Thus, the synthesis of the cell wall is suppressed.

2) Inhibition of protein synthesis – proteins plays a vital role in the life processes of all living organisms. Any change which can inhibit the synthesis of proteins, in turn can destroy the cell. The synthesis of proteins involves two main processes – transcription and translation. In the first stage of protein synthesis, the information from DNA is handed down by mRNA in the form of codons and is transferred to the ribosome, a factory for protein synthesis. In the ribosome, translation of m-RNA occurs and there are three steps involves in this process: initiation, elongation and termination. There are two types of protein inhibitors – 30s ribosome and 50s ribosome inhibitors. In the case of the 50s ribosome inhibitors, the antibiotic inhibits the initial step of protein translation or the elongation phase of the synthesis of proteins. Antibiotics that interfere with the approach of amino acyl–tRNAs to the ribosome are known as 30s ribosome inhibitors.
3) Hindrance of nucleic acid synthesis – the disturbance in nucleic acid synthesis, caused by an antibiotic, has a great effect on the survival posterity of bacterial cells. The activity of the antibiotic is associated with the hindrance in replication or stopping of transcription. DNA replication involves the unwinding the double helix structure by the enzymatic action of helicase enzymes. Quinolones, a class of antibiotics, whose mode of action involves stopping the synthesis of nucleic acids, interferes in the performance of that particular enzyme and as a result, the replication of DNA does not occur. In the same manner, fluoroquinolones (FQ) interfere with the action of DNA gyrase which is responsible for nicking the strands of DNA, making negative supercoils and resealing the nicked strands.
4) Retardation in folic acid metabolism – folic acid plays an important role in the metabolism of nucleic acids and amino acids. A particular substrate is needed for the synthesis of folic acid in bacterial cells. The two antibiotics, sulfonamides and trimethoprim, display their inhibitory action at different places in folic acid metabolism. Due to the higher affinity of sulfonamides for the natural substrate, p-aminobenzoic acid, it inhibits the enzyme dihydropteroate synthase. On the other hand, trimethoprim inhibits the enzyme dihydrofolate reductase at a later stage of folic acid synthesis. In short, these antibiotics act as substrate mimics in their mode of action.
5) Collapse in cell membrane structure – antibiotics, whose main target is the cell membrane, are very specific in their action due to the nature of the lipids present in the cell membrane of microorganisms. The polymyxins, for example, interact with specific lipids of a lipopolysaccharide and result in disintegration of the cell membrane. Another

example is the antibiotic daptomycin, which cases disruption of the cell membrane due to depolarisation of calcium-dependent membranes.[2]

1.1.2 Antibiotic resistance:

Antibiotic resistance is due to a mechanism that the bacteria possesses to overcome the lethal effect of antibiotics. These organisms can offer antibiotic resistance by inhibiting the entrance of a drug or the distribution of a drug, by making a change in the target site or by producing an enzyme which can degrade the antibiotics. Following the introduction of the sulfonamides and the penicillins, the first classes of antibiotics, the first cases of antibiotic resistance were reported in the late 1930s (for the sulfonamides) and then in the 1940s (penicillins).[3] Fleming discovered penicillin in 1928 but his co-workers found a bacterial penicillinase in 1940, even before the use of penicillin as a therapeutic. The identification of bacterial penicillinase affords an interesting question as to whether the antibiotic or antibiotic resistance came first. [4]

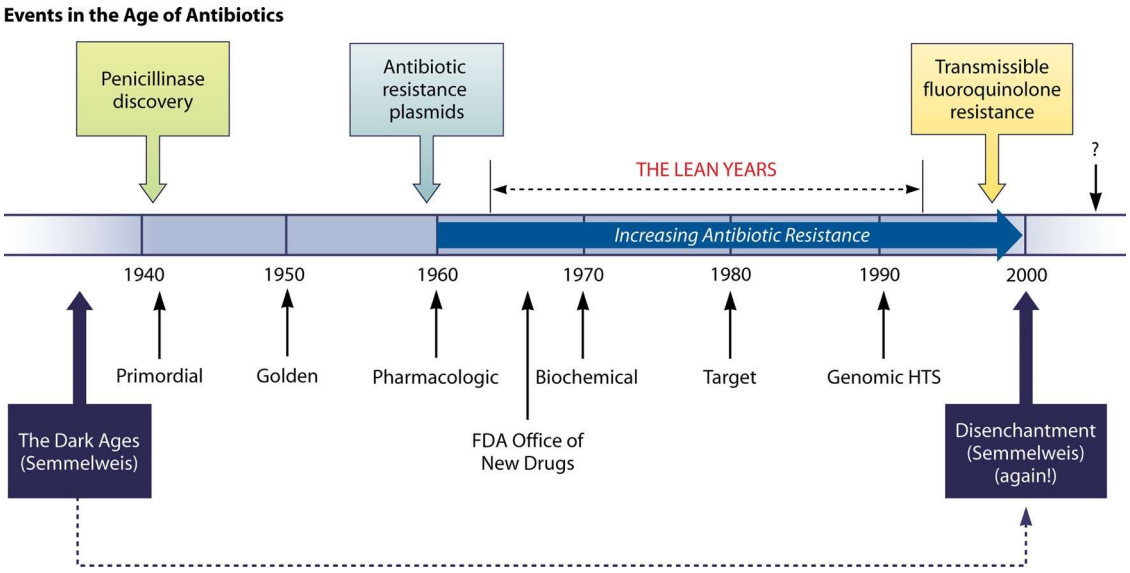

Figure 2. History of antibiotic resistance[4]

In the first 25 years of development of antibiotics, antibiotic resistance was a threat for hospitalised patients, but with the passage of time, this threat is spreading to affect also the lives of the community, outside of the hospitals.[3]

1.1.3 Causes of antibiotic resistance:

The main cause of antibiotic resistance is overuse of antibiotics. The founder of first antibiotic, Alexander Fleming warned that the "public will demand [the drug and] then will begin an era …of abuses".[5] There are two mechanism of bacterial resistance – biological mutation and gene transfer. In general, it can be said that bacterial resistance has its foundation at the genetic level. This means that in most cases of bacterial resistance, changes in the genetic makeup of the previously susceptible bacteria takes place, either via a mutation or by the introduction of new genetic information. The expression of these genetic changes in the cell result in changes in one or more biological mechanisms of the affected bacteria and ultimately determine the specific type of resistance that the bacteria develops, resulting in a myriad of possible biological forms of resistance.[3] Below we will review briefly both the biological and the genetic mechanisms of resistance:

1.1.3.1 Biological mutation

Resistance gained from the mutation of genetic material can be natural or be the result of selection pressure.[3] Natural resistance means that the mutation of a gene occurs in the absence of selective pressures from the presence of antibiotics. This type of resistance is much less common. What is more common is the selection of genetic changes due to the overuse of antibiotics. Different mechanisms by which bacteria are able to achieve resistance include:

(i) Efflux pumps – Efflux pumps are membrane proteins which can remove antibiotics from the cell. These proteins are present in the cytoplasmic membrane. When antibiotics enter a cell, efflux pumps are able to remove them until the concentration of antibiotic is lower than the required concentration for it to have antibiotic action. This mechanism is used by bacteria to resist numerous different classes of antibiotics including the tetracyclines, macrolides and fluoroquinolones (FQ), but are not effective against the polymyxins.[6] These efflux pumps were first discovered for the tetracycline and macrolide antibiotics.[3]

(ii) Modification of the target molecule – The action of antibiotics is dependent upon its interaction with target binding sites. A small change in a target site can resist the activity of antibiotics. These changes are associated with mutations of a bacterial gene on the chromosome. These natural variations and acquired change in target sites inhibit the binding of antibiotic, which are very specific in nature.[3] Examples of alterations in target sites include:

a) Glycopeptides, vancomycin and teicoplanin can inhibit the synthesis of cell wall in Gram-positive bacteria. But the residue D-alanyl-D-alanine of peptidoglycan precursors can be changed by some bacteria to D-alanyl-lactate, and therefore the binding of glycopeptides with this residue is not possible and resistance occurs.

b) In Gram-positive bacteria, the alteration of the transpeptidase protein and in Gram-negative bacteria, the formation of β-lactamases is the reason for resistance. The mutation in the transpeptidase protein is responsible for reducing the effectiveness of β-lactam antibiotics.

c) Some antibiotics are able to inhibit the synthesis of proteins, e.g. tetracycline, macrolides, chloramphenicol and aminoglycosides. To perform their antibiotic action, aminoglycosides interact with the 30s ribosomal unit while macrolides, lincosamides and streptogramim B interact with the 50s ribosomal unit. These ribosome units offer resistance to these antibiotics by modification of the binding site.[6]

Table 1. Mechanisms of antibiotic resistance[4]

Antibiotic class	Example(s)	Target	Mode of resistance(s)
Aminoglycosides	Gentamicin, streptomycin, spectinomycin	Translation	Acetylation, efflux, altered target, phosphorylation, nucleotidylation
Glycopeptides	Vancomycin, teicoplanin	Peptidoglycan biosynthesis	Reprogramming peptidoglycan biosynthesis
Tetracyclines	Minocycline, tigecycline	Translation	Monooxygenation, efflux, altered target
Macrolides	Erythromycin, azithromicin	Translation	Hydrolysis, glycosylation, phosphorylation, efflux, altered target
Streptogramins	Synercid	Translation	Acylation, efflux, altered target, C-O lyase
Lincosamides	Clindamycin	Translation	Nucleotidylation, efflux, altered target
Phenicols	Chloramphenicol	Translation	Acetylation, efflux, altered target
Oxazolidinones	Linezolid	Translation	Efflux, altered target
Quinolones	Ciprofloxacin	DNA replication	Acetylation, efflux, altered target
Lipopeptides	Daptomycin	Cell membrane	Altered target
Rifamycins	Rifampin	Transcription	ADP-ribosylation, efflux, altered target
Cationic peptides	Colistin	Cell membrane	Altered target, efflux
Sulfonamides	Sulfamethoxazole	C_1 metabolism	Efflux, altered target
Pyrimidines	Trimethoprim	C_1 metabolism	Efflux, altered target
β – Lactams	Penicillin, cephalosporins, Penems, monobactams	Peptidoglycan biosynthesis	Hydrolysis, efflux, altered target

(iii) Destruction or transformation of an antibiotic – The cause of this destruction is the production of specific enzymes by bacteria, which are able to cause certain changes in the structure of the antibiotic which hinder the activity of the antibiotic. Three main enzymes of this type are: β-lactamases, aminoglycoside-modifying enzymes (AME'S)

and chloramphenicol acetyltransferases (AACs). All β-lactam antibiotics having ester and amide bonds can be hydrolysed by β-lactamases.

AME's affect the interaction of aminoglycoside molecules with the 30s ribosomal subunit by neutralising it to prevent binding from aminoglycosides and fluoroquinolones. In Gram-positive and Gram-negative bacteria, an enzyme chloramphenicol transacetylase is present, which acetylates the hydroxyl groups of chloramphenicol and inhibit their binding with the 50s ribosomal unit.

1.1.3.2 Genetic mechanism of antibiotic resistance

Perhaps of greater threat to our communities is the ability of bacteria to gain resistance by the transfer of genetic material. Such transfer of genetic material encoding resistance can occur vertically as well as horizontally. This is achieved by two mobile DNA elements called transposons and integrons. The transposons contain genes that codify the resistance. The movement of resistant genes from one plasmid to another and the integration of genes are achieved through transposons and integrons respectively. Integrons are present in Gram-negative as well as Gram-positive bacteria and are able to confer multiple drug resistance. After a genetic alteration occurs in bacterial DNA, the genetic material can be transferred to other bacteria through a number of different mechanisms:

Conjugation – a popular mechanism of resistance transmission in bacteria is conjugation. It is normally mediated by a plasmid and transmission of plasmids occurs through a hollow tubular structure called a pilus, which is formed between closely placed bacteria.

Transformation – during transformation, the transfer of free DNA occurs from one bacterial cell to another. The free (naked) DNA is produced from dead bacteria or bacteria broken apart in the vicinity of the receiving bacteria. The incoming DNA is introduced into the cytoplasm of the receiving bacteria.

Transduction – this mechanism involves viruses which contain resistance genes. These viruses infect the bacterial cell and transfer the genetic material to the cell. In some cases, bacteriophages (viruses capable of infecting bacteria) transfer viral DNA to a receiving cell and then compels the cell to produce a greater number of the infecting virus until the cell dies and distributes infectious viruses so that they can infect other bacteria.[3]

1.2 The Polymyxin antibiotics

Polymyxins are a class of antibiotics which were discovered from different species of *Bacillus polymyxa*.[7] There are five different chemical compounds related to this class of antibiotics: polymyxin A, B, C, D and E (colistin). Out of these five polymyxins, only polymyxin B and E have been used in the medical field.[7] These polymyxins are used as last resort antibiotics to treat infections caused by Gram-negative bacteria, including *Pseudomonas aeruginosa* and *Acinetobacter baumannii*, because these antibiotics can also cause nephrotoxicity and neurotoxicity. Due to the adverse effects of the polymyxins, the use of polymyxins waned in the 1970s.[7-8] Other antibiotics which had lower toxicity as compared to polymyxins were preferred in the clinic. However, due to an increase in antibacterial resistance, there are increasing reports of Gram-negative bacteria that are resistant to all other antibiotics except polymyxins. Therefore, polymyxins are being used to treat near-fatal infections caused by Gram-negative bacteria. According to new clinical data, the use of colistin is safe if certain precautions are followed.[9]

1.2.1 Chemical Structure of the Polymyxins:

Polymyxins are non-ribosomal cyclic lipopeptides that can be depicted by the general structure shown in Figure 3.[8]

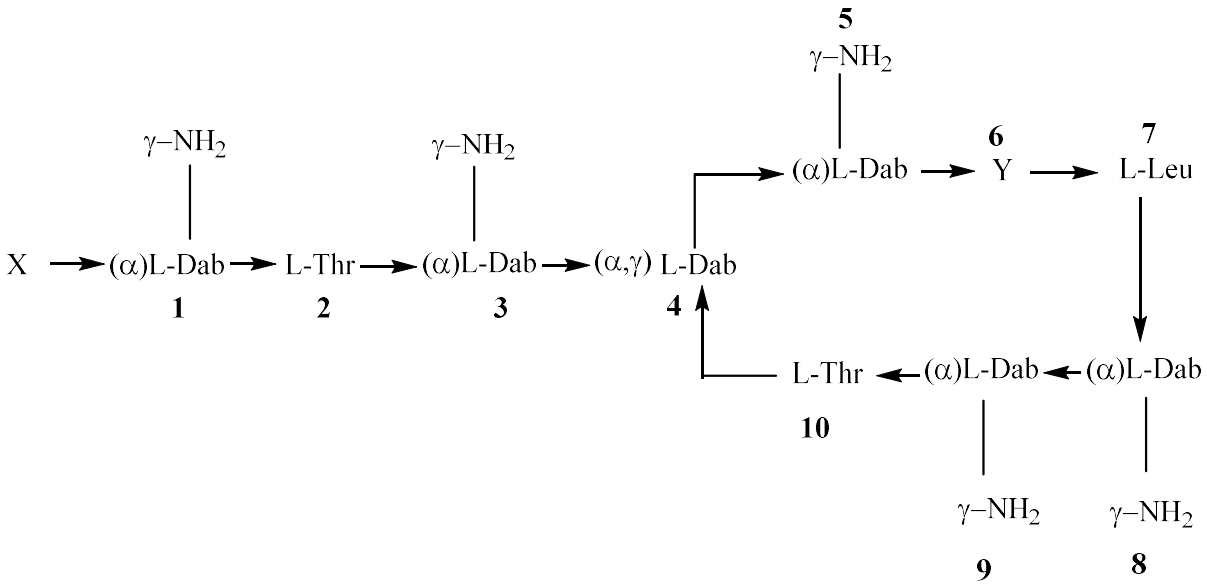

Figure 3. General structure of the polymyxins[8]

In the above Figure 3, represents the fatty acid residue 6-methyloctanoic acid for colistin A and polymyxin B_1 and 6-methylheptanoic acid for colistin B and polymyxin B_2. Y represents the amino acid D-Leu for colistin and D-Phe for polymyxin B.

A decapeptide sequence is present in the polymyxins, involving a cyclic loop of a heptapeptide between the 4-position and the 10-position at which the amino group of the side chain of diaminobutyric acid (Dab) and the carboxyl group of the C-terminal threonine is located respectively. The other main features of the structures are: (1) the presence of five non-proteogenic Dab residues, which are responsible for the polycationic nature of the polymyxins; (2) hydrophobic residues at positions 6 (D-Lue for colistin and D-Phe for polymyxin B) and 7 (-Lue); and (3) an N-terminal fatty acyl group. There is one crucial property of the polymyxins, its amphipathcity, which is responsible for their action as antibiotics. The origin of this property is the presence of both lipophilic and hydrophilic groups within polymyxin.

The configuration of all amino acids present in both types of polymyxin is the natural L-configuration except at position 6. This means that, at position 6, polymyxin B has D-phenylalanine and polymyxin E (colistin) contains D-Leucine.

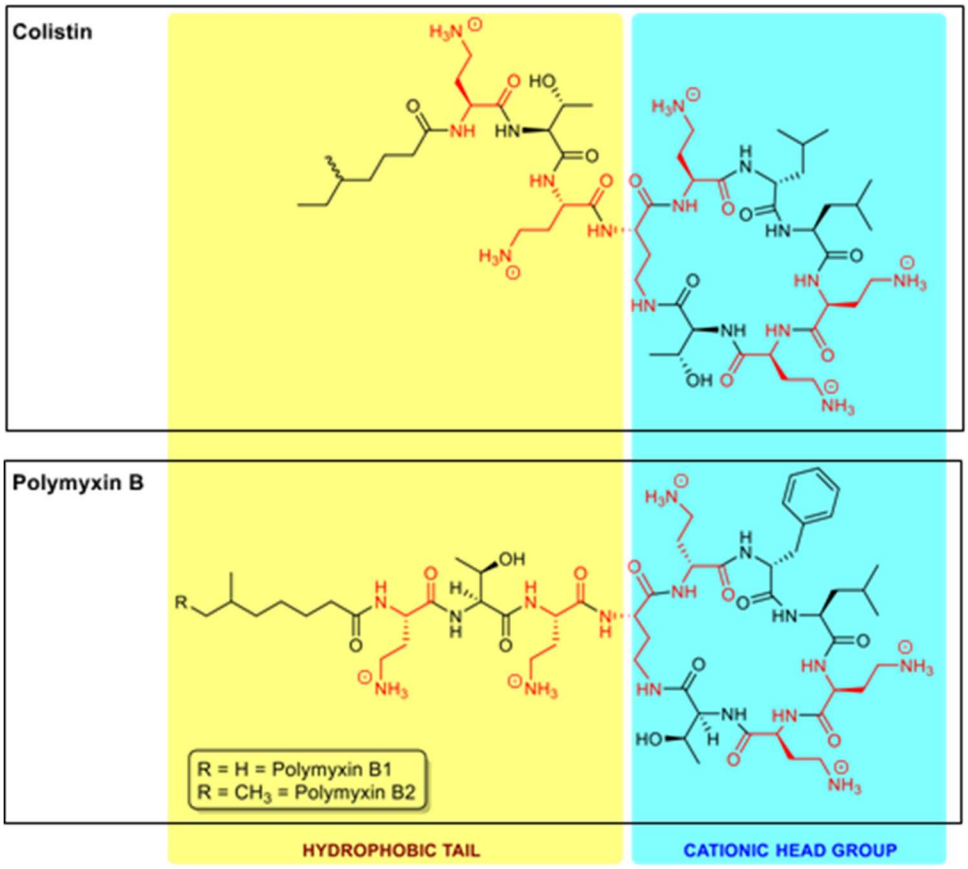

Figure 4. Structure of colistin (polymyxin E) and polymyxin B[10]

1.2.2 Mechanism of the antibiotic action of the polymyxins:

It was demonstrated in previous studies that the main target of the cationic peptide polymyxin is the cell membrane.[8] Polymyxins are used against Gram-negative bacteria, which contain a thick negatively charged outer layer. The polymyxins directly interact with this outer cell membrane of Gram-negative bacteria. In order to get a clear idea of the antibiotic activity of the polymyxins, it is important to understand the membrane structure of Gram-negative bacteria. The outer membrane contains an inner phospholipid leaflet and an outer leaflet

involving phospholipids, proteins and lipopolysaccharides (LPS). There are three further distinct units present in LPS: a core oligosaccharide region, an *O*-antigen chain and lipid-A.[8]

The interaction of polymyxin with lipid-A is responsible for the action of polymyxin against Gram-negative bacteria. The structure of lipid-A is shown below as a β-1'-6-linked D-glucosamine disaccharide that is phosphorylated at the 1'- and 4'-positions.[10]

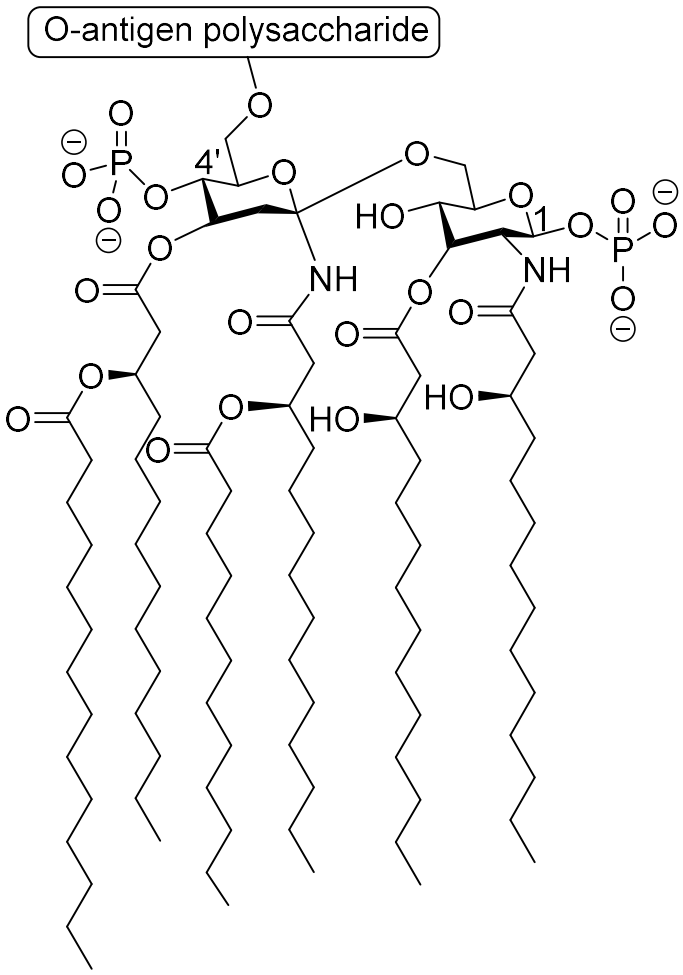

Figure 5. Structure of lipid-A[8]

Gram-negative bacteria are able to resist the action of many antibiotics due to the presence of the highly repulsive anionic charge of lipid-A and the phosphate and carboxylate functional groups of O-antigen sugars. But the polymyxins are able to inhibit the action of Gram-negative bacteria because of its amphipathic nature. According to a 'self-promoted uptake' pathway, there is an electrostatic interaction between the protonated amines of the Dab residues of the

polymyxins and the anionic lipid-A. As a result, displacement of Ca^{2+} and Mg^{2+} occurs which allows the *N*-terminal fatty acyl group and positions 6 and 7 of the polymyxins to enter into the outer membrane. This insertion causes the expansion of the outer membrane and the resulting osmotic imbalance likely results in the death of the cell.[8]

1.2.3 Resistance to colistin and the *mcr-1* gene

Colistin is a member of a family of cationic polypeptide antibiotics having a lipophilic side chain of fatty acids. As stated earlier, it is normally used to treat the lethal effect of Gram-negative bacteria which are resistant to other antibiotics. However, in 2015, Gram-negative bacteria were found that also offers resistance towards colistin. The main cause of this resistance is related to the modification of lipid-A of LPS. This modification involves the neutralisation of a negative charge at the 1'- or 4'- position of lipid-A which is important for the interaction of polymyxin with lipid-A.[11] There are three ways in which the bacteria can alter the structure of lipid-A: (a) adding L-aminoarabinose (L-Ara4N) to the 1(or 4')-phosphate position; (b) adding a phosphoethanolamine (pEtN) group to the 1 (or 4'') and (c) addition of glycine to a 3'-linked secondary acyl chain.[10]

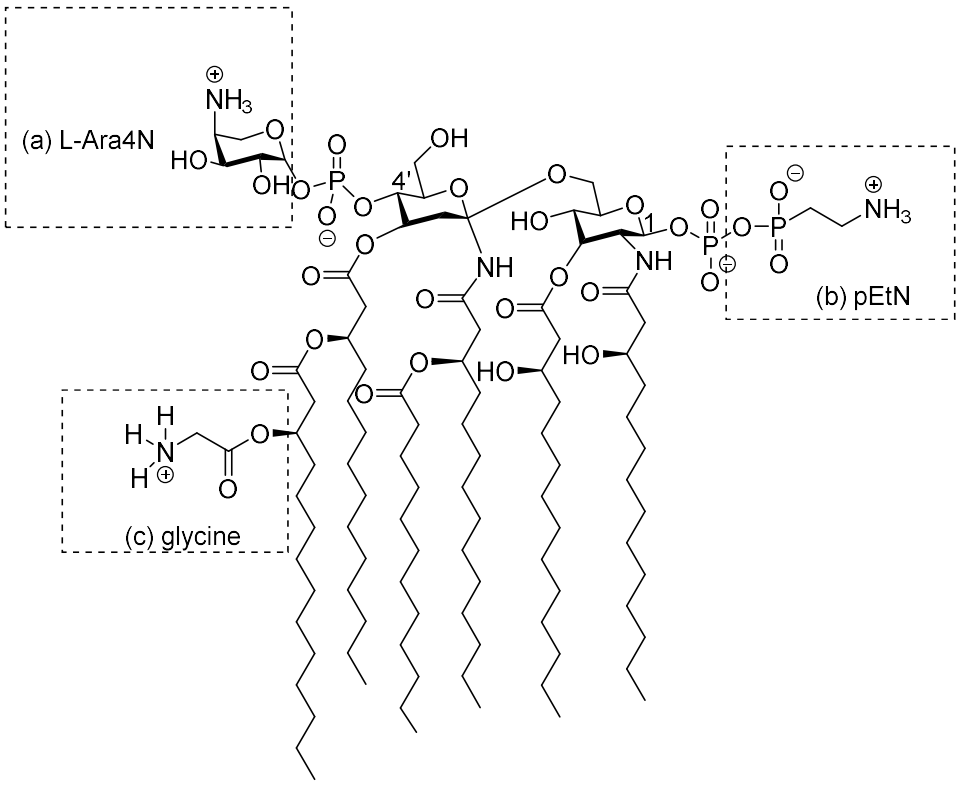

Figure 6. Modifications in the structure of lipid-A causes polymyxin resistance[10]

1.2.4 Role of MCR-1 in colistin resistance:

MCR-1 is the protein that is encoded by the *mcr-1* gene. The primary function of MCR-1 is to transfer the phosphoethanolamine (pEtN) to either the 1 or 4' position of lipid-A (Figure 7).

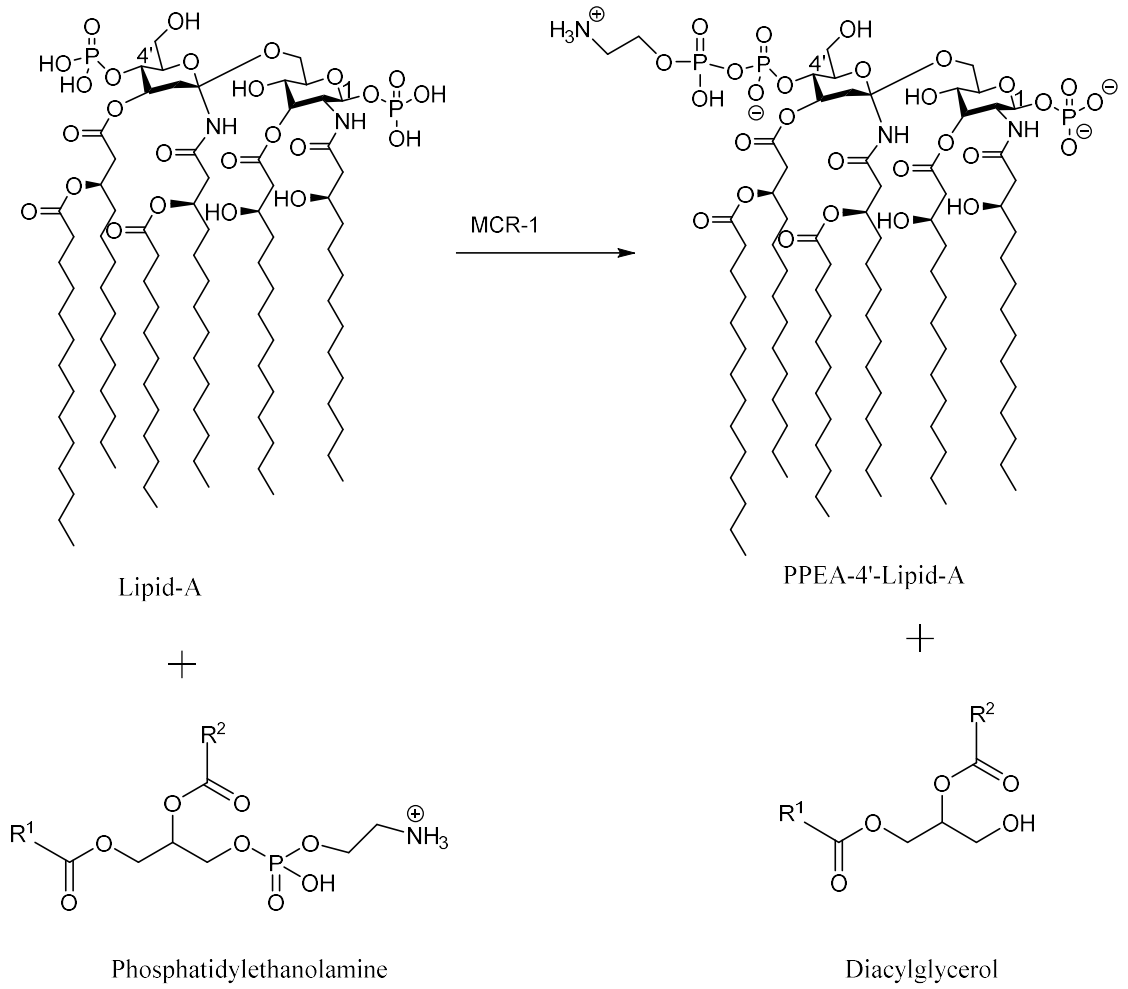

Figure 7. Transfer of phosphoethanolamine moiety from phosphatidyl-ethanolamine to lipid-A[11]

Both *in vivo* and *in vitro* experiments have been performed to show that MCR-1 acts to attach phosphoethanolamine to lipid-A of lipopolysaccharide (LPS). This attachment at the 1 or 4' position of lipid-A decreases the negative charge on this site, which prevents the electrostatic interaction of polymyxin with lipid-A.[10]

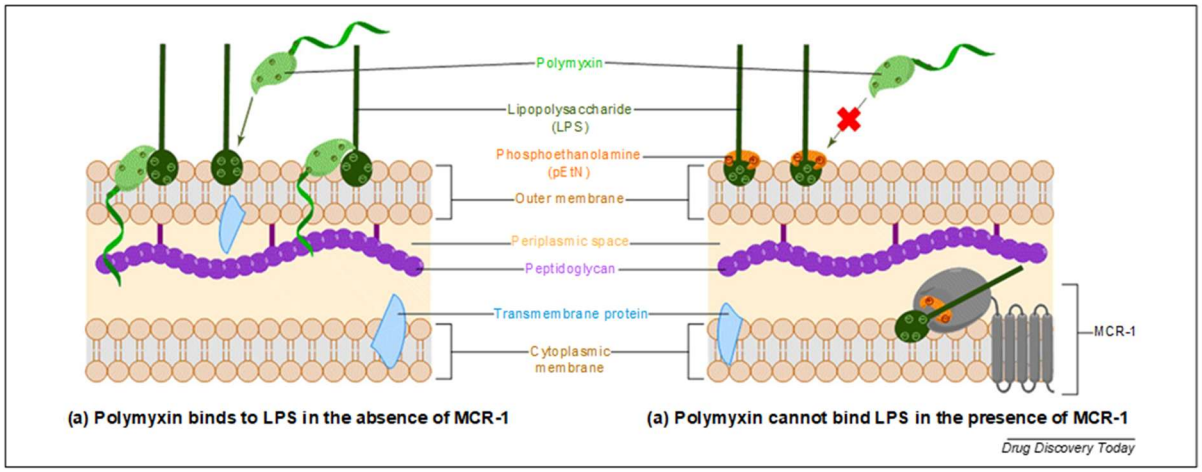

Figure 8. Action of polymyxin in the absence and presence of MCR-1[10]

In the *in vitro* experiment performed by Xu et al., full length MCR-1 was incubated with nitrobenzodiazole-labelled glycerol-3-pEtN (NBD-glycerol-3-pEtN) at room temperature for 20 hours. It is clear from the result of thin layer chromatography that MCR-1 took up pEtN from NBD-glycerol-3-pEtN. The spot of NBD-glycerol was positioned at the top of TLC plate (Figure 9a).

In an *in vivo* experiment, a strain of *E. coli* having plasmid expressing full length MCR-1 was placed under observation. In mass spectrometry, there was a single charge state at m/z = 1797.356 corresponding to unmodified lipid-A in a control plasmid sample while lipid-A from a MCR-1 positive strain showed a two charge state at m/z = 1797.416 for unmodified lipid-A and m/z = 1920.501 for the pEtN-modified lipid-A (Figure 9b).

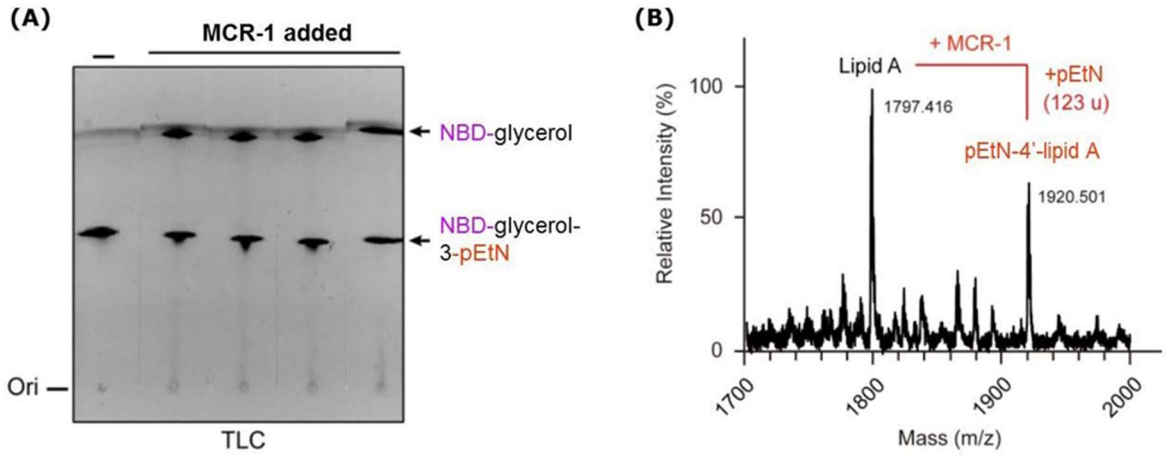

Figure 9. Evidence of lipid-A modification by MCR-1[10]

A two-step mechanism of MCR-1 activity was confirmed by mass spectrometry, X-ray crystallography, computational modelling and site-directed mutagenesis. The first step of the mechanism involves the binding of phosphoethananolamine (PE) with MCR-1 and transfer of pEtN from PE to MCR-1. At this point, a MCR-1/pEtN complex forms. In the second step, this complex binds to lipid-A and transfers pEtN to lipid-A at the 1 or 4' position.[10]

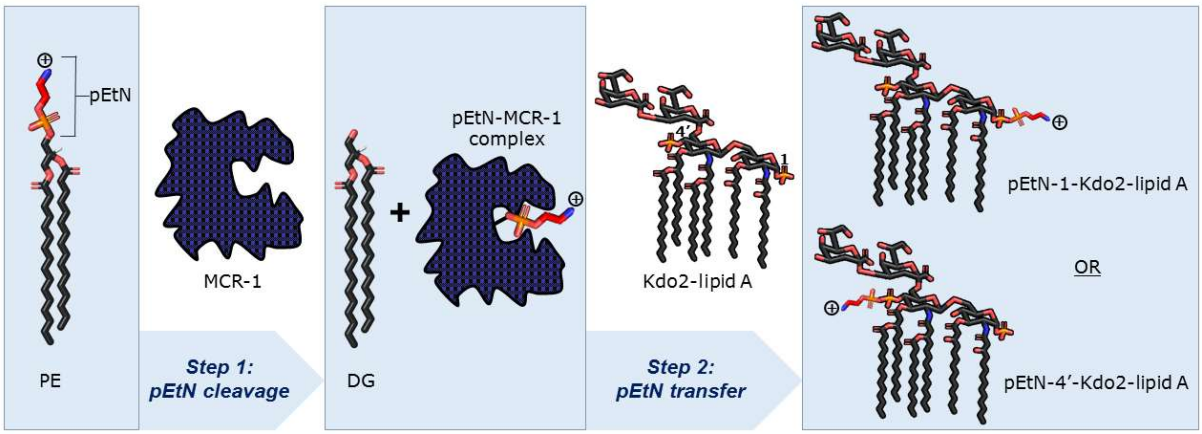

Figure 10. Two-step mechanism of MCR-1 action[10]

Hinchliffe *et. al*. used density functional theory (DFT) calculations in order to get mechanistic insights into MCR-1 function. With this technique, all possible transition states of MCR-1 were examined for the transfer of pEtN using both the mono as well as the di-zinc forms of MCR-1. In the case of the mono-zinc model, firstly a glutamic acid residue (246) abstracts a proton from threonine (285), then T285 acts as a nucleophile to cleave the phosphate group of PE. As a result of this nucleophilic attack, an adduct is formed by removal of the acyl group (R) of PE. E246 and D465 have the same energy and the required geometrical orientation to abstract the proton from T285 and to initiate the mechanistic pathway of MCR-1. In the di-zinc model, the relative potential is higher than the mono-zinc model because in former case, the activation is performed by D465 instead of E246 and dissociation of T285 from the zinc ion occurs.[10]

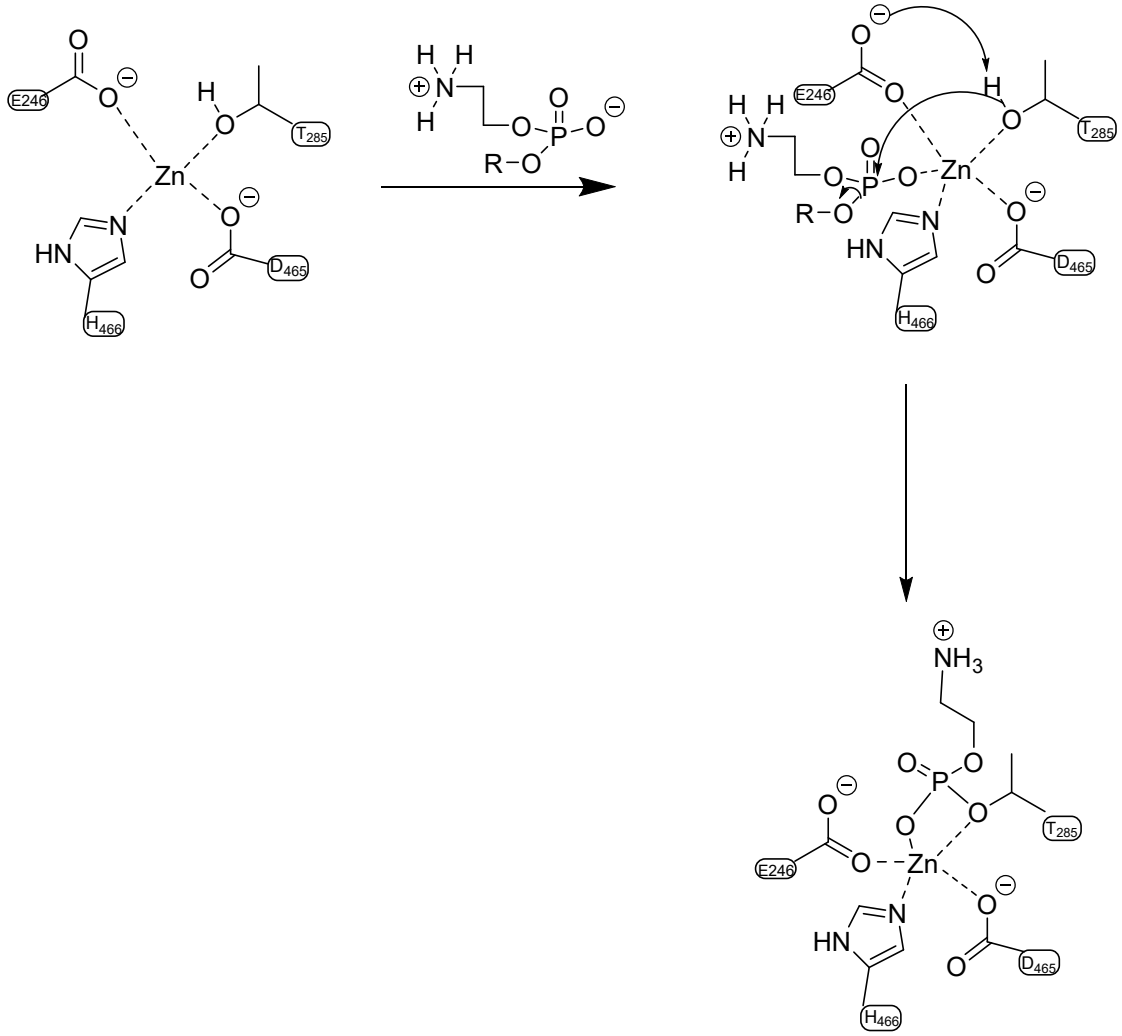

Figure 11. Postulated phosphorylation pathway of a single zinc-containing MCR-1

In 2015, it was found that resistance to colistin could be conferred by the mobilised colistin resistance (*mcr-1*) gene. The *mcr-1* gene is able to spread resistance by horizontal transfer, mediated by plasmids, and this was the first example of transferrable resistance towards the polymyxins.

1.2.5 Significance of *mcr-1* and colistin resistance

According to the World Health Organisation (WHO), antibiotic resistance is the one of the greatest threats to human health. This scenario is very serious particularly in the case of multi drug resistance (MDR) Gram-negative bacteria (*Pseonas, aeruginosa, Acinetobacter*

baumannii and Klebsiella pneumonia).[8] They are resistant to three main classes of antibiotics: (a) the β-lactams which include the plasmid-encoded β-lactamases (ESBLs), hydrolysing cephalosporins and the carbapenemases which hydrolyse carbapenems; (b) the aminoglycosides with 16S rRNA methylases which modify their cellular targets to confer pan-aminoglycoside resistance; and (c) the fluoroquinolones mostly with topoisomerase mutations. The last option for treating infections caused by MDR Gram-negative bacteria are the polymyxins, i.e. colistin and polymyxin-B. There was thus major concern when transferrable resistance to colistin was discovered.[12]

The resistance against colistin is not a new concept because there are a number of bacterial species which have natural resistance to colistin and resistance can be acquired by chromosomal mutations.[12] This resistance is unstable in nature and it cannot be spread from one bacteria to another, meaning that it is not transferrable.[13] However, the discovery of plasmid-mediated colistin resistance by transfer of the *mcr-1* gene was a new discovery in 2015 .[12] The theory that distribution of *mcr-1* was via farmed animals in South China is supported by the high prevalence of *mcr-1* in *E. coli* isolates from animals.[13]

There are main three factors related to *mcr-1* which make it global concern: **1.** The stability of the *mcr-1* plasmid as well as their transferrable nature to human pathogens such as *E. coli* strains; **2.** The movement of people across the border of China; and **3.** The selective pressures provided by the regular use of colistin in the veterinary sector, both within and outside China.[13]

The main concern of plasmid-borne colistin resistance is its recent identification in different parts of the world. In 2015, this resistance was first identified in China, but by 2017, it was found in more than 30 countries on five continents.[9] The occurrence of resistance is detected worldwide in animals, hospital-acquired pathogens and in the environment. It is a worrisome concept that the main host of the *mcr-1* gene is *E. coli* which is easily exchanged among humans, animals and the environment. The spread of *mcr-1* is related to different types of genetic events which occurred independently in geographical areas which are distantly related to each other. This fact is supported by the identification of the *mcr-1* gene on many plasmid backbones.[12]

1.3 Goals and objectives of the project

The goal of this project is to design and synthesise small molecule inhibitors of MCR-1, the protein that is encoded by the *mcr-1* gene. This is an area of hot research currently, given the importance of MCR-1 to polymyxin resistance.[10] For example, the metal-chelating agent ethylenediaminetetraacetic acid (EDTA) has been reported to inhibit MCR-1, as the enzyme is dependent on zinc co-factors.[14] Other structural analogues such as glucose and ethanolamine have also been shown to inhibit MCR-1.[15] However, currently there are no drug-like inhibitors reported for the MCR-1 protein.

This project is a collaboration between the groups of Dr Jack Chen (organic synthesis), Dr Ivanhoe Leung (protein crystal structure, protein-based assays), Dr Johannes Reynisson (computational docking) and Dr Viji Sarojini (cell-based assays). In order to know what molecules to begin to synthesise, the project began with an understanding of the crystal structure of the MCR-1 protein and the mechanism of colistin resistance.

1.4 The crystal structure of MCR-1 and potential binding sites

In order to understand the mechanism of colistin resistance, it is necessary to know the structure and active site of the MCR-1 protein. MCR-1 shows 41% and 40% resemblance to the lipooligosaccharide-modifying enzyme LptA and the phosphoethanolamine transferase enzyme EptC respectively. The catalytic domain of MCR-1 is similar to LptA and EptC transferase but the number and position of active site zinc ions are different as compared to these two transferases.[14]

Two different domains are present in the MCR-1 protein: An *N*-terminal transmembrane domain made up of five α-helixes and a soluble *C*-terminal α/β/α sandwich domain (MCR-1c). An extended periplasmic loop and bridging helix (BH) is the means of attachment between these two domains. So far, no crystal structure has been reported for the full-length protein. However, the soluble domain has been successfully crystallised under a variety of conditions and extensively studied. The soluble domain of MCR-1 is hemispherical in shape and contains a centrally positioned β-sheet having seven strands, flanked between two α-helices. Three

potential binding sites for small-molecule inhibitors have been identified: the Zn binding site, the ethanolamine binding site and the lipid binding site.[10, 14]

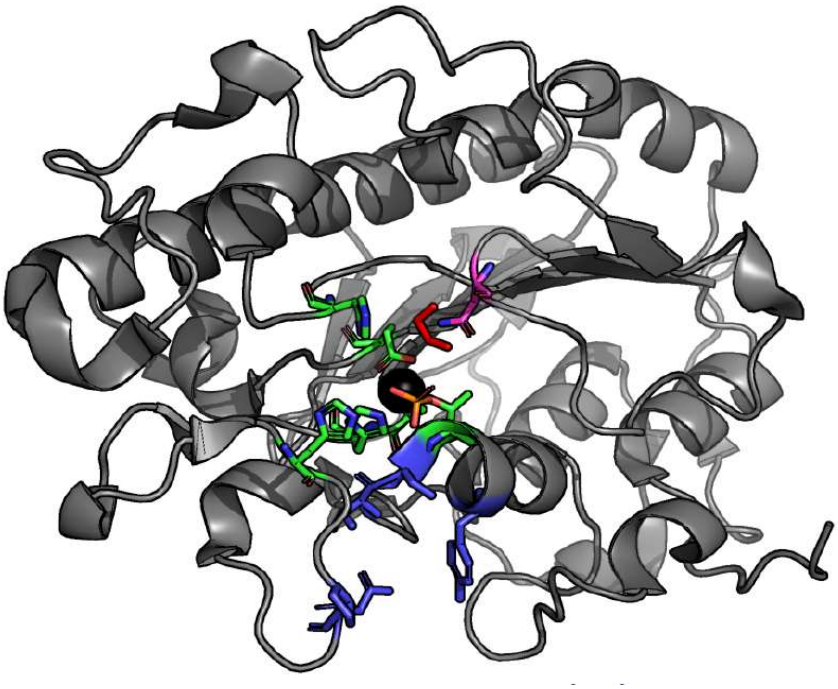

Figure 12. Crystal structure of MCR-1 soluble domain[10]

1.4.1 The Zn binding site

It is clear from the crystal structure of MCR-1 that it is a zinc metalloprotein. The active site for the zinc ion is located in a shallow depression in the soluble domain. Six amino residues are critical in binding to zinc ions, these being E246, T285, H395, D465, H466 and H478. Depending on the crystallisation conditions of the protein, the number of zinc ions present in the binding site can vary from 1 to 4. Removal of zinc from the protein results in a non-functional protein and site-directed mutagenesis of the 6 amino residues have showed that all of them can impair MCR-1 function. The threonine residue in particular is critical for the transfer of the phosphor group from PE to lipid-A.[11, 14]

1.4.2 The lipid-A binding site

It is proposed that the lipid-A binding site is present in close proximity to the Zn binding site. Even though the crystal structure of lipid-A bound to MCR-1 has no yet been reported, various mimics of lipid A, including D-sorbitol, [11]D-glucose, glycerol[14] and D-xylose[16] were shown to bind in this lipid-A binding pocket. The amino acid residues T283, S284, Y287, P481 and N482 are believed to be important in forming the binding pocket close proximity to a phosphorylated T285. In case of glucose, it was observed that glucose was flanked by Y287 and P481 with binding interactions to T283, S284 and N482 at the lower face.[11, 15]

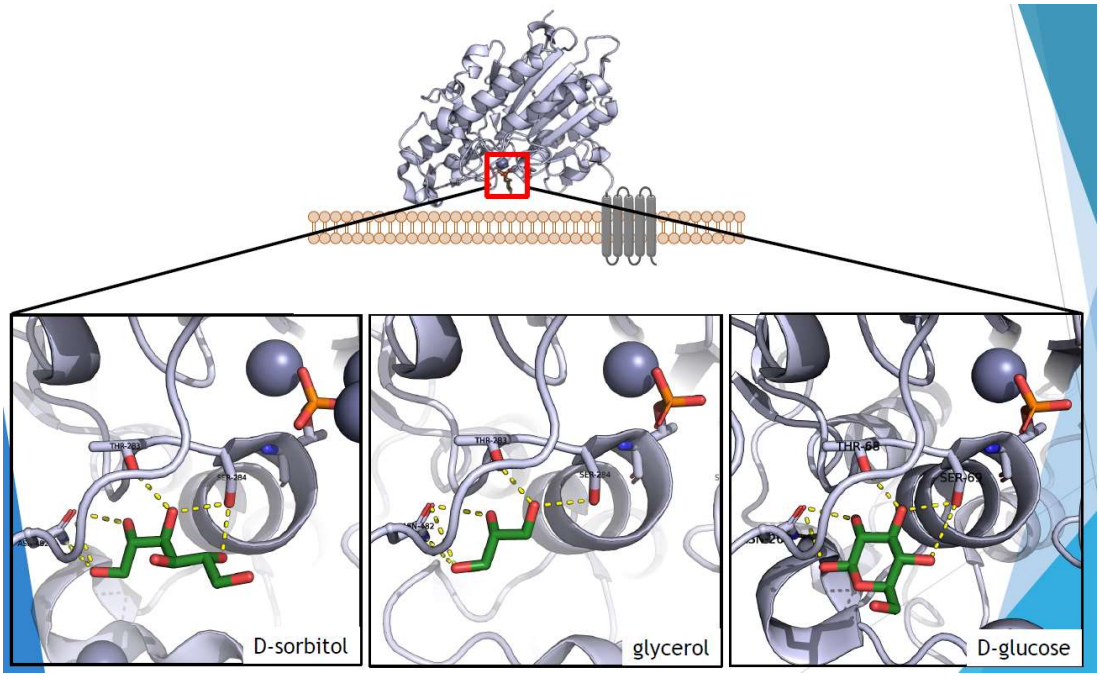

Figure 13. Lipid-A binding site of MCR-1

1.4.3 The ethanolamine (EtN) binding site

The natural substrate pEtN has never been co-crystallised with MCR-1 because the cMCR-1 protein does not contain the *N*-terminal transmembrane domain which is responsible for binding of this substrate.[15] In the absence of this domain, MCR-1 binds to pEtN weakly. Besides this, the phosphoester bond between the phosphate group and ethanolamine (EtN) tends to break instead of forming a new bond from the phosphate group to T285 due to the

absence of lipid A in close proximity. As a result of this, the EtN moiety will be lost. The EtN moiety has been found co-crystallised in the active site of MCR-1, where is stabilised by hydrogen bonding with N239, phosphorylated T285 and a water molecule. It is clear from comparison between EtN-bound and non-bound crystals, that the residue H395 rotates 50° to accommodate the EtN. Furthermore, in inhibition studies using the concentration range from 0 – 10 mM of EtN, it was found that in the presence of 4 mg/L polymyxin B, EtN concentration-dependent growth inhibition was seen. [15]

1.5 Virtual Screening for the selection of lead compounds

To determine the structure of the molecules to synthesise, virtual screening studies were initially performed by collaborators in the group of Dr J. Reynisson. These initial screening studies were performed against the Zn(II) binding site of MCR-1, using published crystal structures in the protein data bank. The screening used both phosphorylated and non-phosphorylated forms of the protein. 28 commercially available compounds were identified as virtual hits and were purchased for further testing in protein binding assays.

NMR-based binding assays were performed by the groups of Dr I. Leung. This involved initially, expression of the MCR-1 protein as a mixture of phosphorylated and non-phosphorylated forms. Binding of the purchased small molecules with the protein was studied using a WaterLOGSY method, due to its ability to identify binding to a protein over a wide range of binding affinities, from the mM to the μM range.

1.5.1 NMR-based Protein-binding assays

WaterLOGSY is an NMR method that is able to differentiate between small molecules in solution and molecules that are interacting with large macromolecules. In this technique, the bulk water is excited, and the magnetisation of the water is transferred by the nuclear Overhauser effect (NOE) to the free ligand and/or a ligand within a protein-ligand complex. The resonances of non-binding molecules appear in opposite sign to molecules that interact with a protein (see Figure 14a).

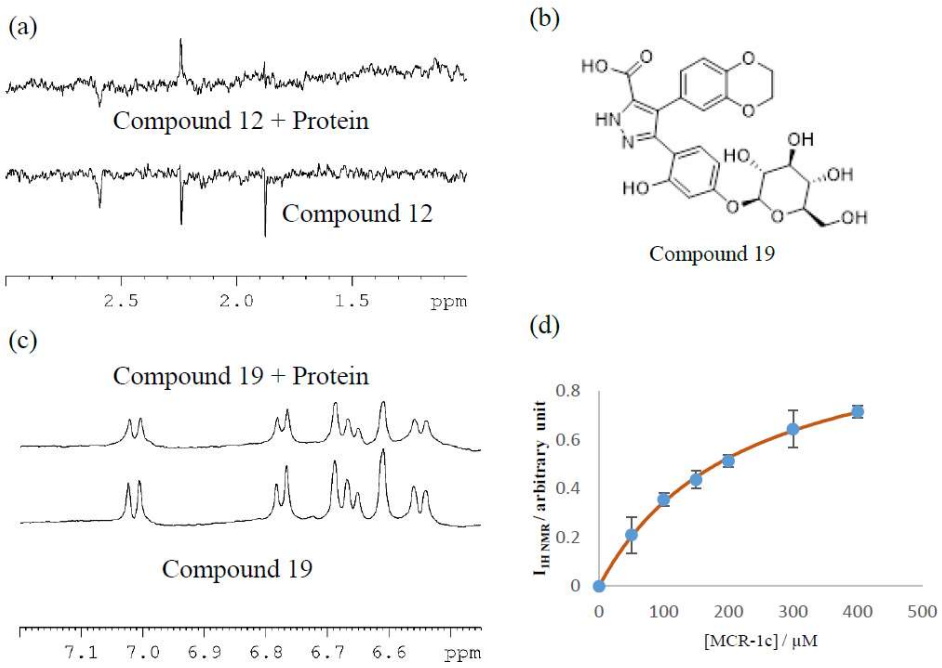

Figure 14. (a) Example of hit screening by WaterLOGSY screen **(b)** Structure of compound 19 **(c)** 1:1 ^{1}H NMR screen of compound 19 **(d)** the binding curve of compound 19

Of the 28 compounds found from the virtual screen, 12 compounds were identified as binders (see Figure 15). Out of these dozen compounds, 8 were identified as being strong binders. These strong binders were further examined using NMR studies so that their affinities with the protein could be ranked. This was achieved by measuring their ^{1}H NMR spectra at a 1:1 ratio of protein to ligand. Molecules that are not bound to the protein would show a strong resonance. On the other hand, molecules that are bound to the protein will tumble slowly in solution and their intensity is reduced (Figure 19). Following these studies, compound 19 was identified as the compound with the strongest affinity to the MCR-1 protein. It was believed that this was likely due to the presence of a sugar moiety, which is similar to MCR-1's natural substrate.

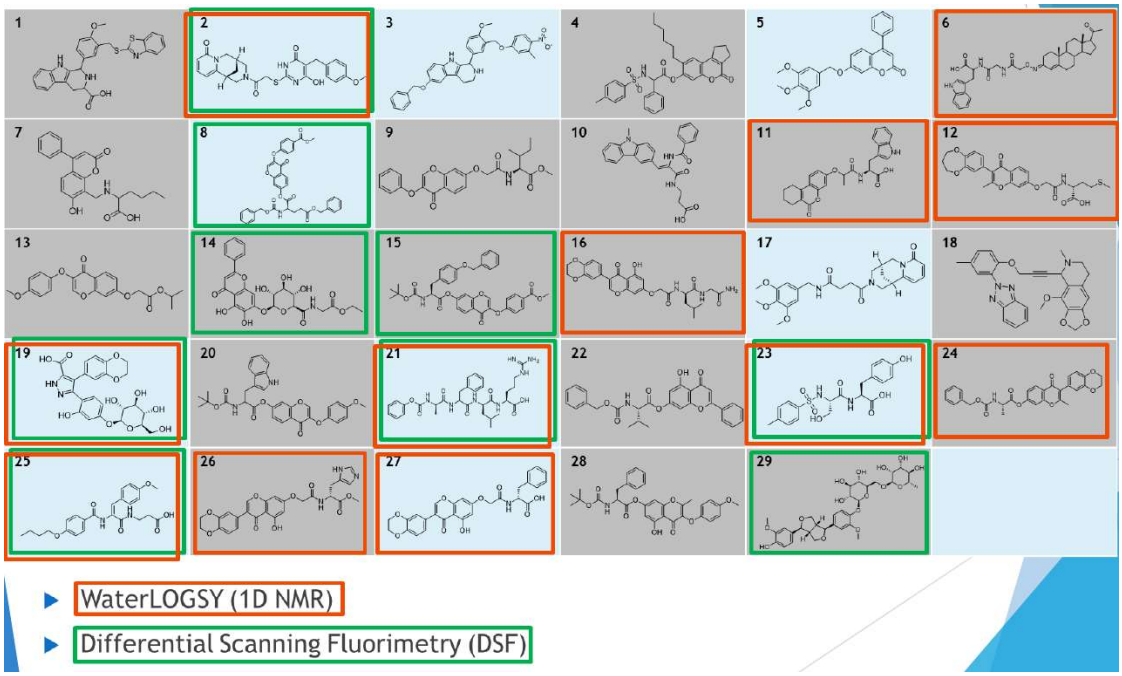

Figure 15. Compounds from the first round of virtual screening

In order to quantify the binding affinity, an apparent binding constant was determined by an NMR titration experiment. The intensity of the compound signal was measured in the presence of increasing amounts of the MCR-1 protein. The binding curve plotted from this experiment gave an apparent binding constant of ~220 μM (Figure 14d). It is important to note that apparent binding constant needs to be taken with caution, as the protein used in a mixture of phosphorylated and non-phosphorylated forms and it was not possible to distinguish the form of the protein that the molecules were bound to.

1.5.2 Second round of screening

The structural features of the hits obtained in the initial screen was used to perform a second round of more focussed virtual screening. This was again performed by the group of Dr Reynisson, with a focus on obtaining structural analogues that were commercially available. The virtual screen identified 30 compounds for further testing using NMR studies. The group of Dr Leung performed another round of 1:1 ^{1}H NMR screening to reveal 9 of these 30 compounds as strong binders. The apparent binding constant was measured for the compound with the highest affinity (compound 11, Figure 16) and was determined to be 10 μM. This

result was an improvement on the previous result and showed the value of a more focussed screen. It is important to note that although binding is observed, these studies are not able to tell us anything about the site of binding. If the binding of the molecule was not at the active site, but was instead due to non-specific binding, the molecule would have a much lower chance of working of inhibiting MCR-1 activity. The easiest way to determine whether the binding is occurring at the Zn(II) binding site or not is to perform competition studies with a known small molecule agonist. However, no such molecule has yet been published.

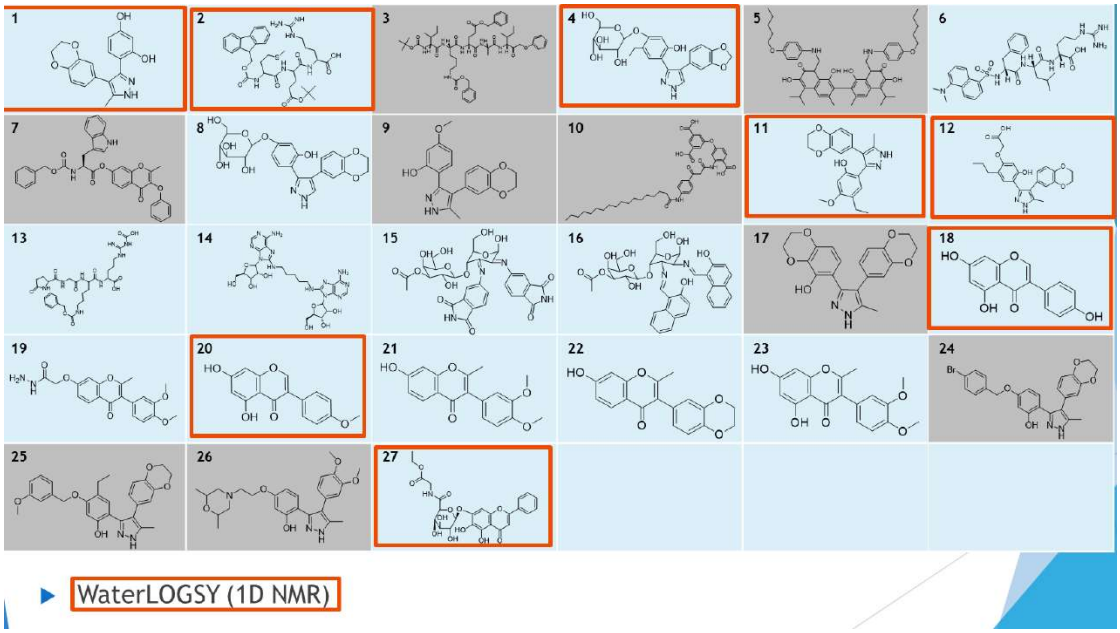

Figure 16. Compounds from the second round of virtual screening

1.6 The need for a synthetic organic chemist

After the initial virtual screens and confirmation of the results by ^{1}H NMR binding studies, a number of potential hits were identified that had significant binding to MCR-1. Ten of the most promising lead compounds are shown in Figure 17. Out of all these compounds, the compound with the strongest binding affinity as determined by ^{1}H NMR binding studies was compound **1** (Figure 17). Due to the lack of a known agonist for the Zn(II) binding site (and therefore the inability to perform competitive binding assays), the logical next step was to use cell-based minimum inhibitory concentration (MIC) assays to see if these hit compounds could be

potentially used as an antibiotic (i.e. if it could kill colistin-resistant bacteria in combination with colistin). However, the amount of compound required for an MIC assay prevented the simple purchase of these molecules from a commercial supplier.

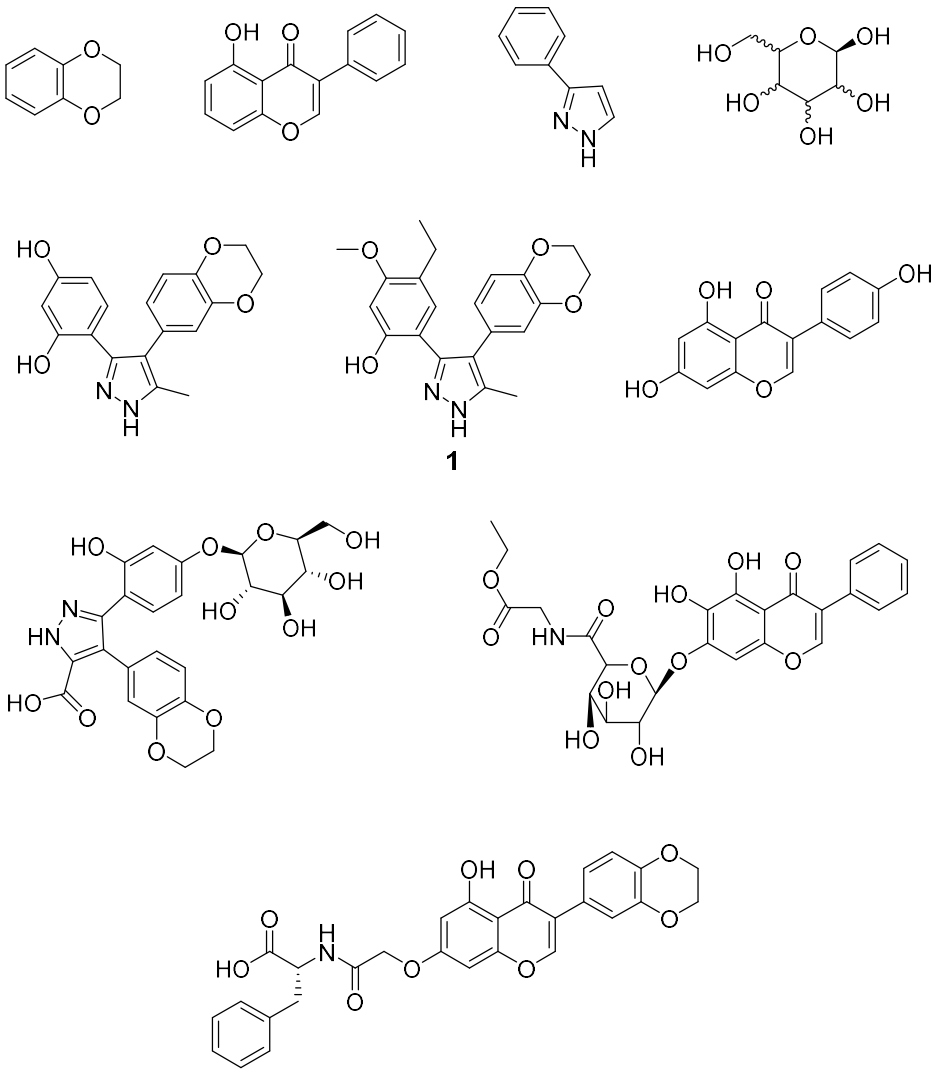

Figure 17. Selected hits from the second virtual screen

1.7 My Aims and Objectives

At this point, there was a need for a synthetic organic chemist. My project is focussed on the synthesis of compounds that are structurally similar to the strongest binder compound **1**. The mains objectives were to: **1.** Synthesise enough compound of a number of the hits from the above studies to be able to use in MIC assays; **2.** To investigate synthetic routes that would allow for range of structural analogues to be made; and **3.** Identify and confirm the first drug-like inhibitor of the MCR-1 protein.

CHAPTER TWO: RESULT AND DISCUSSION

2.1 Synthesis of 3,4-diarylpyrazoles

2.1.1 Rationale and Retrosynthesis

The strongest binder of the MCR-1 protein found after two rounds of virtual screening and NMR binding assays was pyrazole **1** (Figure 18). This heterocycle had aromatic substituents in the 3- and 4- positions of the central pyrazole ring and a methyl substituent on the 5- position. Given that there were several other hits that possessed the same 3,4-diarylpyrazole core structure, we decided to focus our synthetic efforts on this motif. The aim was to find a synthetic method that would allow entry into these series of compounds as quickly as possible so that their activity in cell-based assays could be determined. We also wanted to use a synthetic method that was modular and flexible, so that a variety of different structural analogues could be made to investigate the structure-activity-relationship (SAR). After investigating methods for the synthesis of 3,4-diarylpyrazoles in the literature we came up with the retrosynthesis below (see Scheme 1).

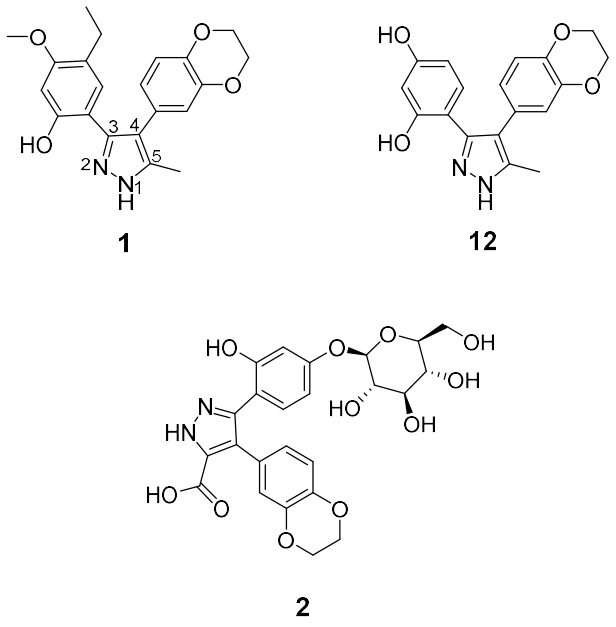

Figure 18. Selected hits having the pyrazole core

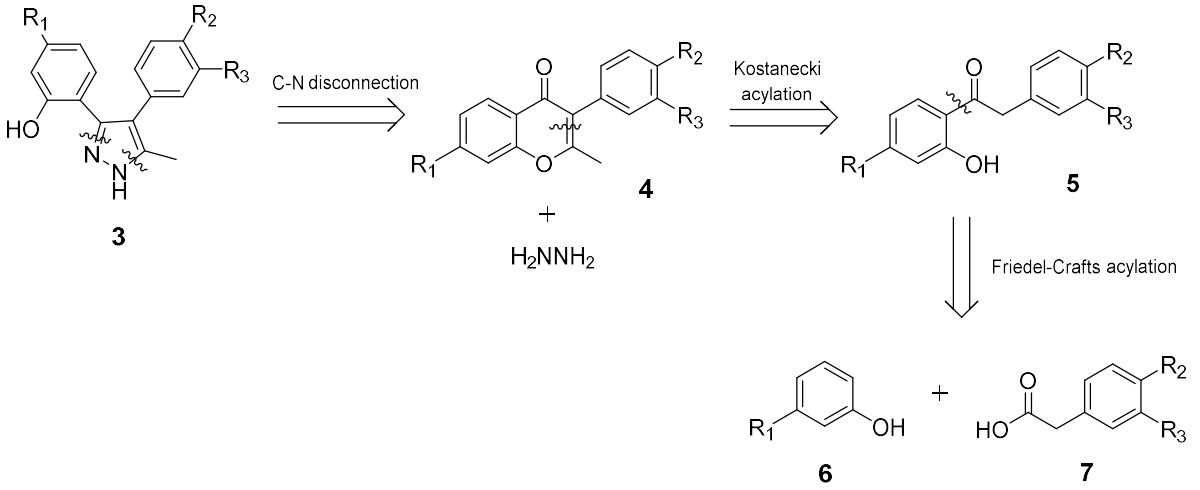

Scheme 1. Retrosynthetic analysis of diarylpyrazoles

Firstly, disconnections across two C-N bonds within the five membered ring gives a hydrazine molecule and an isoflavonoid which can be formed from an aza-Michael addition involving the hydrazine followed by rearrangement. This isoflavanoid **4** can be further disconnected α to the carbonyl group, which is formed in the forward direction by a Kostanecki acylation involving acetic anhydride. Finally, a disconnection adjacent to the ketone gives a phenol (**6**) and substituted phenylacetic acid (**7**) which can be joined together by a Friedel-Crafts acylation.

This retrosynthesis was favoured as the synthesis was short and it was clear that a diverse range of analogues could be made by using phenols and phenyl acetic acids with different substitution patterns. Another interesting aspect was that the intermediate isoflavones scaffolds (**4**) that are formed during the course of the synthesis are also present in many of the hits as determined by the initial screenings performed by Dr Reynisson and Dr Leung. These structures are also of interest and will also be submitted for binding assays/biological testing. Below is shown the general scheme used for the synthesis the diarylpyrazoles[17-18] (Scheme 2).

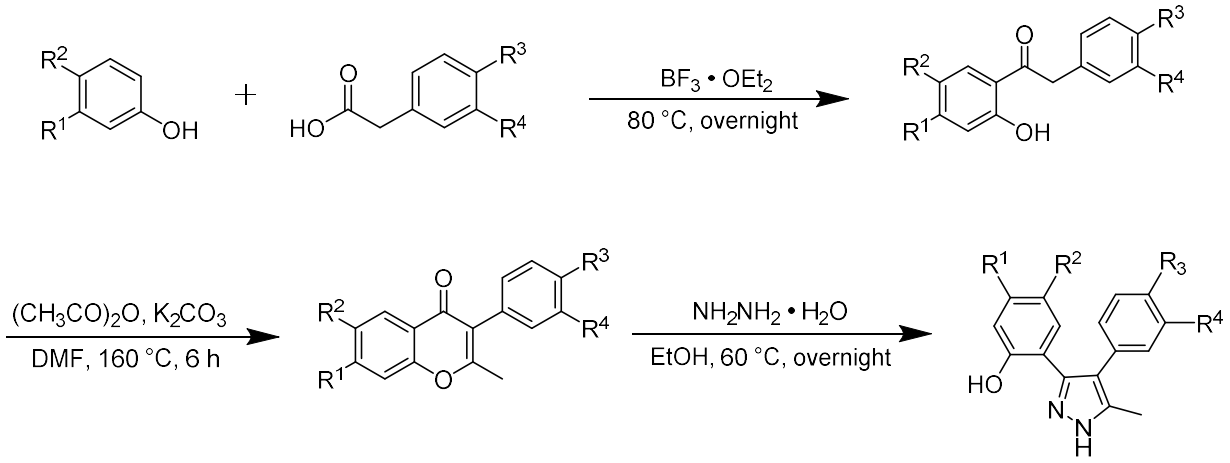

Scheme 2. General scheme for preparation of diarylpyrazoles

2.1.2 Friedel-Crafts acylation for the synthesis of ketone 10

We began to investigate this reaction sequence by testing out the Friedel-Crafts acylation of resorcinol **8** and phenyl acetic acid **9**. Both reagents were dissolved in boron trifluoride diethyl etherate and heated overnight at 80 °C under a nitrogen atmosphere. In this reaction, boron trifluoride diethyl etherate acts as solvent as well as a reagent.[17-18] In acylation reactions, a stoichiometric amount of the Lewis acid is required because Lewis acid can also complex to the carbonyl in the product. In the following reactions, several equivalents of Lewis acid are used due to the presence of other oxygen atoms within the substrate.

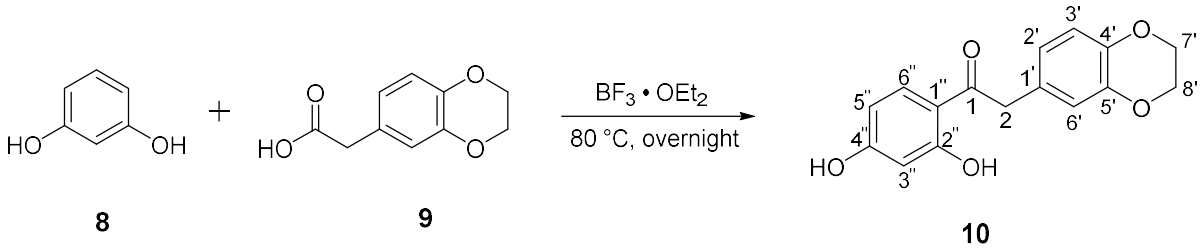

8 **9** **10**

Scheme 3. Synthesis of phenylbenzylketones

The Friedel-Crafts reaction is a commonly used procedure first discovered is 1877. The mechanism of the reaction first involves the combination of an acyl chloride or acid anhydride with a strong Lewis acid to produce a reactive acylium ion (Scheme 4). This highly-reactive carbocation is attacked by the benzene nucleophile in an electrophilic aromatic substitution

reaction. Loss of a proton then neutralises the positive charge and re-forms the aromatic ring. The acyl group in the product withdraws electrons from the π system making multiple substitution harder. This is in contrast to Friedel-Craft alkylations which is often complicated by overalkylation.[19-20]

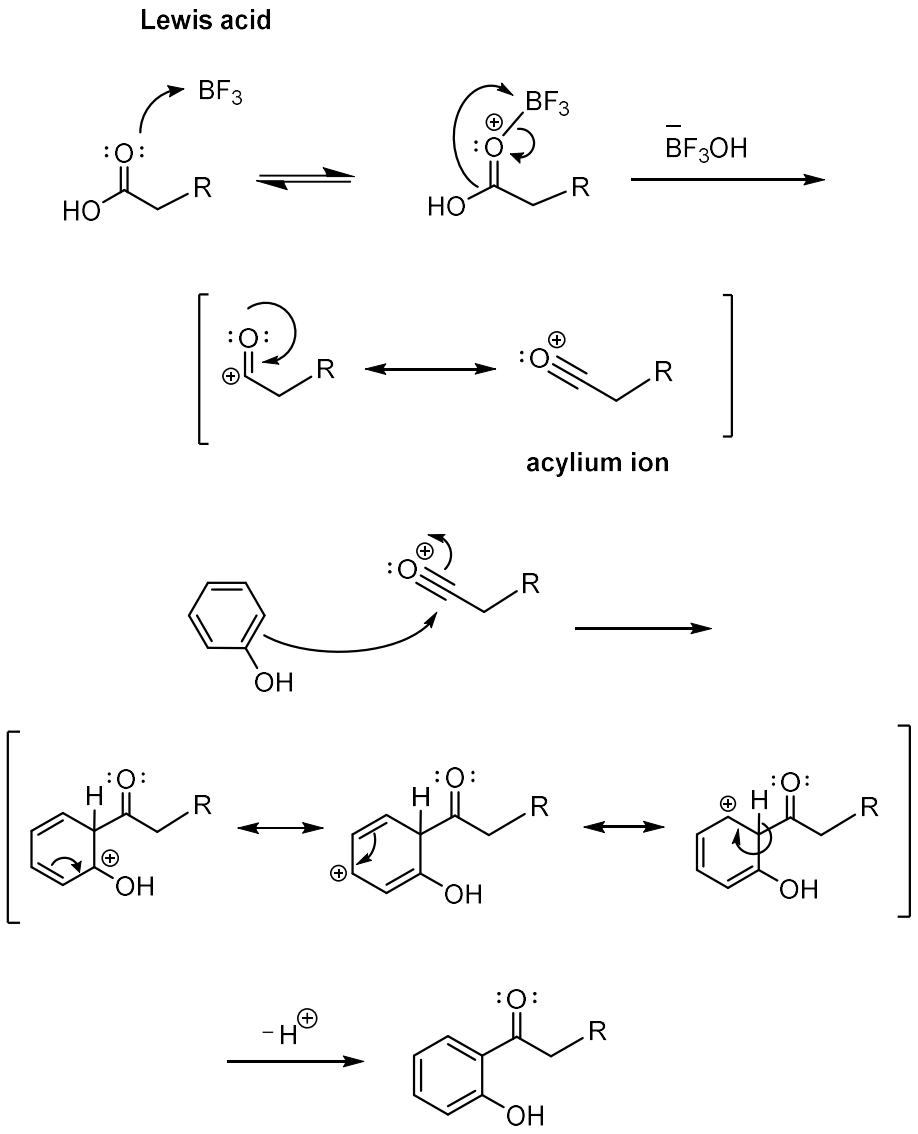

Scheme 4. Mechanism of Friedel-Crafts acylation

In our case, the Lewis acid used was $BF_3 \cdot OEt_2$ and a large equivalent was used because of the multiple hydroxyl groups present in the starting material resorcinol.[21] After work-up and flash column chromatography, the product was obtained in 30% yield. While the yield is not particularly high, this compares well with Friedel-Craft acylations of similar substrates used in

the literature.[22] An addition, our main focus was to synthesise a range of structures rather than optimising the reaction yield.

The formation of ketone **10** was confirmed by NMR analysis. In the ^{1}H NMR spectrum, the proton signal for 2-H appeared as a singlet at 3.95 ppm and there are six aromatic signals in the region 6.15 to 7.70 ppm which confirms the presence the two tri-substituted aromatic rings. (see Scheme 3).

2.1.3 Kostanecki reaction for the synthesis of isoflavanoid 12

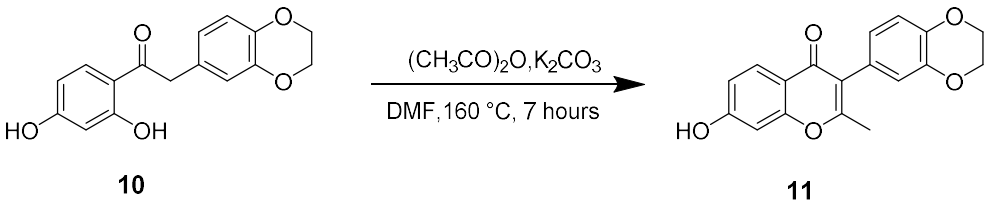

10 11

Scheme 5. Synthesis of isoflavanoid[17]

To prepare isoflavanoid **11**, ketone **10** was dissolved in acetic anhydride and potassium carbonate in a reaction called the Kostanecki acylation that was first reported by Nagai and Tahara in 1892.[23] This is a crucial step in the synthesis because this method can be used to form the isoflavone core structure. Initially, this reaction was carried out overnight, but this resulted in the formation of a complex mixture and the desired product was not obtained. The reaction was repeated with carefully monitoring by TLC for the disappearance of the starting materials, which established that the reaction was finished in 7 hours.

If aliphatic anhydrides are used in the Kostanecki acylation, two possible products can be formed. Two different mechanisms are possible to form either chromones or coumarins.[24] On the other hand, if an aromatic anhydride is used in the reaction then we only observe the formation of isoflavones and not coumarins. This version of the Kostanecki acylation involving aryl anhydrides is called the Allan-Robinson reaction and was first reported in 1924.[25-26] It can be said that the Allan-Robinson reaction is an extension of the Kostanecki acylation and it is an important reaction for the preparation of chromones. The two different mechanisms leading to the formation of either chromones or coumarins is shown below is Scheme 6 and 7.

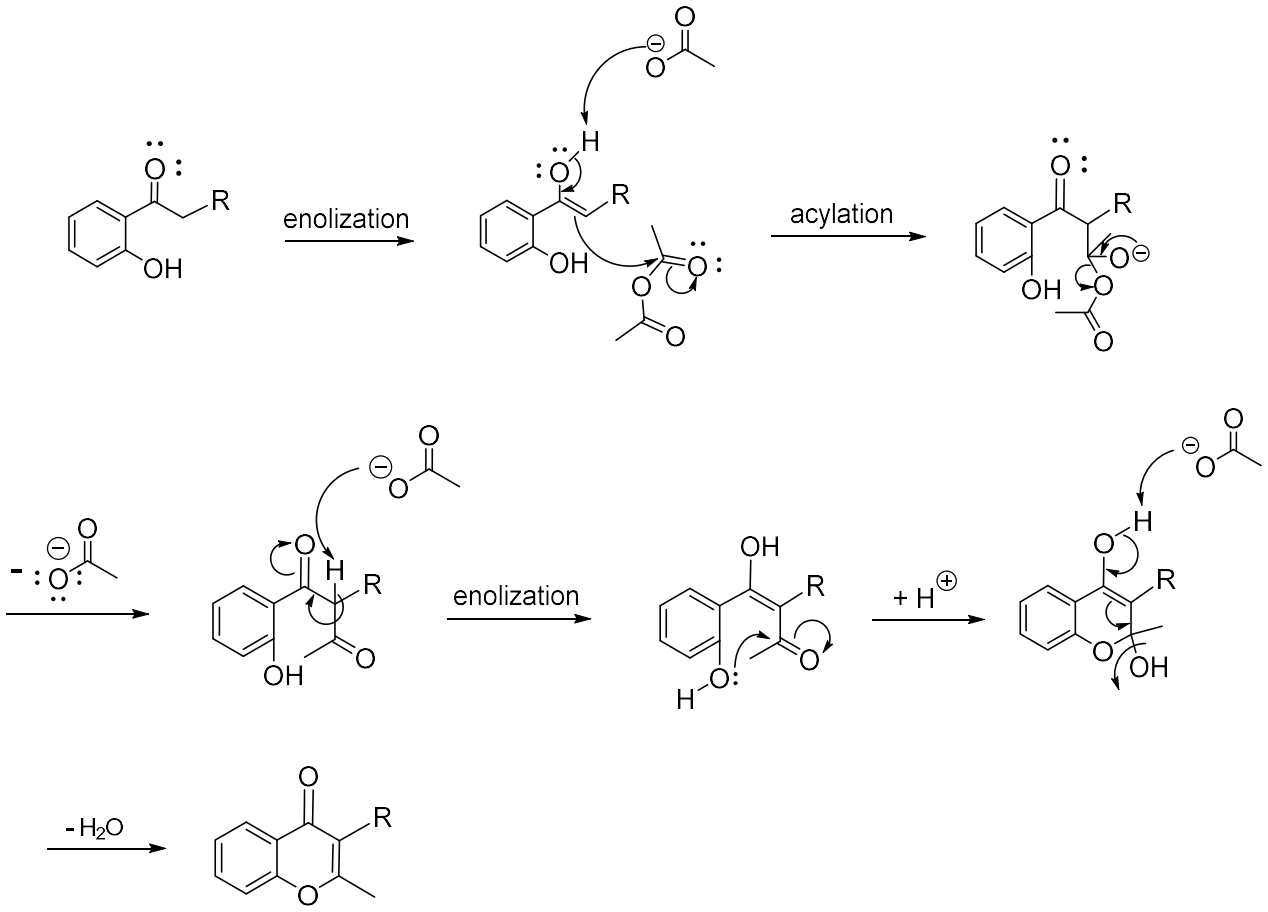

Scheme 6. Mechanism A: Formation of chromones

During this reaction, the ketone group of the molecule is first converted to the enol form by tautomerisation. The enolate next attacks acetic anhydride, which loses an acetate group resulting in the formation of a 1,3 diketone. Another tautomerization then forms an enol acetate. An intramolecular cyclization and loss of water then forms the isoflavone structure. This is the main product that is formed with our starting material ketone **10**.

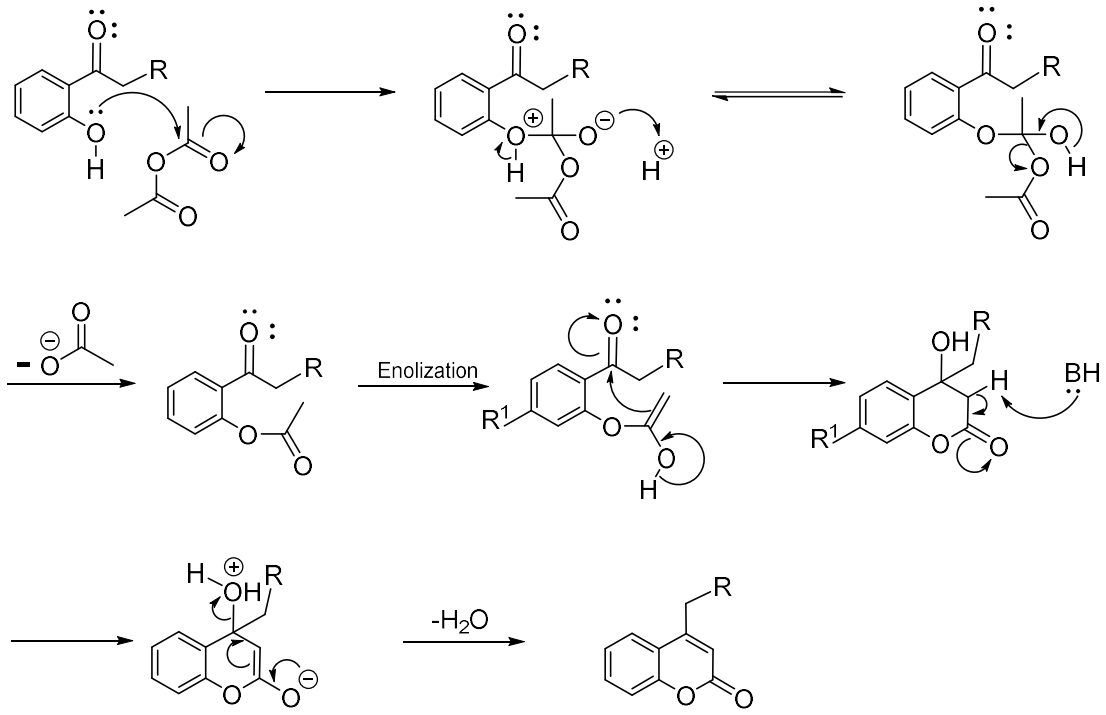

Scheme 7. Mechanism B – formation of coumarins:

The mechanism for the formation of coumarins begins by attack of the phenolic oxygen atom on the carbonyl carbon of the aliphatic anhydride. This initially forms a tetrahedral intermediate which collapses to form an ester. The ester next undergoes enolization and an intramolecular aldol condensation occurs to affect ring closure and formation of a hydroxydihydrochromone. Finally, loss of water by an E1cB mechanism forms the coumarin ring.

In our particular reaction, our major product was the chromone rather than the coumarin. This is likely due to the presence of an aromatic ring as the R group – which would stabilise the formation of the initial enolate as shown in Scheme 6. This enolate should form much easier than the enolate that needs to be formed in Scheme 7 and would drive the reaction towards the formation of the chromone.

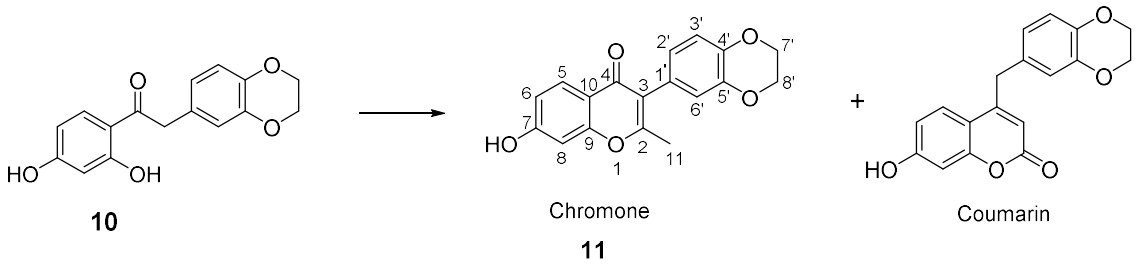

Scheme 8. Formation of chromones and coumarins

In the Kostanecki acylation, other substituents on the ring, for example: alkyl, alkoxyl, halogen, acyl, nitro and cyano groups remains intact in their original form as they are not affected during the reaction. However, hydroxyl groups have the possibility to be acylated due to the presence of acetic anhydride. The yield of this reaction was always very low, often 10 to 20% and the purification was always very difficult due to the presence of a mixture of products. We believe this was due to the formation of the coumarin a side product and also a mixture of acetylated products.[23, 26]

The ^{1}H NMR spectrum of **11** showed a new peak at 2.19 ppm for 11-H which confirmed the addition of the methyl group in the molecule. This crude material was taken directly to the next step.

2.1.4 The Aza-Michael reaction – treatment with hydrazine for the synthesis of pyrazole 13

In the last step of synthesis, hydrazine hydrate is used to react with flavone **11** to form the desired pyrazole after a series of rearrangements. This reaction was firstly monitored by TLC and the reaction stopped after the disappearance of the starting material (6 hours); but after work-up, the peaks of the product were not found in an ^{1}H NMR of the crude material. The reaction was then repeated, and this time allowed to stir at 60 °C overnight. The formation of the desired product was this time confirmed by crude NMR. The purification of the final compound was difficult due to the presence of products with very similar R_f values. Eventually, pure compound was obtained by an initial flash column followed by preparative TLC to remove close-moving impurities.

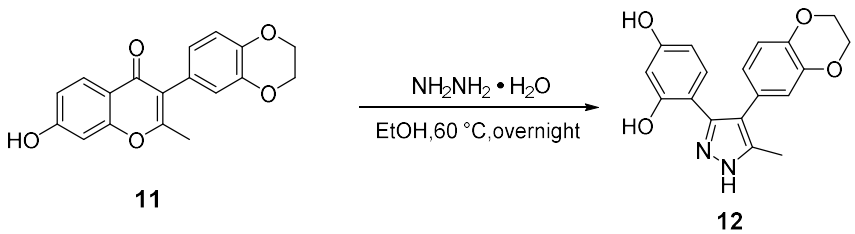

Scheme 9. Synthesis of pyrazoles

The mechanism of the reaction involves an initial aza-Michael addition with hydrazine. The aza-Michael addition reaction was first discovered by Heintz, Sokoloff and Latschinoff in 1874. In this reaction, nitrogen containing nucleophiles act as Michael donors and add to a molecule having a C=C double bond conjugated with an electron withdrawing group (Michael acceptor). This reaction allows the formation of *β*-amino carbonyl derivatives which is useful in the preparation of a large number of antibiotics, bioactive natural products and chiral auxiliaries.[27] The mechanism of this reaction is shown in Scheme 10.

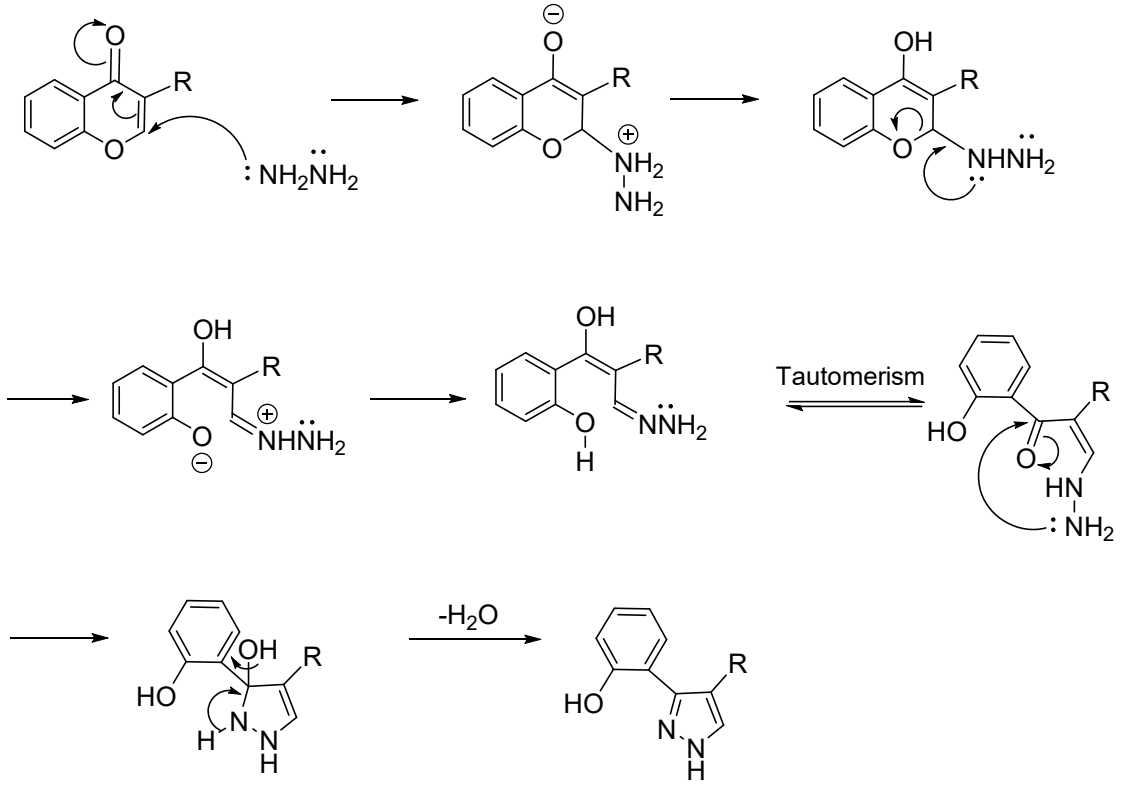

Scheme 10. Mechanism of Aza Michael addition

Firstly, hydrazine attacks the *β*-position of the arylchromone which induces the opening of the bicyclic ring system and liberation of the phenol (Scheme 10). Tautomerisation then reforms the ketone and cyclisation of the alkylhydrazine onto the ketone forms the pyrazole ring following the elimination of water.

Formation of the desired product was confirmed by a combination of NMR, IR and mass analysis. The ^{1}H and ^{13}C NMR were assigned with the help of HSQC and HMBC experiments

(see Figures 19 and 20). The peaks for C-3 and C-5 were initially not found in the ^{13}C NMR but C-3 was able to be identified at 138 ppm with help of the HMBC spectrum. C-5 was not able to be found but all other data, including high resolution mass spectrometry confirmed the successful synthesis of the pyrazole. It is clear from IR data that the important peaks of the molecule are present in the spectra. The peak for N-H stretching is present at 3203 and two peaks for free hydroxyl groups are present at 3819 and 3501. The yield of this molecule over three steps was 7%.

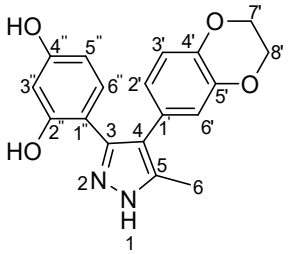

12

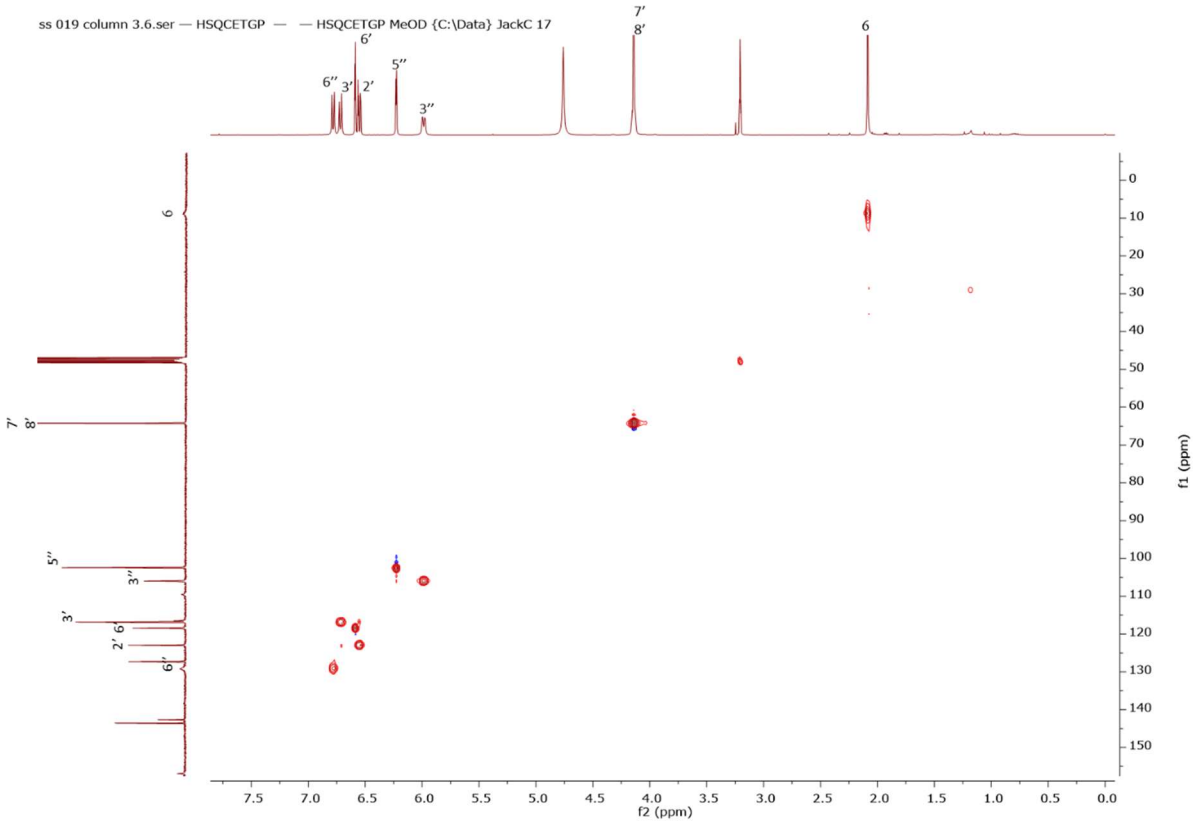

Figure 19. HSQC spectrum of pyrazole **12,** MeOD.

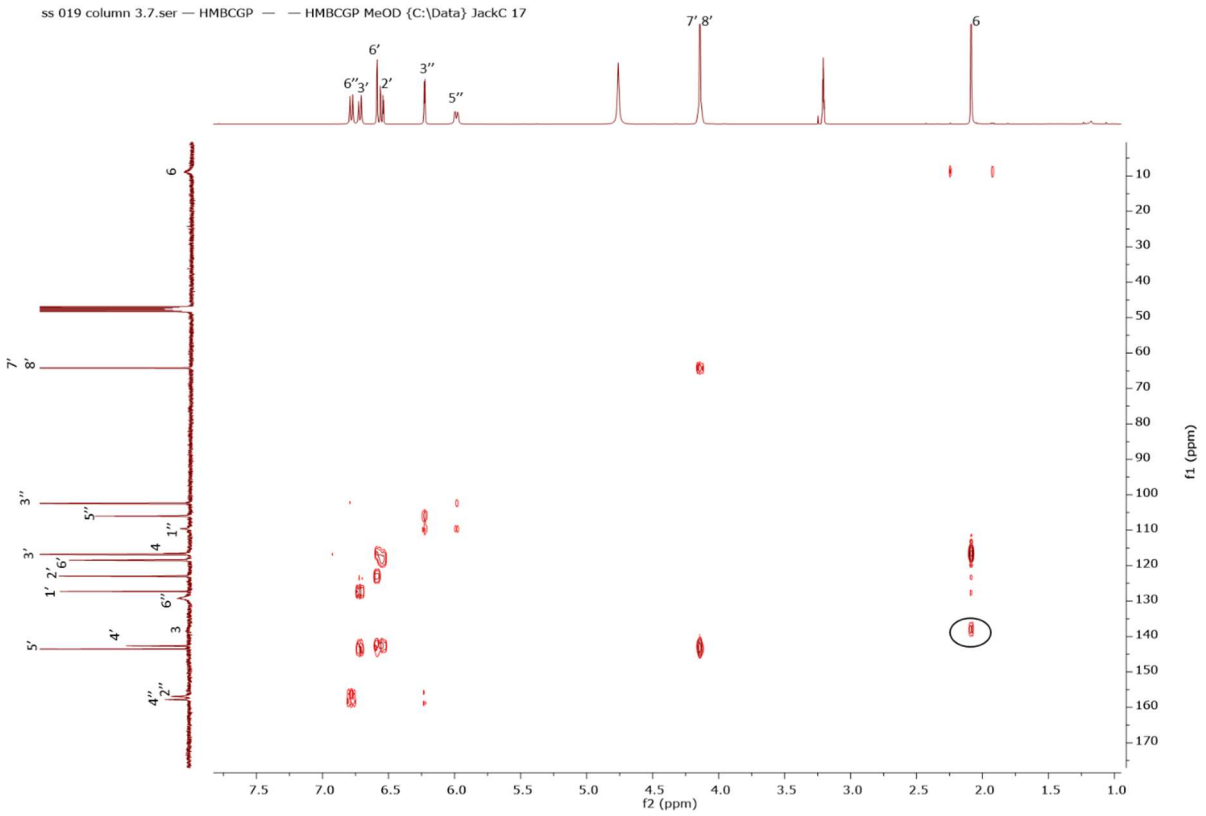

Figure 20. HMBC spectrum of pyrazole **12**, MeOD.

By successfully synthesising pyrazole **12**, which was one of the binders found in the second protein-based screening assay (compound 2.01, see figure 16), we were able to demonstrate that our chosen method is viable for the synthesis of diarylpyrazoles. This is a synthesis that should be readily modifiable for the synthesis of structural analogues. Our next goal was to synthesise pyrazole **1** (compound 2.11 in the 2nd screen, see figure 16), because this structure was the strongest binder found in the pyrazole series. This molecule is structurally more complicated to make as it contains an aromatic ring in which one of its two phenols is selectively methylated. This could be tricky to synthesise, but we decided that we would attempt the methylation at the end of the synthesis. Even if selective methylation could not be achieved, we will still be able to synthesise structural analogues that will be useful for SAR determination.

The synthesis of pyrazole **17** began with ethyl resorcinol **13** and phenylacetic acid **14**. Below is the scheme that was followed. After several attempts at performing this reaction, we found that performing a column after the first step, but not after the second step was able to improve

the yield. At the end, 23% yield over 3 steps were able to be achieved. We were able to confirm that the product was formed by comparing to the proton and carbon NMR to literature data.[17]

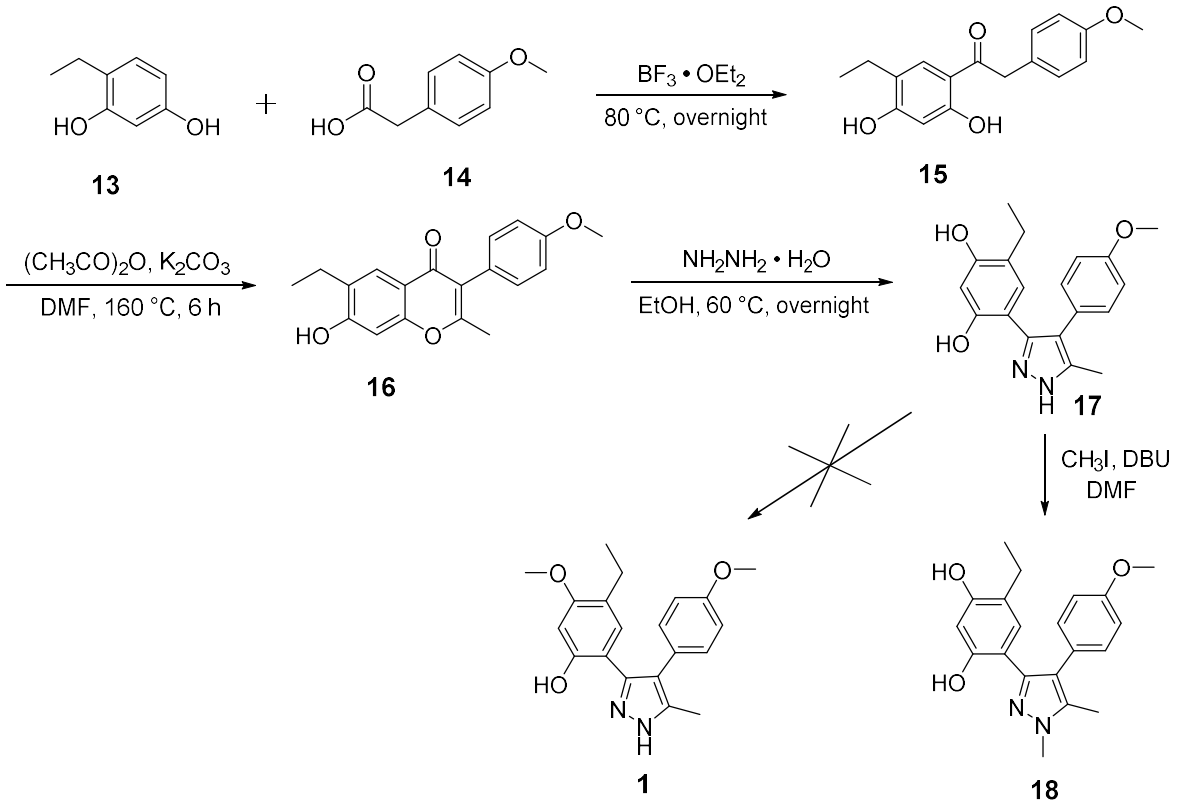

Scheme 11. Procedure for synthesis of pyrazole **17** and **18**

2.1.5 Selective methylation of the phenol

After successful synthesis of pyrazole **17**, we investigated methods for the conversion of pyrazole **17** to the previously tested compound pyrazole **1** (compound 2.11 in the initial screens). This required a selective methylation of one of the phenol groups. We began by testing a simple methylation procedure that used a bulky base, which we believed may deprotonate preferentially the hydroxyl group on the benzene ring which was *ortho* relative to the pyrazole. Thus we treated pyrazole **17** with the bulky base 8-diazabicyclo[5.4.0]undec-7-ene (DBU) and used methyl iodide as the methylating agent. The introduction of one methyl group onto the molecule was confirmed by ^{1}H NMR as there was one new peak was found at 3.85 ppm. However, the position of the methylation was impossible to determine using just ^{1}H NMR and ^{13}C NMR. Fortunately, on closer examination of the HMBC spectrum, which gave ^{1}H-^{13}C ^{2}J and ^{3}J heteronuclear correlations, we were able to determine that methylation actually

occurred on the pyrazole nitrogen instead of the hydroxyl group. We were able to make this conclusion because we observed a correlation between the C1 methyl protons and the carbon at C5 (Figure 21).

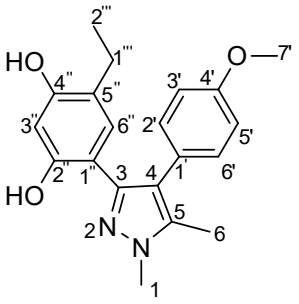

18

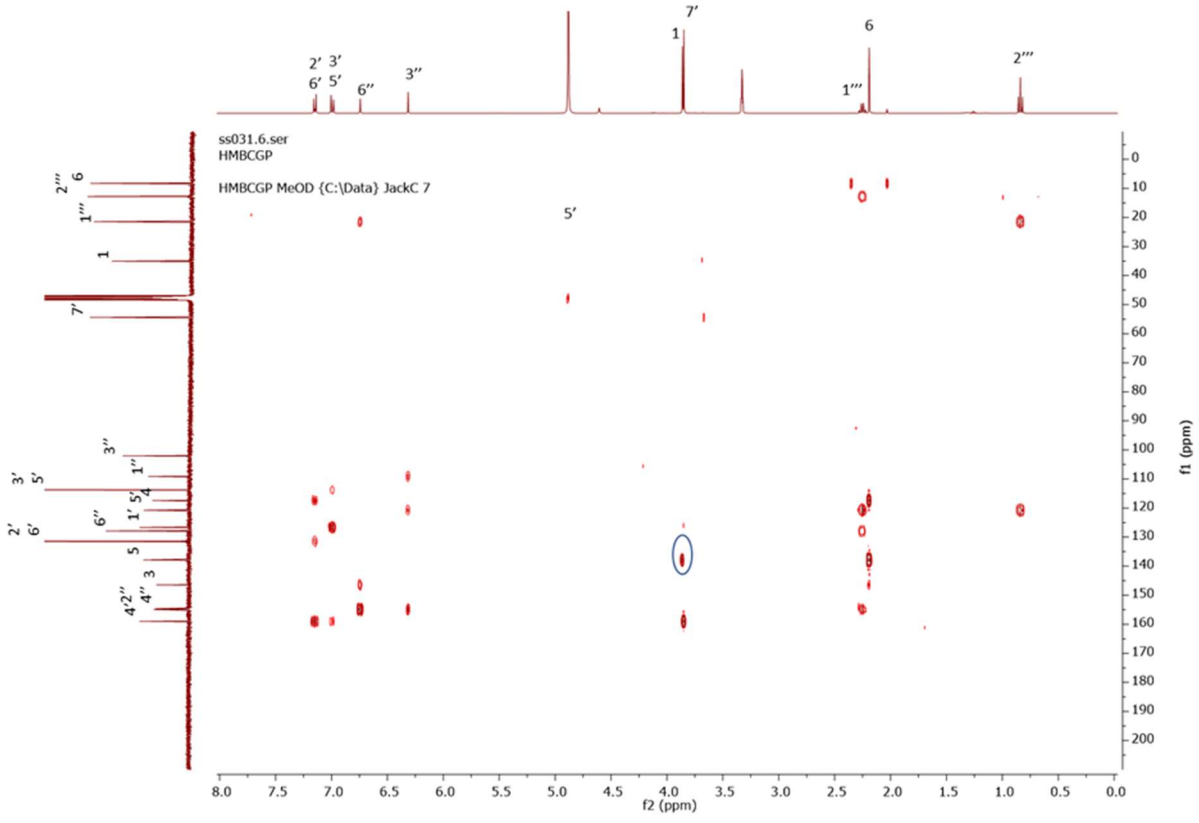

Figure 21. HMBC spectrum of pyrazole **18**, MeOD.

While this was not our intended product, this molecule was also an important analogue and could be used to determine the importance of the NH of pyrazole on the inhibitory action of the molecule. By comparing the result of MIC assay for these molecules, it will be clear

whether the binding interaction changes in the absence of the pyrazole NH, which will give us useful SAR information.

In the next attempt to convert the hydroxyl group of the resorcinol ring into a methoxy group, we tried to perform methylation of the phenol one step before, at the isoflavone stage. In this molecule, only one hydroxyl group was free, as the other forms part of the structural core of the isoflavone (Scheme 12).

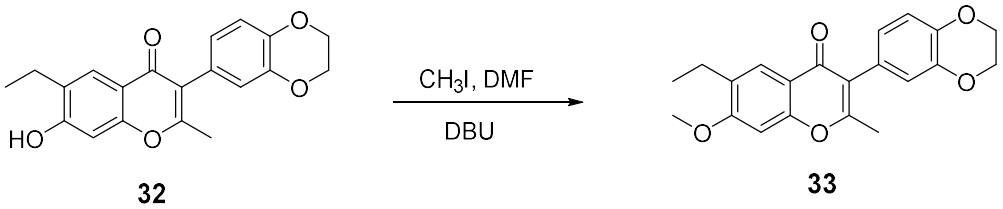

Scheme 12. Methylation of isoflavones

Under these conditions, the hydroxyl group was successfully converted into the methoxy group. The formation of product was confirmed by analysing ^{1}H NMR. However, we did not continue on with the synthesis of the final compound at this stage as we did not have enough material to continue (we needed around 20 mg for MIC studies), and also at this stage, biological results were suggesting us to pursue different analogues (see below for further discussion).

2.1.6 Synthesis of pyrazoles with increased water solubility

Attempts at protein-binding studies indicated low water solubilities with both compounds **12** and **17**. This suggested that there would be difficulties preparing samples for the measurement of minimum inhibitory concentrations (MIC's). As water solubility would be of great importance if these compounds were to be used as antibiotics, we decided to design a series of compounds that would be more water soluble. At the same time, we wanted to systematically change the substitution pattern around the ring so that we could obtain some initial SAR information. The compounds that we decided to synthesise are shown in Scheme 13.

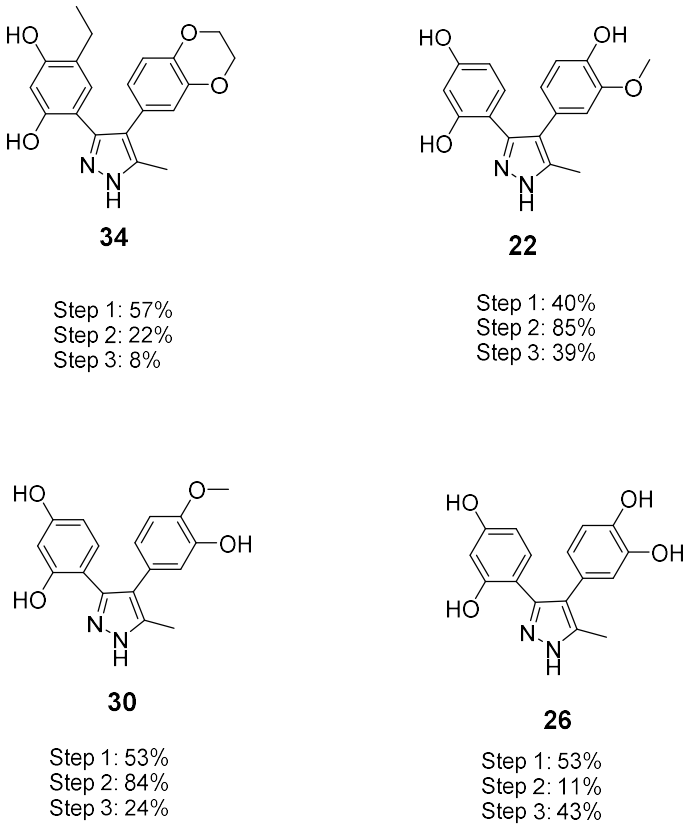

Scheme 13. Compounds with increased water solubility

One of these compounds (**34**) retained the ethyl substituent on the phenol ring but included two hydroxyl groups on the phenylacetic acid to increase the water solubility of the final molecule. Three other analogues (**22, 26** and **30**) had the ethyl substituent removed, which would test the importance of the ethyl group in binding. Two analogues were made with different methylation patterns on the hydroxyl groups that were on the ring derived from the phenylacetic acid.

Using the methodology previously outlined, we were able to synthesise pyrazole **34** in 1% overall yield over 3 steps. The other pyrazoles, **22**, **30** and **26** were synthesised in 13, 10 and 2% yields respectively.

2.1.7 Solving the problem of over-acetylation

As mentioned earlier, the conversion of ketone **10** to isoflavone **11** was often problematic due to the presence of several products that made purification very difficult. These problems became worse with these current analogues which have more hydroxyl groups present in the molecule. At this point, we assumed that the main impurities were due to poly-acetylation of the hydroxyl groups.

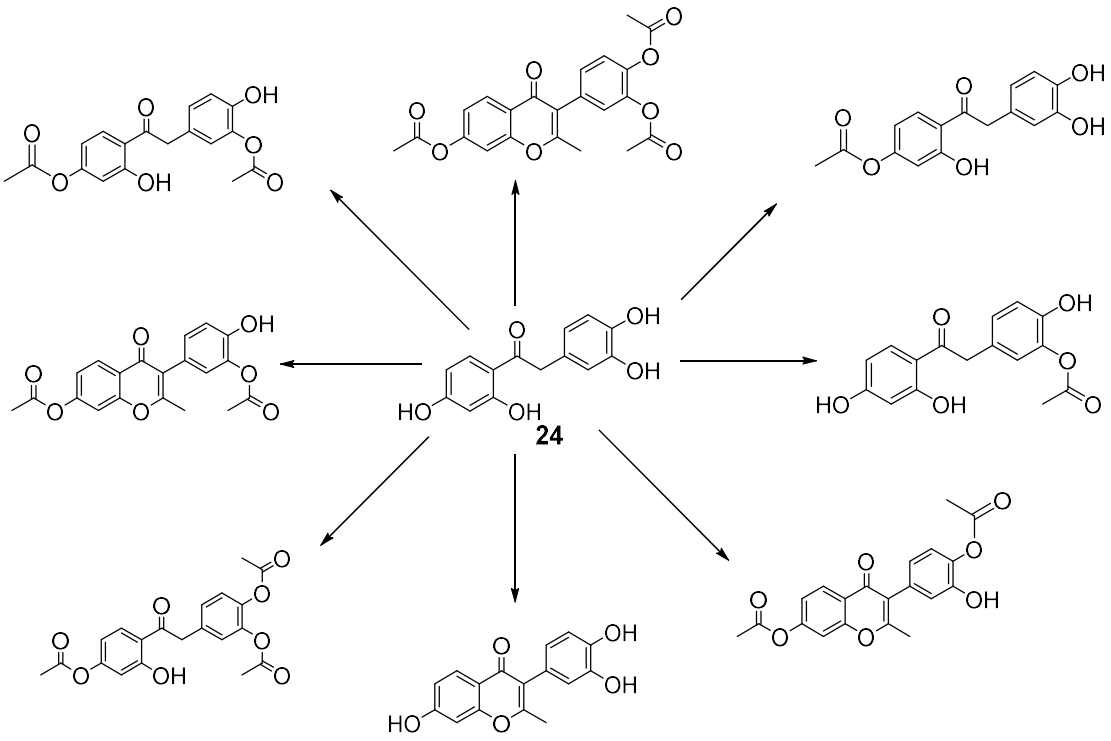

Scheme 14. Formation of mixture products during Kostanecki reaction

We thought that one way to solve this problem would be to introduce a subsequent step to remove the acetate groups from the hydroxyl groups. To this effect, we stirred the crude product with 10% HCl solution in methanol and monitored any changes using TLC analysis. We were hoping that if the side products were due to over-acetylation, then transesterification would occur to liberate again the phenol groups (Scheme 15).

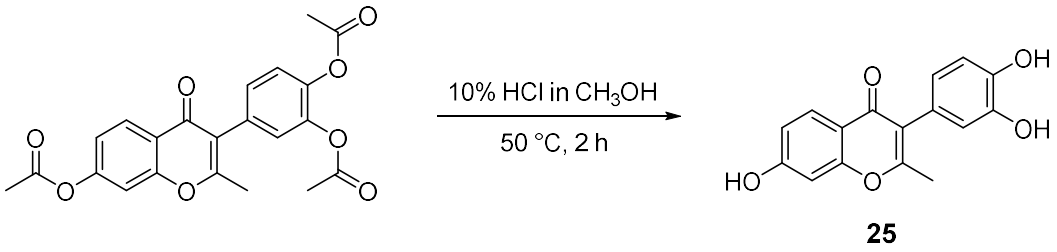

Scheme 15. Transesterification

Below is shown the mechanism of the transesterification reaction (Scheme 16). In the beginning of the reaction, the acetate group is protonated by acid (HCl) and the carbonyl is now activated for nucleophile attack. Methanol acts as a nucleophile and attacks the carbonyl carbon to form a tetrahedral intermediate. Proton transfer occurs between the oxygen of the original alcohol and oxygen atom of original ester. The protonated carboxyl oxygen of the original ester is then removed.

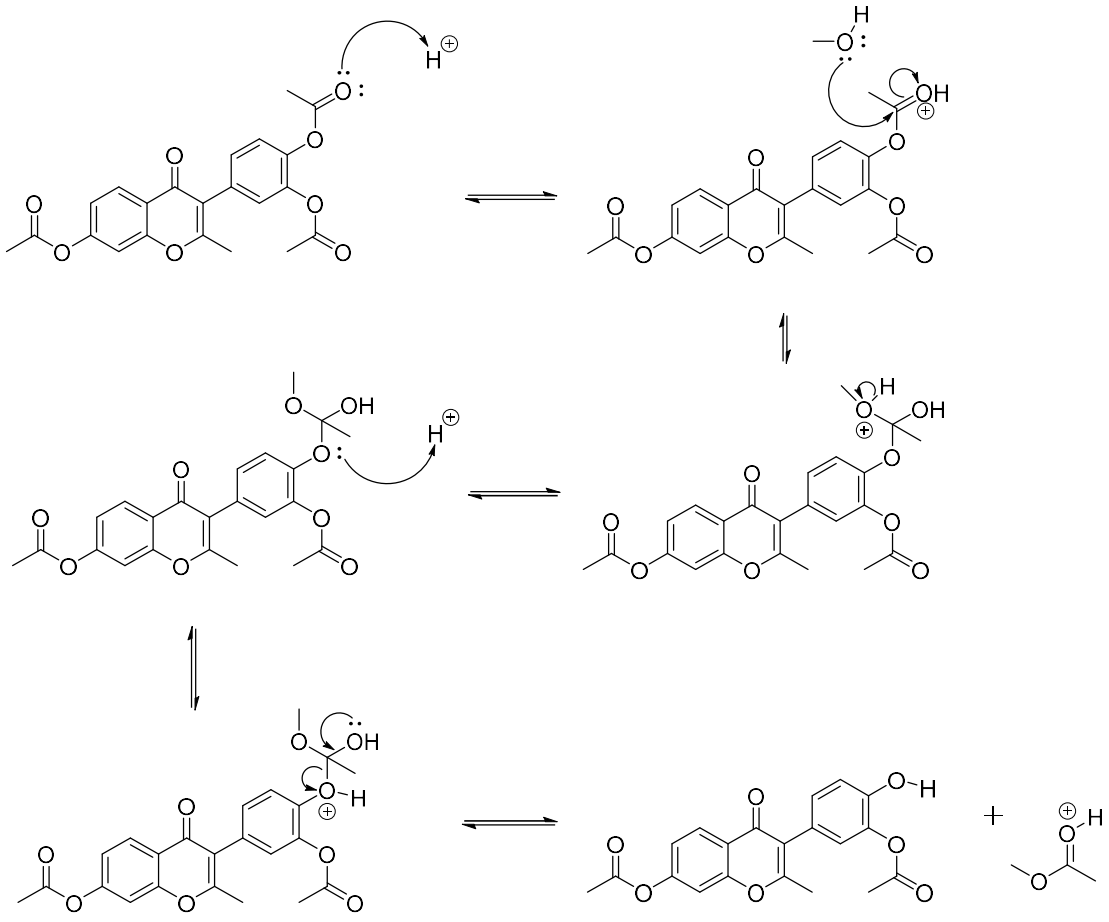

Scheme 16. Compounds with increased water solubility

To our delight, when we followed this transesterification reaction by TLC analysis, we observed a starting reaction mixture with several spots slowly merge into one main spot (Figure 22). NMR analysis confirmed that the main spot that is formed was indeed the desired isoflavone with free phenol groups

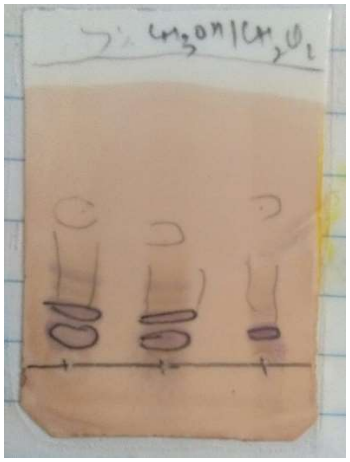

Figure 22. TLC of the transesterification reaction (on the left is the reaction mixture before transesterification, on the right is the reaction mixture at completion of transesterification and the centre is the mixed spot)

2.2 Synthesis of disubstituted pyrazoles

2.2.1 One-pot Synthesis

After preparing a series of analogues of substituted diaryl pyrazoles (with and without the ethyl group, and with different methylation patterns on the phenols) we decided to make a pyrazole analogue without the methyl substitution in order to determine the importance of the methyl group on the inhibition of MCR-1. We initially focused on a one-pot synthesis first described by Drysdale in 1973 for the preparation of chromones.[18] The general scheme for this one-pot synthesis is shown below (Scheme 17).

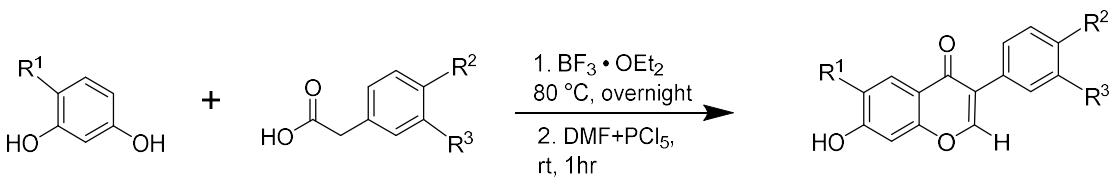

Scheme 17. One-pot synthesis of isoflavones

This reaction sequence is similar to the procedures that we have used so far. The key difference is the use of the Vilsmeier reagent instead of acetic anhydride to add the C-5 of the pyrazole ring. The Vilsmeier reagent was prepared by a reaction between dimethylformamide (DMF) and PCl_5.[28] This involves the initial nucleophilic attack of DMF via the carbonyl with the highly electrophilic PCl_5 (Scheme 18). Attack by chloride on the resulting iminium cation and expulsion of phosphorus oxychloride gives the chloroiminium cation known as the Vilsmeier reagent.[18]

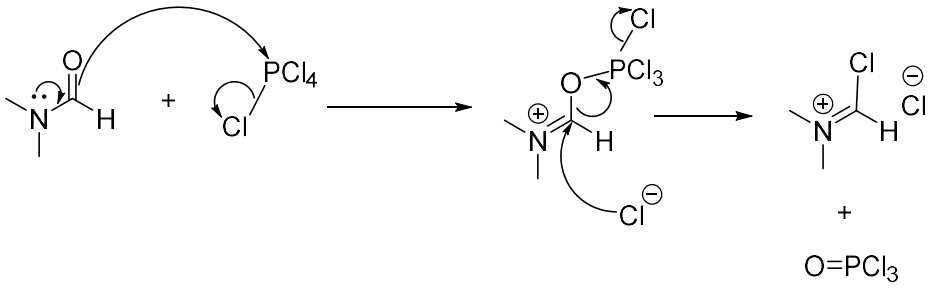

Scheme 18. Formation of Vilsmeier reagent

This freshly prepared Vilsmeier reagent then reacts with the ketone-BF_3OEt_2 complex formed from the Friedel-Crafts acylation (Scheme 19). In this mechanism, the Vilsmeier reagent is attacked by the enol form of the ketone[29] to form a new C-C bond. Following this, a neighbouring phenol is able to make a second attack on the iminium cation, allowing the formation of the third ring. Finally, treatment with acid triggers deamination and formation of the isoflavone product.

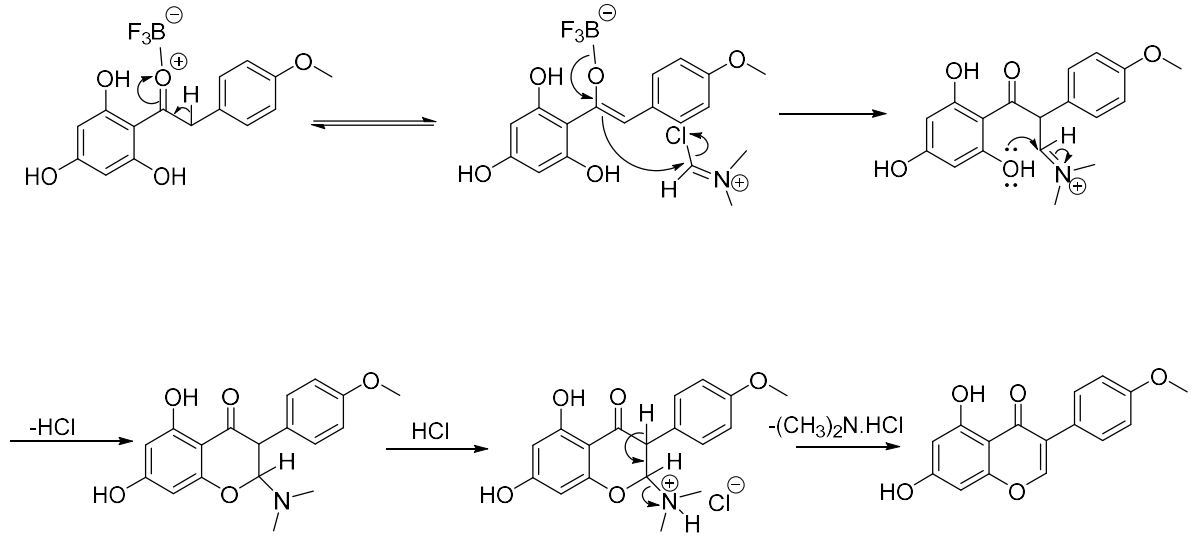

Scheme 19. Mechanism of One-pot synthesis

As we had already introduced hydroxyl groups on the phenyl acetic acid ring to increase the water solubility of inhibitors, we decided to make analogues also with extra hydroxyl groups on the phenol ring (Scheme 20). We thus decided to test out this sequence using phloroglucinol **26** and phenyl acetic acid **15**. The first and last steps of this procedure were the same as the previously adopted procedure, with the only difference being the second step.

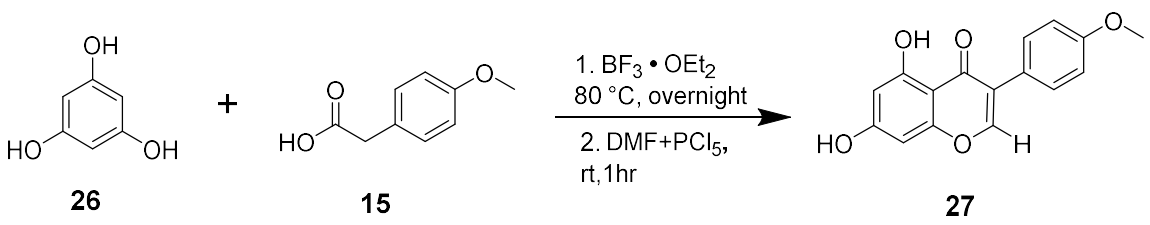

Scheme 20. One-pot synthesis using DMF and PCl_5

Phloroglucinol and phenyl acetic acid were treated with $BF_3 \cdot OEt_2$ and the Vilsmeier reagent, but in our hands, the desired product could not be found. We thought that a possible reason behind this could be the unsuccessful synthesis of the Vilsmeier reagent by PCl_5 and DMF. At this point, we decided to try using a commercially available equivalent, namely dimethyl formamide dimethyl acetate (DMF-DMA) instead of the Vilsmeier reagent.

Scheme 21. One-pot synthesis using DMF-DMA

However, using DMF-DMA still did not allow synthesis of the desired product. At this point, we realised that the phloroglucinol that we had was actually in the form of phloroglucinol hydrate and that the water of hydration present was likely interfering with the of $BF_3 \cdot OEt_2$ in the Friedel-Crafts acylation. Besides this, it was clear from TLC analysis that during this reaction, a mixture of products was formed which would be difficult to separate. We therefore tried another procedure to form this analogue in which the presence of water should not interfere. This reaction sequence involves instead the formation of an ester followed by a Fries rearrangement to form the required ketone (Schemes 22 and 23).

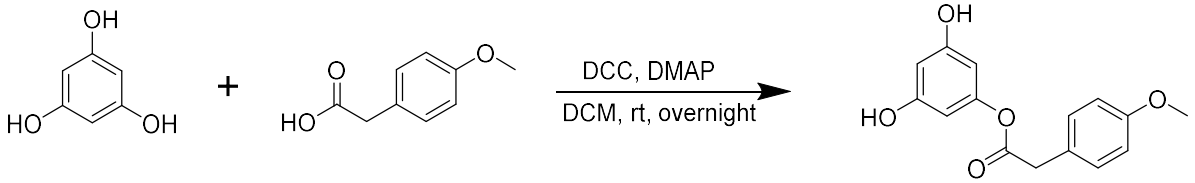

Scheme 22. Steghlich Esterification

(A) Ester formation and Fries rearrangement

To prepare the required ester, phloroglucinol was stirred with phenyl acetic acid in the presence of dicyclohexylcarbodiimide (DCC) and 4-dimethylaminopyridine (DMAP) overnight. After extraction with ethyl acetate and filtration, the crude material was treated with an excess of aluminium trichloride to induce the Fries rearrangement.

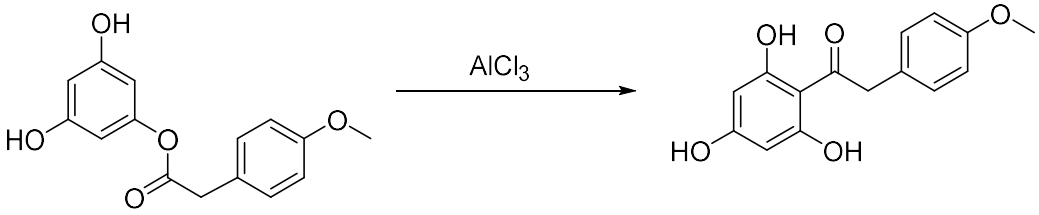

Scheme 23. Fries rearrangement

Steglich Esterification

This reaction is a modern method to synthesis esters from sterically hindered alcohols and carboxylic acids[30] by using a carbodiimide as coupling reagent and 4-dimethylaminopyridine (DMAP) as a catalyst. It was discovered by Wolfgang Steglich in 1978. It is mild reaction and occurs at room temperature.[31]

(B) Mechanism of DCC coupling for formation of esters

Initially, the acid molecule is activated by DCC to form an *O*-acylisourea intermediate on which DMAP attacks and a rearrangement of electrons occurs. As a result of this, a molecule of dicyclohexylurea (DHU) is lost and an acyl pyridinium intermediate is formed. Then, alcohol attacks this intermediate and after losing DMAP as leaving group and proton transfer, the ester is formed. In this reaction, DMAP acts as a nucleophilic catalyst and is used to supress the formation of unproductive acyl migration by-product.[32]

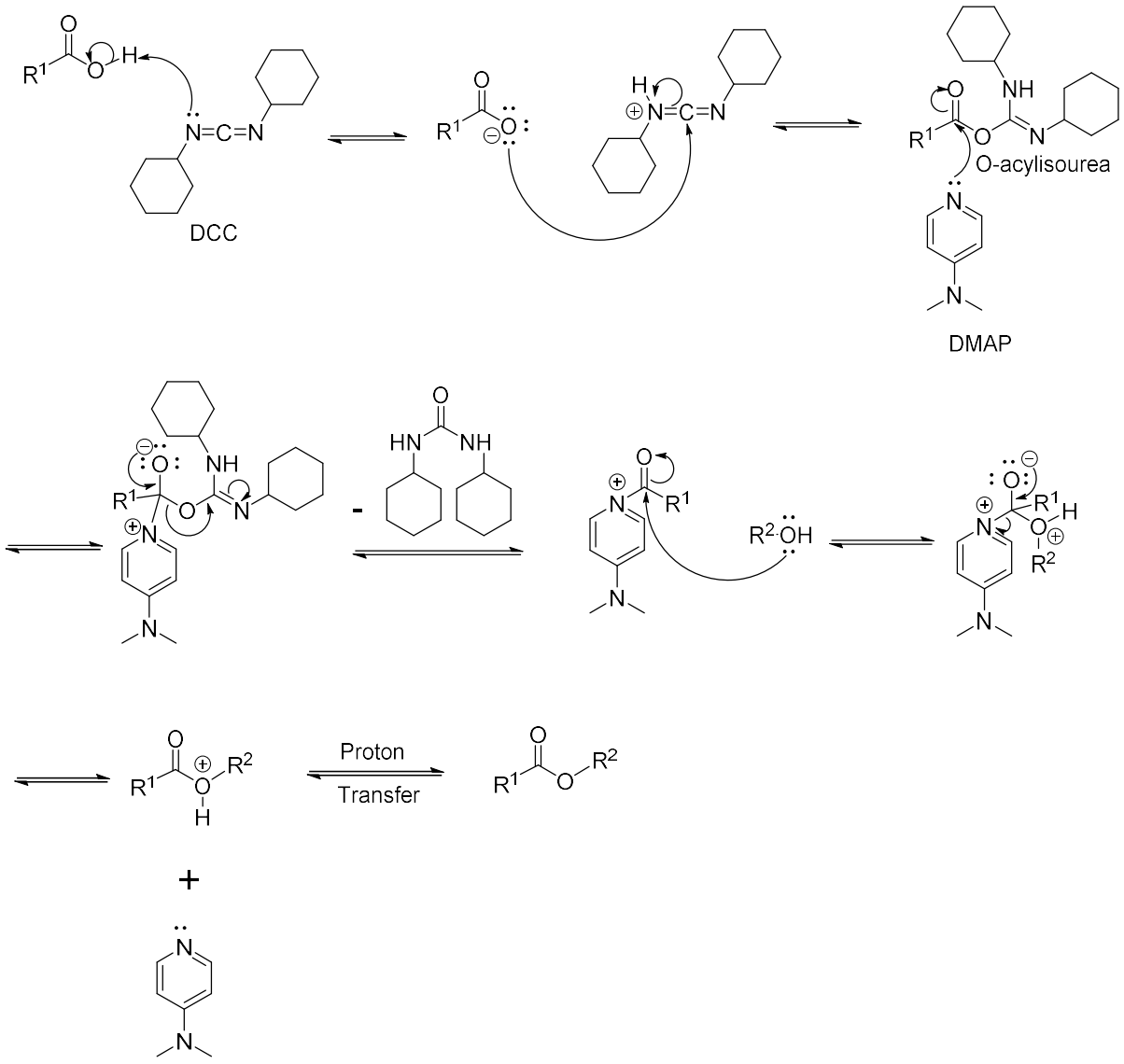

Scheme 24. Mechanism of the ester formation with DCC and DMAP

(C) Fries Rearrangement

The Fries rearrangement was first discovered by Fries in 1908 by using a Lewis acid as a catalyst to convert aryl esters into hydroxy carbonyl compounds. Both *ortho* and *para* products were formed in this reaction. The formation of products is highly depending on temperature, reaction medium and the choice of catalyst. Low temperatures favour the production of *para* products and high temperatures result in the formation of *ortho* products.[33] The mechanism of this reaction is still not obvious, it may be completely intermolecular or intramolecular or it may be partially inter- and intramolecular.[20, 33]

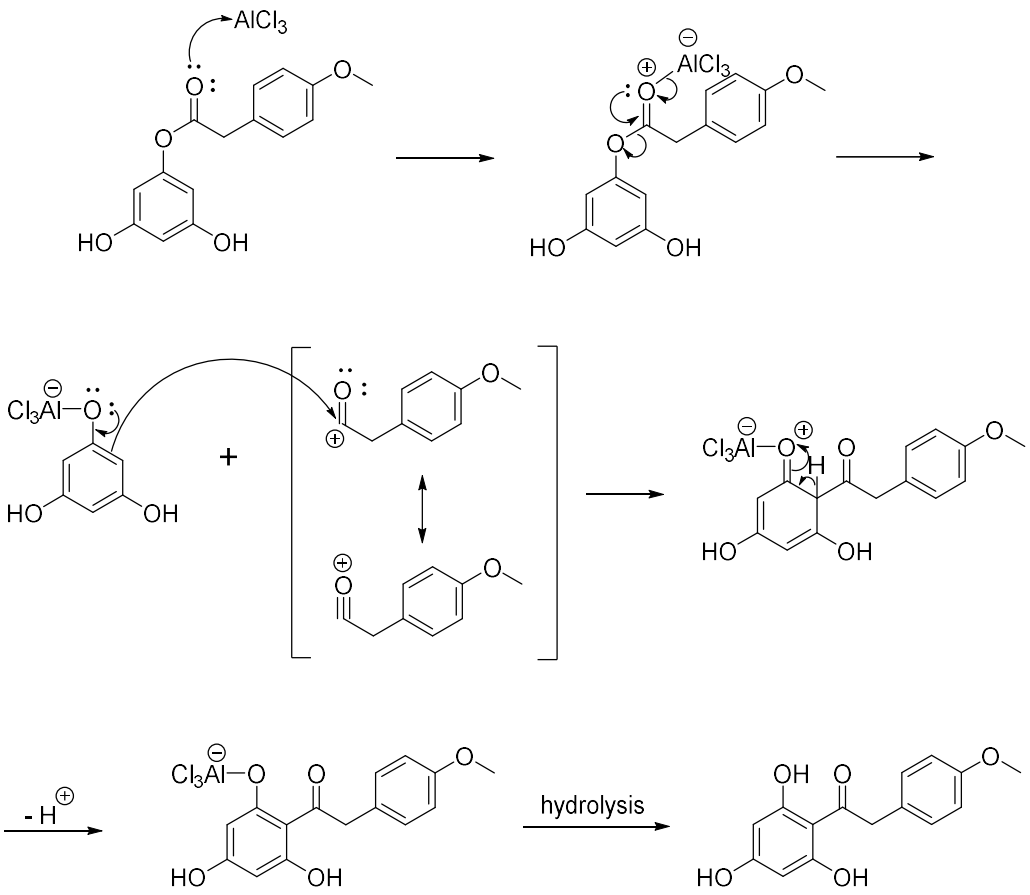

Scheme 25. Mechanism of the Fries rearrangement

In this rearrangement, the oxygen atom of carbonyl group is more electron rich compared to phenolic oxygen atom and behaves as the Lewis base. Therefore, it attacks the aluminium chloride which behaves as a Lewis acid in this reaction. Electrons move from the carbonyl oxygen to the phenolic oxygen, resulting in the formation of an acylium cation. The phenol then is able to attack the acylium ion via an electrophilic aromatic substitution, which forms the final product upon hydrolysis. However, in our hands after several attempts we were not able to obtain the desired product. It is possible that this is due to the presence of numerous hydroxyl groups in our starting materials which may interfere with the reaction. At this point, we decided to investigate the use of the Suzuki cross-coupling reaction to synthesise further analogues.

2.2.2 New analogues using Suzuki cross-coupling

After an examination of the literature, we found that 3,4-diarylpyrazoles (without substitution in the 5-position) have been previously synthesised using Suzuki cross-coupling methodology. This was an interesting route to explore due to the availability of boronic esters which could potentially allow access to a wide variety of structurally diverse analogues.

The retrosynthetic analysis of 3,4-diarylpyrazoles using a Suzuki disconnection is shown in Scheme 26. It shows that two couplings partners are needed: a 3-iodochromone **41** and an arylboronic acid **42**. The boronic acid is chosen over organometallic compounds because these acids shows stability towards air and inertness towards different functional groups.[34] Besides this, many boronic acid are commercially available.

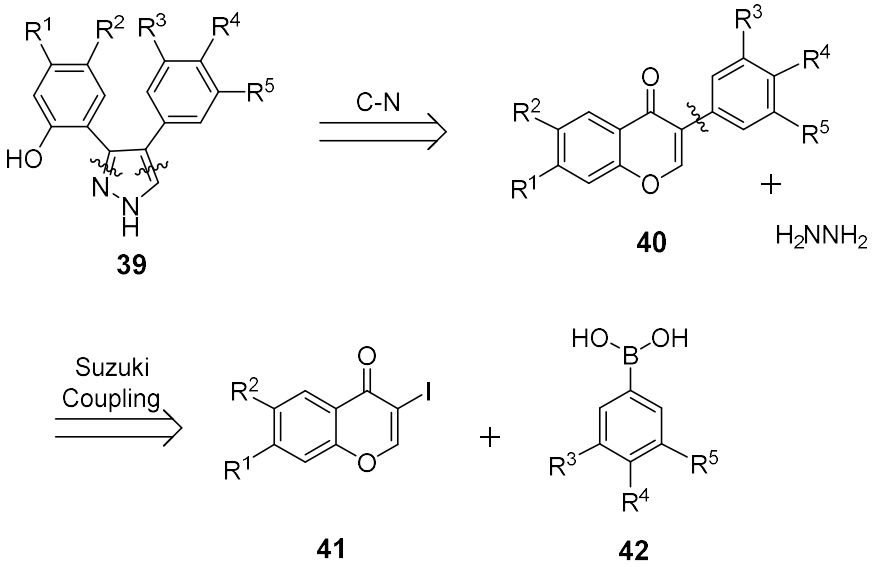

Scheme 26. Retrosynthesis using a Suzuki cross-coupling disconnection

The Suzuki cross-coupling was first published in 1979 by Akira Suzuki and Norio Miyaura.[35-36] It is also known as the Suzuki reaction and Suzuki-Miyaura coupling.[34] At the time, it was a novel approach to carbon-carbon bond formation involving the usage of boronic acids and a transition metal catalyst. The Suzuki reaction describes specifically the coupling of organic halides or triflates with organoboranes under basic conditions. This coupling is catalysed by palladium complexes.[37]

The mechanism of the Suzuki cross-coupling involves three steps: oxidative addition, transmetalation and reductive elimination, with the oxidative addition being the rate determining step.[35] During this step, phosphine complexes of Pd(0) undergo oxidative addition with vinyl or aryl iodides. A stable trans-palladium(II)complex forms during the oxidative addition of alkenyl, allyl, benzyl and aryl halides.[38-39] Aryl and alkenyl halides are activated by electron withdrawing groups.[37]

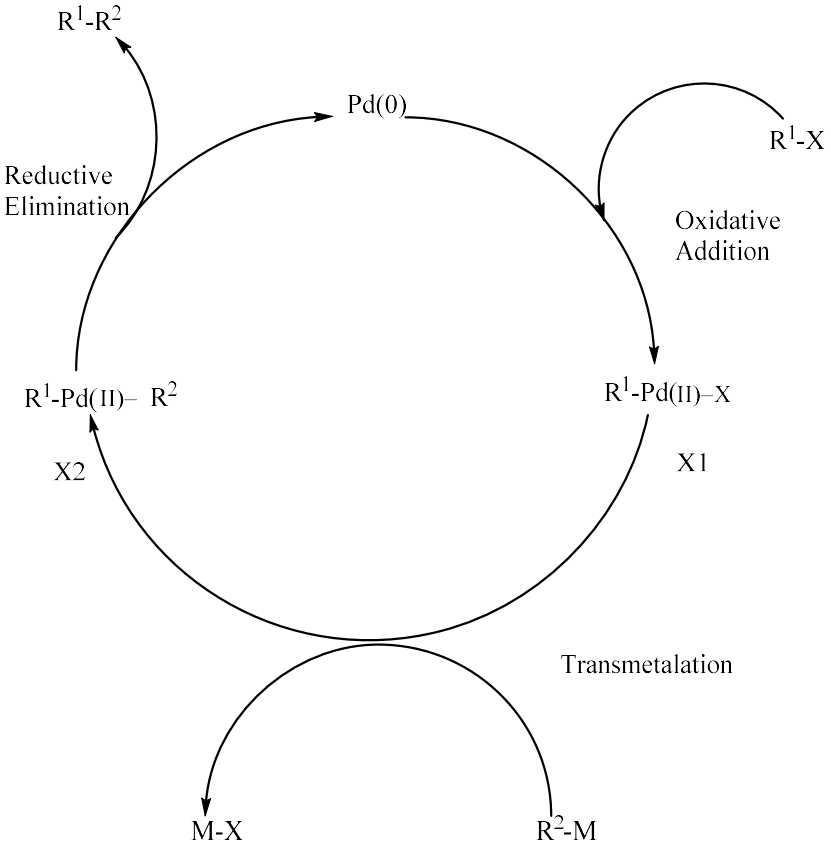

Scheme 27. Mechanism of Suzuki Coupling reaction

The second step is the transmetallation. This involves the transfer of a ligand from one metal to another metal. Two possible pathways have been suggested for the mechanism of the transmetalation in the Suzuki reaction. According to Path A, an organoboron compound reacts with a base and converts into a nucleophilic boronate. It is then able to attack the palladium(II) halide. On the other hand, Path B describes the formation of a nucleophilic palladium hydroxo complex which reacts with a neutral organoboron compound as shown in Scheme 28.[40]

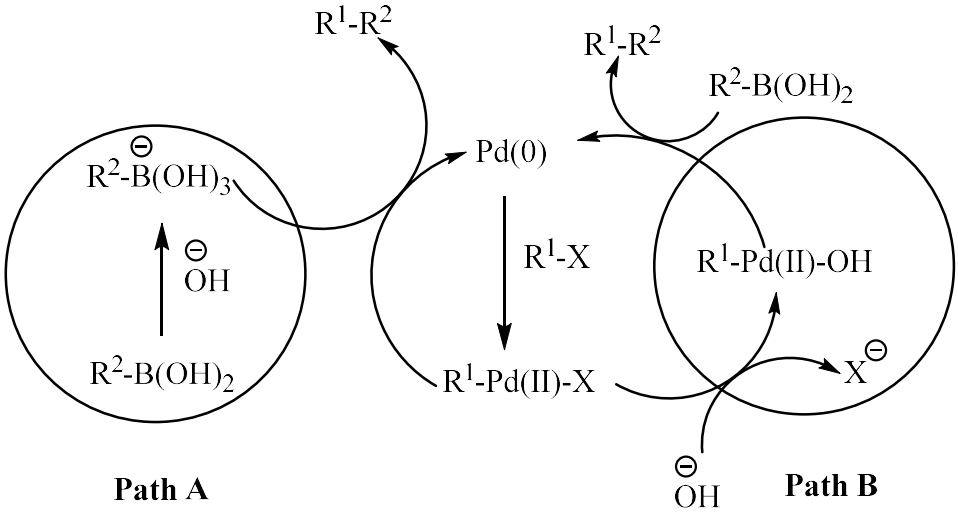

Scheme 28. Two possible pathways of transmetallation

The last step of the mechanism is reductive elimination, in which the oxidation state and coordination number of the palladium are reduced by two and bond making and bond breaking occurs simultaneously. The palladium (0) complex is regenerated by reductive elimination of organic groups from X2 shown in the catalytic cycle. The reaction occurs through a *cis*-X2 complex and *trans*-X2 must first isomerise into *cis*-X2 before reaction. After this reductive elimination, the palladium(0) regenerated to complete the catalytic cycle and is able to undergo oxidative addition again.[35, 38-39]

The general scheme for the preparation of 3,4-diarylpyrazoles by Suzuki coupling is shown in Scheme 29 below. The synthesis begins with the synthesis of the iodochromone, which is the key coupling partner for the Suzuki reaction.

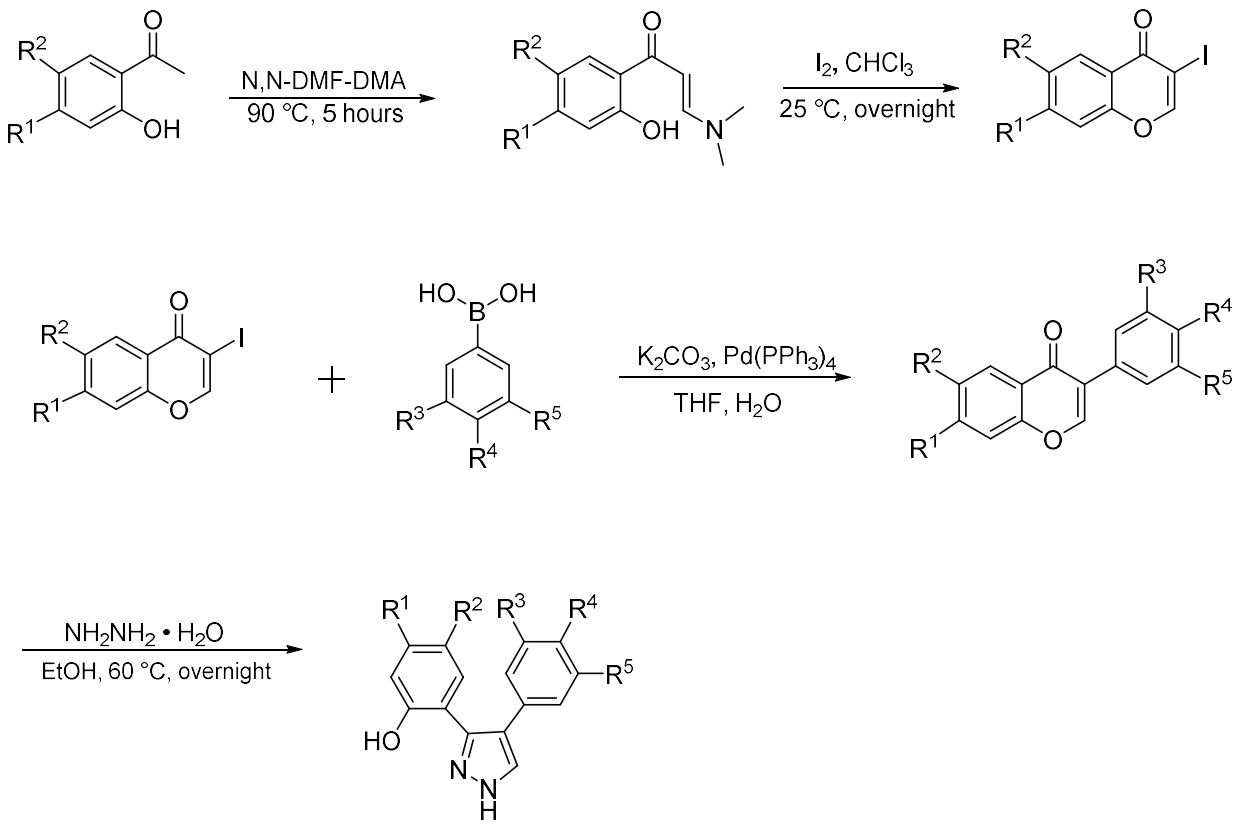

Scheme 29. An alternative synthesis using Suzuki cross-coupling

(A) Synthesis of the iodochromone

Synthesis of the required iodochromone required 2-hydroxyacetophenone starting materials. We began investigation this synthesis by using 2-hydroxy-5-methoxyacetophenone **43** (Scheme 30). It has been shown that condensation between 2-hydroxyacetophenones and dimethylformamide dimethylacetal (DMF-DMA) produces enamines that can be cyclized to directly 3-idochromones without purification using iodine in the presence of $CHCl_3$ or MeOH, a reaction reported by Gammil.[41] This reaction has also been called a modified Vilsmeier-Haack reaction.[29] In some cases it was reported to be more efficient to purify the crude enamines chromatographically prior to iodinative cyclisation. [41]

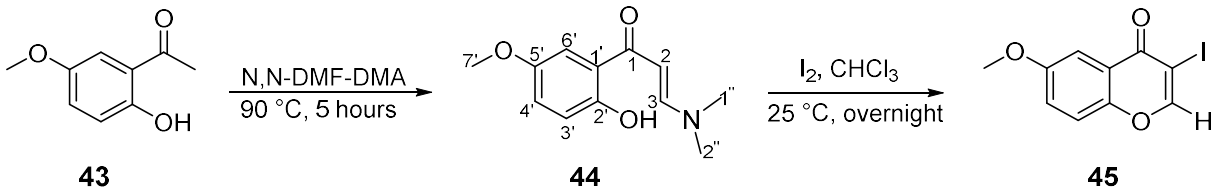

Scheme 30. Formation of iodochromones

During this reaction DMF-DMA is activated by loss of methoxide to an electrophilic iminium cation, similar to the Vilsmeier reagent (Scheme 31). The methoxide anion is able to act as a base to remove the α-hydrogen from 2-hydroxy acetophenone and converted it into an enolate which in turn attacks the activated molecule of DMF-DMA. This generates an enamine that is conjugated to the acetophenone. In the next step, iodine is added, and it acts as an electrophile. Reaction of the iodine with the enamine followed by an intramolecular Michael addition allows the formation of a six membered ring. Finally, loss of the dimethyl amine gives the final iodochromone product (Scheme 32).

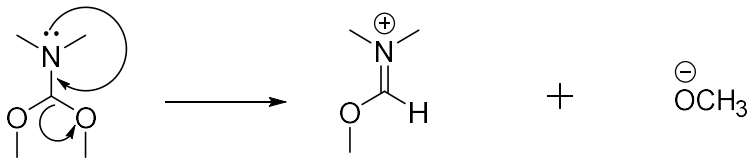

Scheme 31. Activation of DMF-DMA

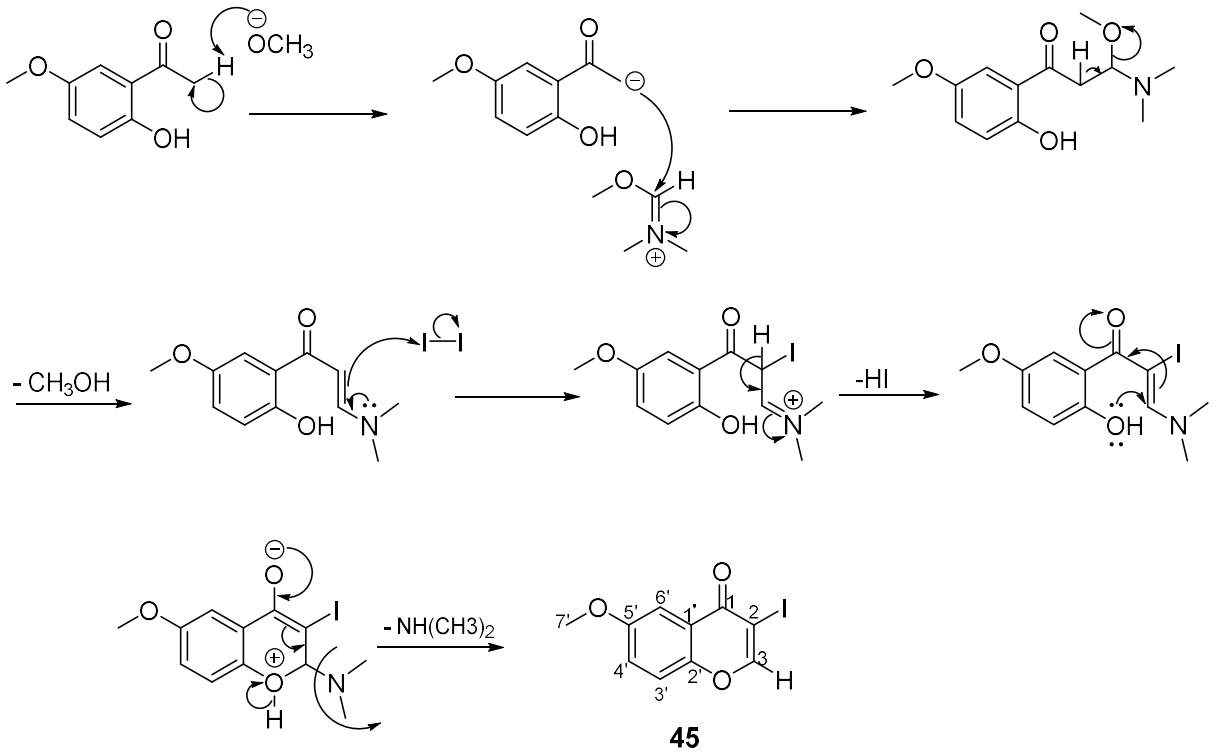

Scheme 32. Mechanism for the preparation of iodochromone

In the ^{1}H NMR spectrum of the enamine, the addition of two methyl groups resulted in two new peaks at 2.95 ppm and 3.19 ppm, indicating the successful conversion of acetophenone into an enamine. The peak at 7.88 ppm showed the presence of 3-H. (Scheme 30). In the case of iodochromone **45**, the preparation of desired product was confirmed by disappearance of two peaks of methyl groups as well as the peak for 2-H proton at 5.72 ppm, which were present in the ^{1}H NMR of the starting material. Moreover, the position of the 3-H proton shifted from 7.87 ppm to 8.20 ppm and appeared as a singlet instead of a doublet which confirmed the absence of any other hydrogen close to it and showed that the cyclisation occurred. (Scheme 32). Our first attempt at this reaction resulted in the formation of two products, with the formation of the non-iodinated chromone **46** as the major product (Scheme 33).

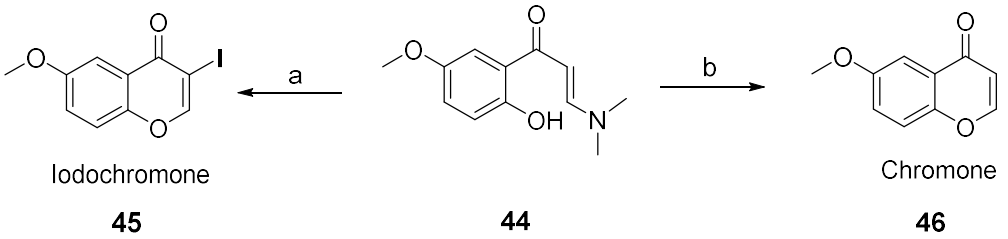

Scheme 33. Two possibilities for product formation

One possible mechanism for the formation of chromone **46**, is ring closure prior to iodination (Scheme 34). Initially, the mechanism is the same as explained above but the attack of lone pair of oxygen from the phenol occurs prior to the addition of iodine and results in the formation of chromone rather than the formation of iodochromone. However, the loss of iodine may also be due to a radical process which occurs after its formation. In fact, we believe that loss of iodine after the iodochromone is formed is likely the dominant mechanism and it can be observed that conversion of the iodochromone **45** to chromone **46** does occur over time.

The presence of both products was confirmed by ^{1}H NMR, the side product had one extra proton signal at 6.26 ppm in the spectrum which was not present in the spectrum of iodochromone **45**.

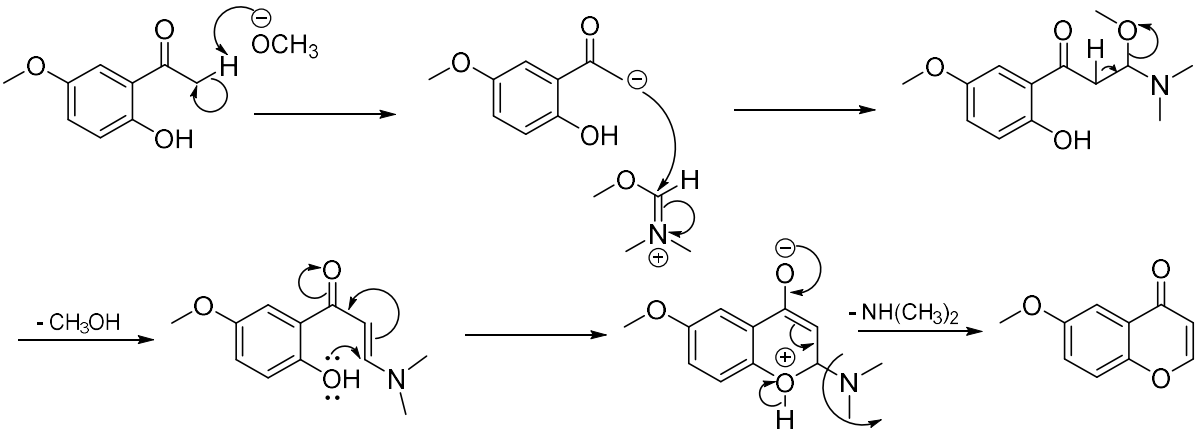

Scheme 34. Formation of the chromone

In an attempt to convert chromone **46** into the required iodochromone **45**, chromone **46** was treated with piperidine in the presence of methanol to form (piperidin-1-yl)propen-1-one which was further treated with iodine and pyridine[42] (Scheme 35).

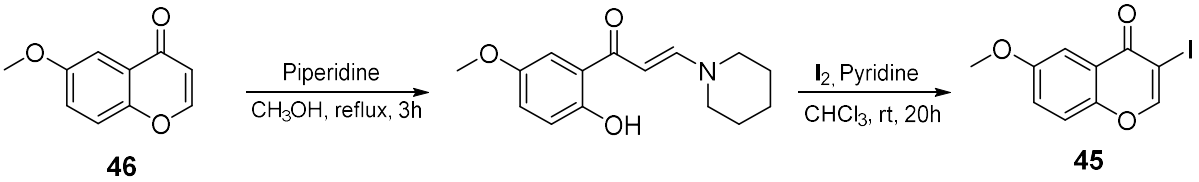

Scheme 35. Preparation of the iodochromone from chromone

The piperidine acts a nucleophile in an aza-Michael reaction, followed by a rearrangement of electrons and opening of the 6-membered ring (Scheme 36). The resulting conjugated enamine is able to attack an iodine molecule and attack of the phenol oxygen allows re-formation of the six-membered ring. Using this method, we were able to covert chromone into iodochromone, but with low to moderate yields. Subsequently, we were able to optimise the reaction conditions of the initial iodination step (Scheme 30), so only minimal amounts of the non-iodinated chromone was formed. We changed the time of reaction from 24 hours to overnight and increased the temperature from 0 °C to 25 °C. Careful storage of the product, in the absence of light also helped to ensure the product did not decompose.

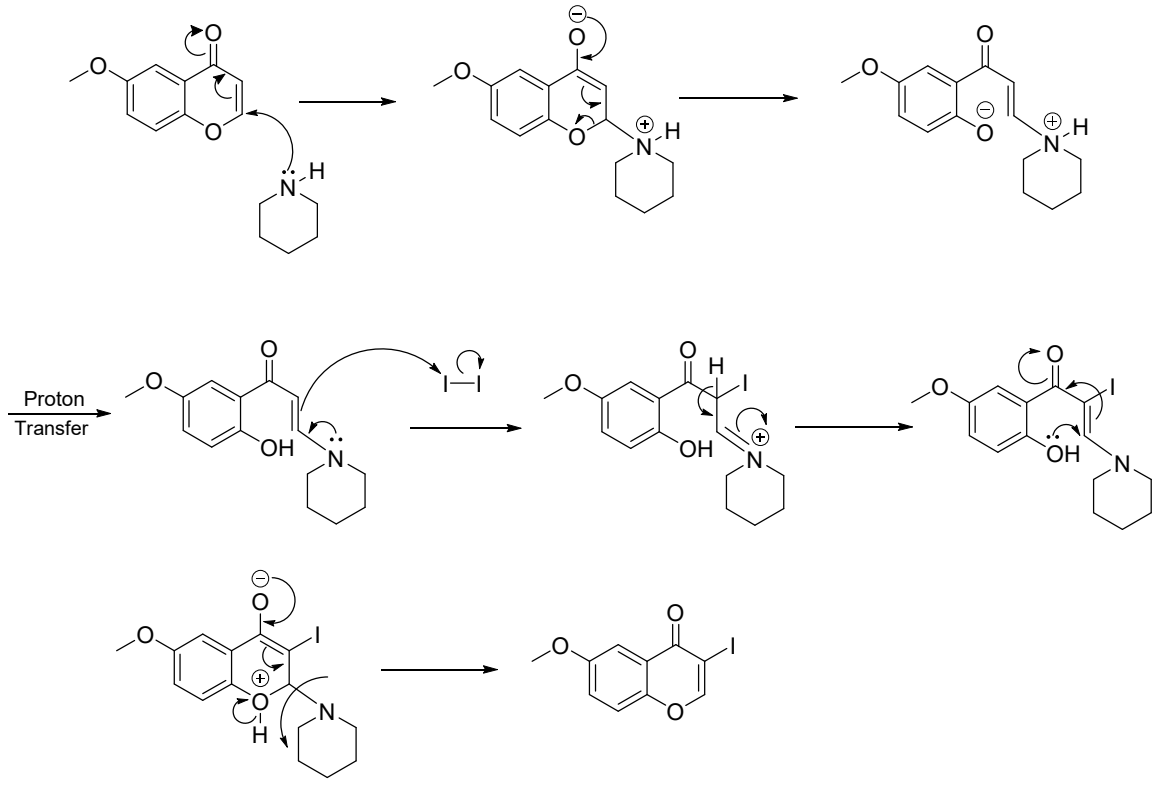

Scheme 36. Formation of the iodochromone

(B) Synthesis of isoflavones

With the required iodochromone **45** in hand, the next steps were the Suzuki coupling with a boronic acid **50** in the presence of $Pd(PPh_3)_4$ catalyst, followed by the addition hydrazine hydrate to form the 3,4-diarylpyrazoles (Scheme 37).

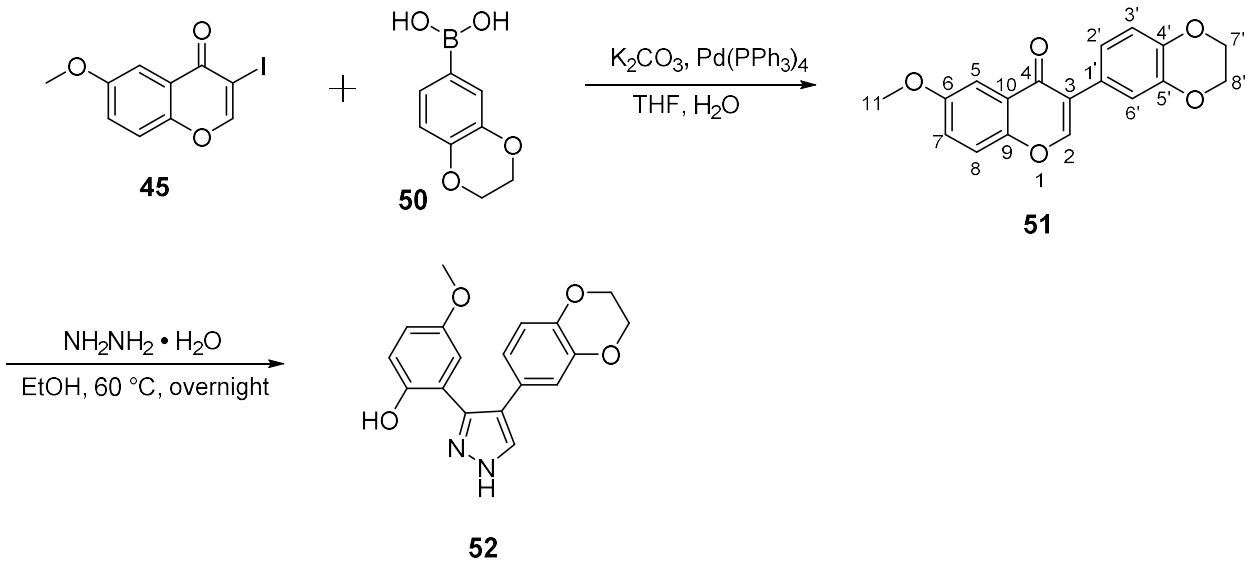

Scheme 37. Completion of the synthesis with Suzuki Coupling and an aza-Michael addition

The final product of the Suzuki coupling was confirmed by ^1H NMR spectra. The peak for 11-H and 2-H from iodochromone **45** was present at 3.85 ppm and 7.91 ppm and one new peak for 7'-H and 8'-H was present at 4.21 ppm which showed a successful coupling occurred between iodochromone and boronic acid. Six peaks were present in the aromatic region from 6.84 ppm to 7.61 ppm, three for each aromatic ring (Scheme 37).

(C) Aza-Michael reaction:

After the Suzuki coupling between iodochromone **45** and boronic acid **50**, an isoflavone **51** was formed. The final step of the synthesis was reaction of the isoflavone with hydrazine hydrate in an aza-Michael addition to prepare the diarylpyrazoles product.

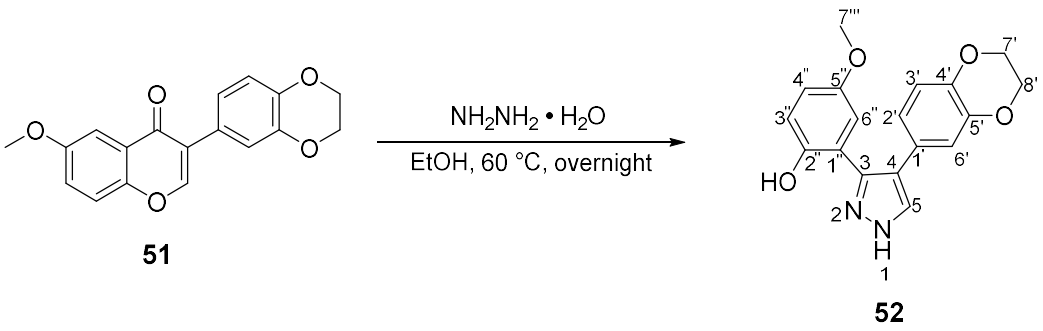

51 52

Scheme 38. Aza Michael addition

The formation of required pyrazole was confirmed by analysis of the ^{1}H NMR spectrum of **51** which showed 5-H as a distinctive singlet at 7.58 ppm which was present at 7.90 ppm in the starting material. The peak of 5-H was used in the HMBC spectrum to assign the quaternary carbons C3 and C4 which were found at 147.81 ppm and 120.26 ppm respectively.

To demonstrate that this synthesis would be amenable for the synthesis of a variety of analogues, we attempted to perform this reaction also with two other boronic acids to make two other analogues using this methodology (Scheme 39). Thus, pyrazole **49** was formed in 50% yield over 3 steps, in a sequence that used (3,5-dimethoxyphenyl) boronic acid, and pyrazole **55** was formed in 20% yield over 3 steps, in a sequence that used benzo[d]-1,3-dioxol-5-ylboronic acid. In the future, the iodochromone starting material will also be modified to produce more analogues.

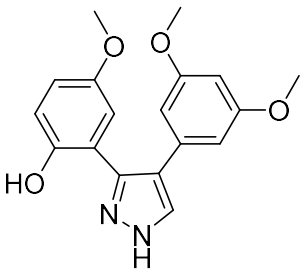

49

Step 1: 69%
Step 2: 83%
Step 3: 89%

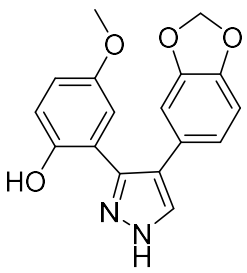

55

Step 1: 69%
Step 2: 46%
Step 3: 66%

Step 1 = Formation of iodochromone
Step 2 = Suzuki Cross Coupling
Step 3 = Aza-Michael Addition

Scheme 39. Analogues from Suzuki Coupling

2.3 Summary of compounds synthesised

In total, 11 isoflavone compounds have been synthesised, with 5 of them being novel compounds (Figure 23). The overall yields of these compounds range from 5 to 38 percent over 2 steps. These compounds are currently in the process of being tested in protein-binding assays and MIC assays by our collaborators.

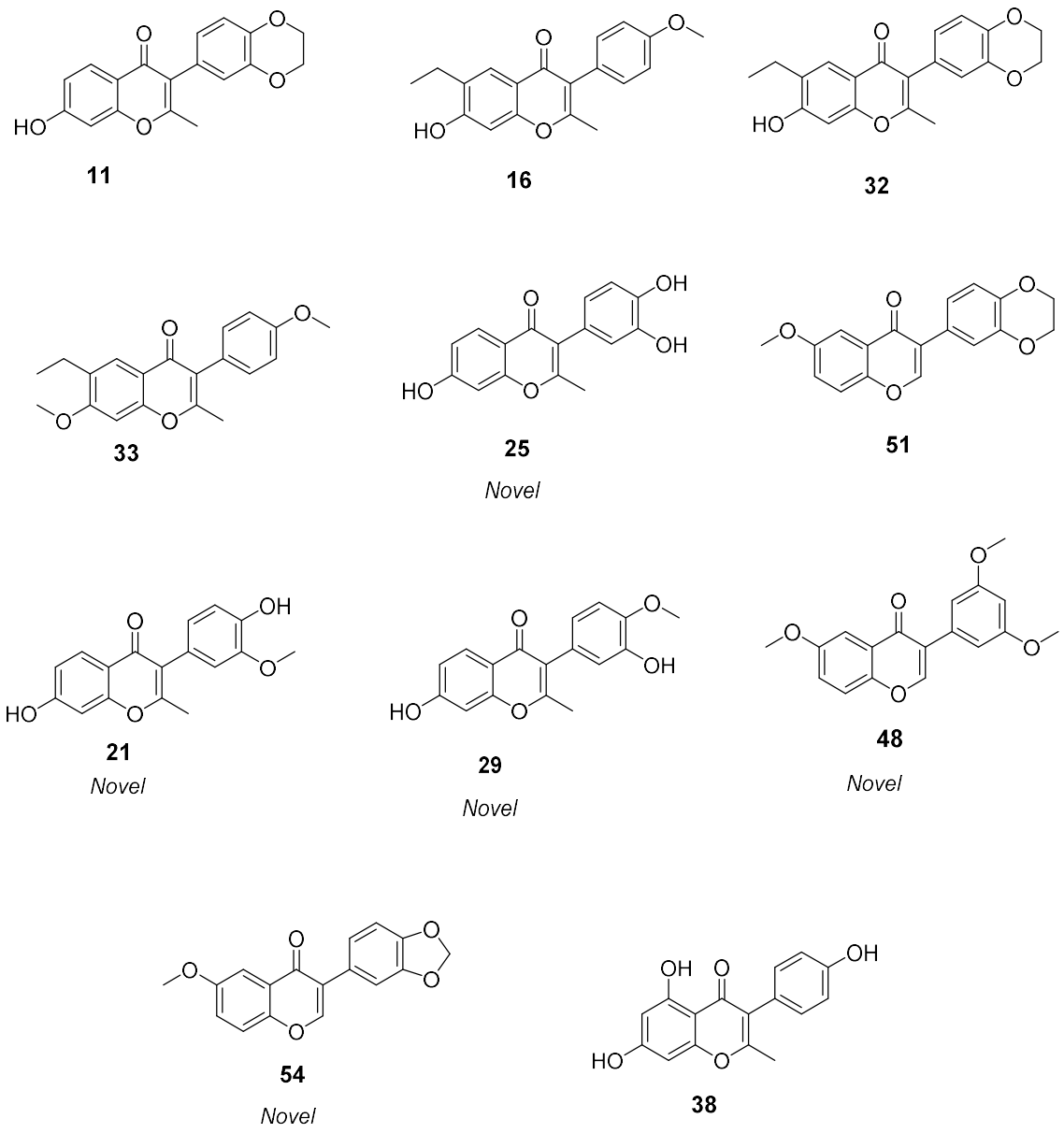

Figure 23. Total number of isoflavones

For the diarylpyrazole analogues, 10 have been synthesised, 7 of which are novel compounds (Figure 24). These compounds are currently with collaborators for both NMR-based protein-binding assays and biological testing to determine MIC values. To date, 13 of the above compounds have been tested in MIC assays against *E. coli* with mcr-1 resistance. Of the compounds tested, 6 have shown significant decreases in the MIC values demonstrating an ability to revert back the antibacterial activity of colistin.

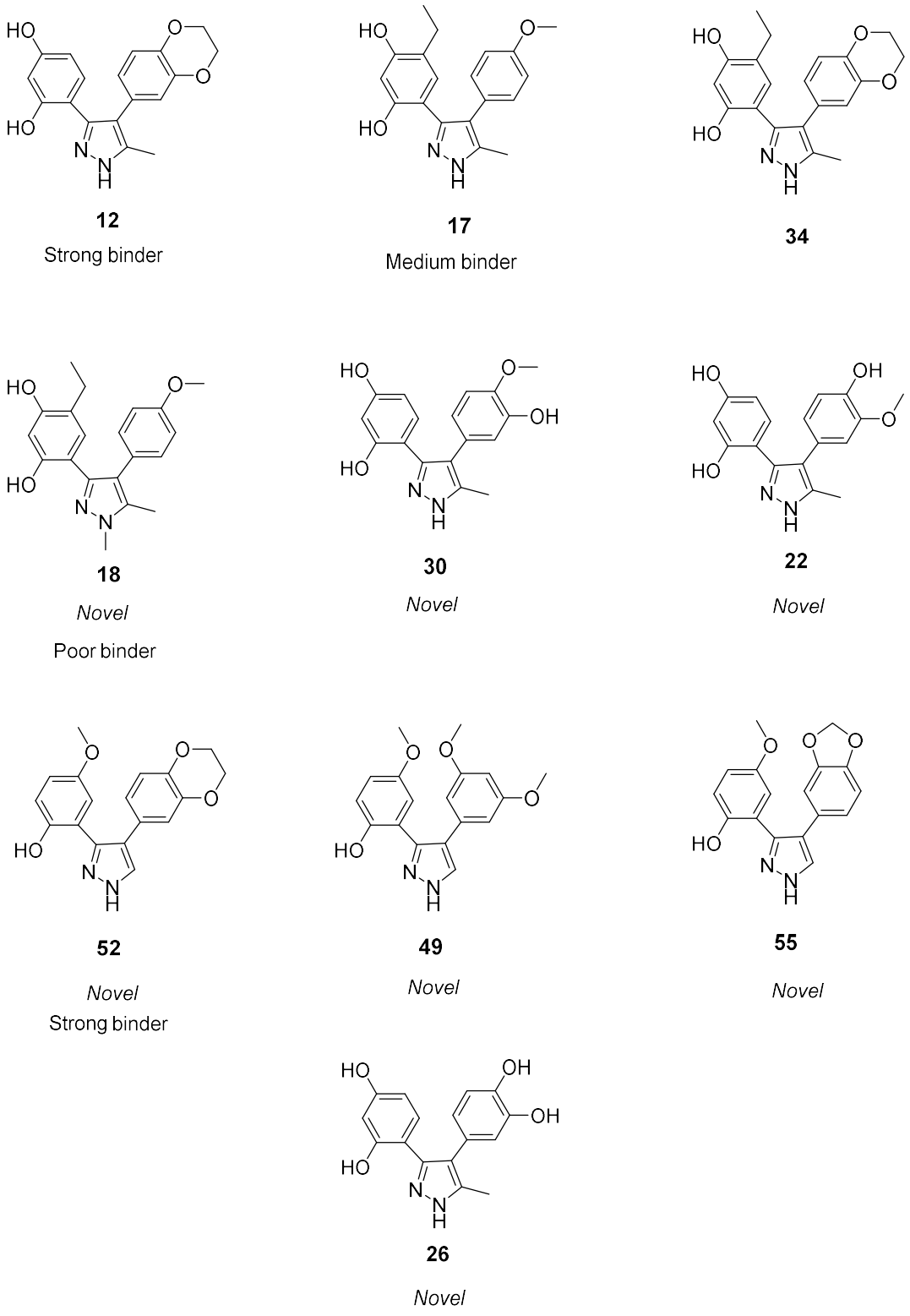

Figure 24. Summary of pyrazoles synthesised

2.4 Initial biological results

Our collaborators are currently performing minimum inhibitory concentration (MIC) assays with our synthesised compounds against *E. coli* with mcr-1 resistance. This involves first incubation of the *E. coli* with polymyxin only, to determine the MIC value in the absence of any potential MCR-1 binders (Figure 25, first column). This value was measured at 1.57 ± 0.55 μM. The MIC of polymyxin is then measured in the presence of our synthesised compounds. Initial results are very promising. Of the 13 compounds tests, 6 have shown significant reduction in the MIC of polymyxin, which indicates that these compounds are able to negate the resistance of *E. coli* towards colistin. The summary of the MIC values for the effective compounds are shown below in Figure 25.

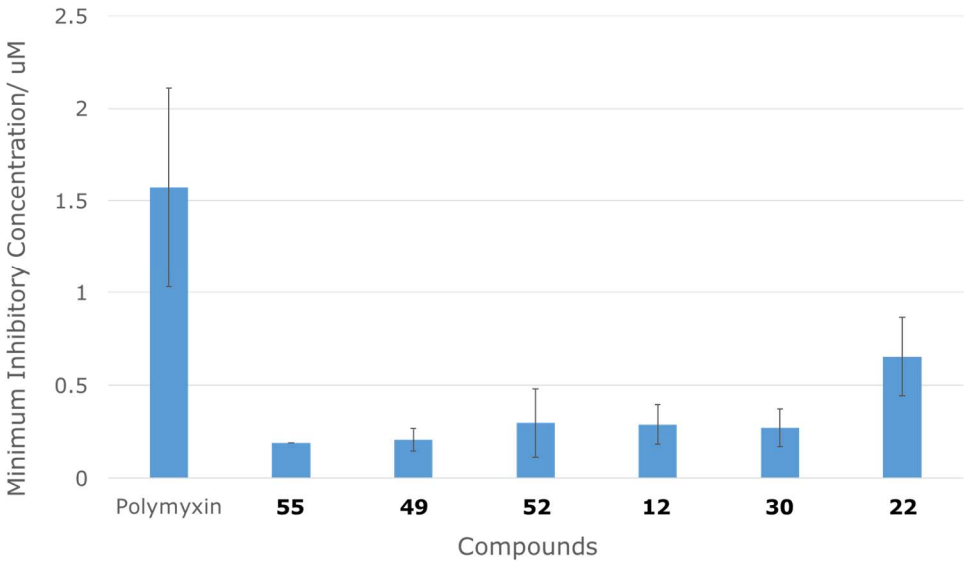

Figure 25. MIC/ μM values in the presence of different pyrazole analogues

2.5 Conclusions and Future Work

In summary, a total of 21 isoflavones and diarylpyrazoles have been synthesised, of which 12 are novel compounds. These compounds have been synthesised using two different synthetic routes – using either a Friedel-Crafts acylation, Kostenecki acylation strategy or a Suzuki cross-coupling strategy. Both routes are short and allow ready generation of analogues by changing the starting materials that are employed in the reaction. During the course of the synthetic work, it became evident that many of the lead compounds were not very water soluble, which would become problematic further along the drug discovery process. Analogues were therefore designed and synthesised which possessed a greater number of free hydroxyl groups.

At present, 6 of the 13 compounds tested have been found to decrease the MIC of polymyxin towards *E. coli* with mcr-1 resistance. This is a remarkably high hit rate and suggests that the prior computational docking and protein-binding studies were performed accurately and to a high standard. At this stage, it is not possible to comment on the structure-activity-relationship for MCR-1 inhibitors as we do not have yet a complete set of biological data. In future work, our aims are to **1.** Continue to synthesise new isoflavone and pyrazole analogues, guided by the biological data and **2.** To build up a picture of the structure-activity-relationship required for MCR-1 inhibition.

CHAPTER THREE: EXPERIMENTAL

3.1 General Details

The organic molecules were synthesized and characterized by ^{1}H, ^{13}C NMR, IR and HRMS and the data compared to literature values where possible.

All organic synthetic reactions were carried out in oven-dried glassware under inert gas. Reactions performed at high temperatures were heated in oil bath with digital thermometer to maintain the defined temperature.

Reagents including *N,N*-dimethylformamide (DMF), *N,N*-dimethylformamide dimethyl acetal (DMF-DMA), tetrahydrofuran (THF) and hydrazine hydrate were purchased from Sigma-Aldrich and NMR solvents including deuterated methanol-d_4 and deuterated chloroform were purchased from EURISO-TOP. Acetone and hexane with analytical quality were purchased from ECP chemicals along with dichloromethane and ethyl acetate of laboratory quality. Hydrochloric acid 37% and methanol were purchased from Thermo Fisher Scientific. Anhydrous magnesium sulfate was purchased from Scharlau.

Analytical thin layer chromatography (TLC) was performed using plates of DC Kieselgel 60 F 254, purchased from Merck. Compounds were visualized by UV light or by staining with methanolic solution of phosphomolybdic acid or ninhydrin. Flash column chromatography was carried out using Silica gel P60 (40-63 μm) purchased from SiliCycle Inc. Solvents were removed by a BUCHI Rotavapor R-300 equipped with BUCHI vacuum pump V-300, BUCHI recirculating chiller F-100 and BUCHI heating bath B-300 Base. Samples prepared for NMR were dried first under high-vacuum.

NMR spectroscopy was conducted using a Bruker Ascend 400 NMR spectrometer operating at 400 MHz for ^{1}H nuclei and 101 MHz for ^{13}C nuclei and analysed using MestReNova 6.0.2-5475. Chemical shifts are reported as parts per million (ppm) from tetramethylsilane ($\delta = 0$) and were measured relative to the solvent in which the sample was analyzed ($CDCl_3$: δ 7.26 for ^{1}H NMR, δ 77.0 for ^{13}C NMR; CD_3OD: δ 3.31 for ^{1}H NMR, δ 49.0 for ^{13}C NMR) and coupling constants (J) are reported in hertz (Hz) to the nearest 0.1 ppm. ^{1}H NMR shift values are reported as chemical shift (δ H), relative integral, multiplicity (s, singlet; d, doublet; t, triplet; q, quartet; m, multiplet; dd, double of doublets; dt, doublet of triplets) and coupling

constant (J Hz). The ^{13}C values were referenced to the residual chloroform peak at δ 77.0 ppm. ^{13}C values are reported as chemical shift (δ C).

Infrared (IR) spectra were recorded using a Nicolet iS10 spectrometer (Thermo Fisher Scientific Inc.) with the absorption peaks expressed in wavenumbers (cm^{-1}) and recorded using a range of 450 to 4000 cm^{-1} . IR spectra were analysed using OMNIC 9.2.86.

High resolution mass spectra (HRMS) were recorded using a VG-70SE spectrometer at a nominal resolution of 5000 to 10000 as appropriate. Major and significant fragments are quoted in the form x (y%), where x is the mass to change ratio and y is the percentage abundance relative to the base peak.

3.2 General Procedures:

3.2.1 General Procedure 1: Synthesis of benzylphenylketones

The phenol (1 equiv.), phenylacetic acid (1 equiv.) and boron trifloride diethyl etherate (3 equiv.) were mixed together and heated at 80 ℃ overnight, under an atmosphere of nitrogen. The reaction mixture was poured into water with the formation of precipitate. The mixture was then extracted thrice with ethyl acetate. The collected organic extracts were washed twice with water and thrice with brine, dried over anhydrous $MgSO_4$ and the solvent was removed *in vacuo* to give the crude product which was then purified by flash chromatography using a mixture of hexane/ethyl acetate as eluent.

3.2.2 General Procedure 2: Synthesis of 2-methyl-3-phenylchromen-4-ones

The benzylphenylketone (1 equiv.) was mixed with acetic anhydride (14 equiv.) and K_2CO_3 (4.96 equiv.) in anhydrous DMF. The reaction mixture was heated at reflux (160 ℃) until completion of the reaction as monitored by TLC (usually between 6 and 7 hours). The reaction mixture was then poured into water. Next, the mixture was extracted thrice with ethyl acetate and the combined organic layers were washed two times with water and thrice with brine solution which formed an emulsion. The solution of 1 M HCl was added into that emulsion and dried over anhydrous $MgSO_4$ and the solvent was removed *in vacuo* to afford the desired product. The crude product was purified using flash chromatography.

3.2.3 General Procedure 3: Synthesis of pyrazoles

The 2-methyl-3-phenylchromen-4-one (1 equiv.) was dissolved in ethanol and hydrazine hydrate (123 equiv.) was added. The reaction mixture was heated at reflux overnight and ethanol was removed *in vacuo*. To this residue with added water and the mixture was extracted thrice with ethyl acetate. The collected organic layers were washed with twice with water, twice with brine and dried over anhydrous $MgSO_4$. Concentration *in vacuo* gave the crude material which was purified by flash chromatography.

3.2.4 General procedure 4: Synthesis of 3-phenylchromen-4-ones

3-Iodo-4*H*-1-benzopyran-4-one (1 equiv.) was dissolved in the solution of THF/H_2O (4:1) and the boronic acid (1.1 equiv.), K_2CO_3 (2 equiv.) and Pd $(PPh_3)_4$ (0.1 equiv.) was added into solution and heated at reflux (70 ℃) overnight. The solvent was removed *in vacuo* and this crude material was purified by flash chromatography.

3.2.5 General procedure 5: Transesterification

The 2-methyl-3-phenylchromen-4-one was dissolved in methanol (10 mL) and added to a solution of 10% HCl in methanol (10 mL). The reaction mixture was stirred at 50 ℃ for 2-3 hours (followed by TLC to see convergence of spots). This mixture was then concentrated *in vacuo*. The residue was dissolved up in ethyl acetate (10 ml) and a saturated solution of sodium hydrogen carbonate (15 ml) was added and the aqueous layer was extracted thrice with ethyl acetate. The combined organic layers were dried over anhydrous $MgSO_4$ and concentrated *in vacuo* to give the crude product which was purified by flash chromatography.

3.3 Experimental Procedure

2-(2,3-Dihydrobenzo[b][1,4]dioxin-6-yl)-1-(2,4-dihydroxyphenyl)ethan-1-one (10)

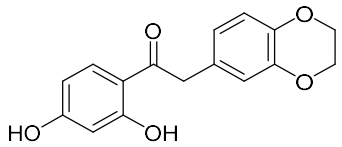

The reaction was carried out following general procedure 1 using resorcinol **8** (165 mg, 1.50 mmol, 1.0 eq.), 2-(2,3-dihydroxybenzo[1,4]dioxin-6-yl)acetic acid **9** (291 mg, 1.50 mmol, 1.0 eq.) and boron trifluoride diethyletherate (3.0 ml, 25 mmol, 17 eq.) and the crude product was purified by flash chromatography on silica gel using a ethyl acetate/hexane (1:4) mixture to afford the title compound **10** as an orange solid (210 mg, 0.73 mmol, 49%).

^{1}H NMR (400 MHz, chloroform-*d*): δ (ppm) 7.58 (d, J = 8.7 Hz, 1H), 6.70 (d, J = 8.2 Hz, 1H), 6.65 (d, J = 2.1 Hz, 1H), 6.60 (dd, J = 8.2, 2.1 Hz, 1H), 6.30 - 6.18 (m, 2H), 4.07 (s, 4H), 3.95 (s, 2H).

3-(2,3-Dihydrobenzo[b][1,4]dioxin-6-yl)-7-hydroxy-2-methyl-4*H*-chromen-4-one (11)

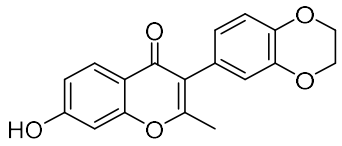

The reaction was carried out following general procedure 2 using ketone **10** (298 mg, 1.04 mmol, 1.0 eq.), acetic anhydride (1.50 ml, 15.8 mmol, 15.1 eq.), potassium carbonate (715 mg, 5.178 mmol, 4.96 eq.) in DMF (5 ml) and the reaction was heated at reflux for 7 hours. The crude material (295 mg) was used in the next step without further purification.

4-(4-(2,3-Dihydrobenzo[b][1,4]dioxin-6-yl)-5-methyl-1*H*-pyrazol-3-yl)benzene-1,3-diol (12)

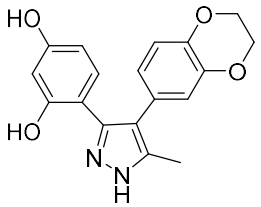

The title compound **12** was synthesised according to general procedure 3 using chromone **11** (295 mg, 0.952 mmol, 1.0 eq.), hydrazine hydrate (5.0 ml, 88 mmol, 92 eq.) and ethanol (5 ml). The crude material was purified by flash chromatography on silica gel using a hexane/ethyl acetate/methanol mixture (8:4:1.5). The columned material required further purification using preparative TLC using the same eluent system to afford the title compound **12** as a light brown solid (50 mg, 0.15 mmol, 16%).

^{1}H NMR (400 MHz, methanol-d_4): δ (ppm) 6.78 (d, J = 8.5 Hz, 1H), 6.72 (d, J = 8.2 Hz, 1H), 6.59 (d, J = 2.0 Hz, 1H), 6.56 (d, J = 2.0 Hz, 1H), 6.54 (d, J = 2.0 Hz, 0H), 6.23 (d, J = 2.4 Hz, 1H), 5.99 (dd, J = 8.6, 2.4 Hz, 1H), 4.14 (s, 4H), 2.09 (s, 3H).

^{13}C NMR (101 MHz, methanol-d_4): δ (ppm) 157.9, 156.9, 143.6, 142.7, 129.2, 127.3, 123.0, 118.5, 116.9, 116.5, 109.6, 106.0, 102.5, 64.3, 64.2, 8.9.

HRMS found (ESI): MH^+ 325.1193, calc for $C_{18}H_{17}N_2O_4$ 325.1183.

IR ν_{max} (film)/cm^{-1} : 3203, 2929, 2360, 1617, 1494, 1454, 1307, 1280, 1243.

1-(5-Ethyl-2,4-dihydroxyphenyl)-2-(4-methoxyphenyl)ethan-1-one (15)

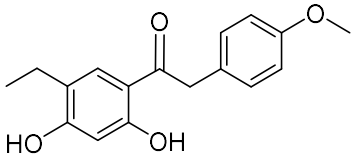

The reaction was carried out following general procedure **1** using 4-ethylresorcinol **13** (413 mg, 3.0 mmol, 1.0 eq.), 4-methoxyphenylacetic acid **14** (498 mg, 3.0 mmol, 1.0 eq.) and boron trifluoride diethyl etherate (6.0 ml, 50 mmol, 17 eq.) and the crude product was purified by

flash chromatography on silica gel by using a ethyl acetate/hexane (1:4) mixture to afford the title compound **15** as a yellow solid (484 mg, 1.69 mmol, 60%).

^{1}H NMR (400 MHz, chloroform-*d*): δ (ppm) 7.58 (d, J = 0.8 Hz, 1H), 7.18 (d, J = 8.7 Hz, 2H), 6.87 (d, J = 8.7 Hz, 2H), 6.29 (s, 1H), 4.15 (d, J = 2.3 Hz, 2H), 3.77 (s, 1H), 2.56 (q, J = 7.5, 0.7 Hz, 2H), 1.20 (t, J = 7.5 Hz, 3H).

6-Ethyl-7-hydroxy-3-(4-methoxyphenyl)-2-methyl-4*H*-chromen-4-one (16)

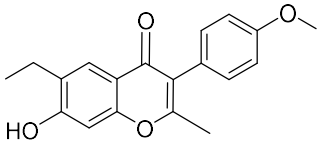

The reaction was carried out following general procedure 2 using ketone **15** (484 mg, 1.69 mmol, 1 eq.), acetic anhydride (2.50 ml, 26.4 mmol, 15.6 eq.), potassium carbonate (1.16 g, 8.38 mmol, 4.96 eq.) in DMF (5 ml) and heated at reflux or 6 hours. A brown solid (421 mg) was formed which was used directly for next step.

4-Ethyl-6-(4-(4-methoxyphenyl)-5-methyl-1*H*-pyrazol-3-yl)benzene-1,3-diol (17)

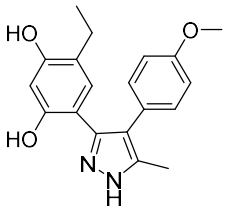

The title compound **17** was synthesised according to general procedure **3** using chromone **16** (421 mg, 1.36 mmol, 1.0 eq.), hydrazine hydrate (8.20 ml, 169 mmol, 124 eq.) and ethanol (7 ml) and the crude material was purified by flash chromatography on silica gel using hexane/ethyl acetate/methanol (8:4:1.5) as eluent. The title compound **17** was obtained as a light brown solid (110 mg, 0.339 mmol, 23%).

^{1}H NMR (400 MHz, chloroform-*d*): δ (ppm) 7.03 (d, J = 8.6 Hz, 2H), 6.82 (d, J = 8.7 Hz, 2H), 6.73 (s, 1H), 6.40 (s, 1H), 3.73 (s, 3H), 2.20 (q, J = 7.4 Hz, 2H), 2.03 (s, 3H), 0.74 (t, J = 7.5 Hz, 3H).

^{13}C NMR (101 MHz, chloroform-*d*): δ (ppm) 157.6, 153.5, 153.1, 146.4, 138.0, 130.6, 127.2, 124.9, 120.0, 115.8, 113.1, 108.8, 102.3, 54.3, 20.6, 12.3, 8.8.

HRMS found (ESI): MH^+ 325.1556, calc for $C_{19}H_{21}N_2O_3$ 325.1547.

IR ν_{max} (film)/cm^{-1}: 3302, 2960, 2924, 1607, 1519, 1462, 1282, 1240, 1172, 1147.

The observed NMR data was in accordance with what is reported in the literature.[18]

4-Ethyl-6-(4-(4-methoxyphenyl)-1,5-dimethyl-1*H*-pyrazol-3-yl)benzene-1,3-diol (18)

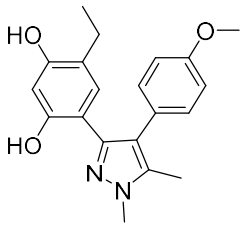

The reaction was carried out by mixing pyrazole **17** (20 mg, 0.062 mmol, 1.0 eq.), methyl iodide (0.050 ml, 0.80 mmol, 13 eq.) and DBU (0.050 ml, 0.33 mmol, 5.4 eq.) in DMF (2 ml) for 5 hours at room temperature. The reaction mixture was quenched with water and then extracted thrice with ethyl acetate. The collected organic extracts were washed twice with water and thrice with brine, dried over anhydrous $MgSO_4$ and the solvent was removed *in vacuo* to give the crude product which was then purified by flash chromatography using hexane/ethyl acetate/methanol (8:4:1) as the solvent mixture. The *title compound* **18** was obtained as a light brown solid (3.9 mg, 0.011 mmol, 19%).

^{1}H NMR (400 MHz, methanol-d_4): δ (ppm) 7.22 - 7.10 (m, 2H), 7.07 - 6.94 (m, 2H), 6.74 (d, J = 0.8 Hz, 1H), 6.31 (s, 1H), 3.85 (d, J = 4.9 Hz, 6H), 2.25 (q, J = 7.5, 0.7 Hz, 2H), 2.19 (s, 3H), 0.84 (t, J = 7.5 Hz, 3H).

^{13}C NMR (101 MHz, methanol-d_4): δ (ppm) 159.0, 154.9, 154.7, 137.9, 131.4, 127.9, 126.7, 120.7, 117.4, 113.8, 109.0, 102.0, 54.4, 35.0, 21.4, 12.8, 8.2.

HRMS found (ESI): MH^+ 339.1700, calc for $C_{20}H_{23}N_2O_3$ 339.1703.

1-(2,4-Dihydroxyphenyl)-2-(4-hydroxy-3-methoxyphenyl)ethan-1-one (20)

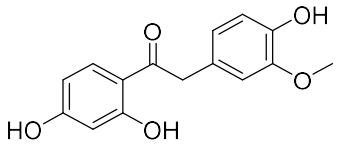

The reaction was carried out following general procedure using 1 with resorcinol **8** (330 mg, 3.0 mmol, 1.0 eq.), 2-(4-hydroxy-3-methoxyphenyl)acetic acid **19** (547 mg, 3.0 mmol, 1.0 eq.) and boron trifluoride diethyletherate (6.0 ml, 50 mmol, 17 eq.) and the crude product was purified by flash chromatography on silica gel by using ethyl acetate/hexane (1:5) and then using ethyl acetate/hexane (1:2) mixture to afford the title compound **20** as a yellow solid (331 mg, 1.20 mmol, 40%).

^{1}H NMR (400 MHz, chloroform-*d*): δ (ppm) 7.73 (d, J = 8.8 Hz, 1H), 6.86 (d, J = 8.0 Hz, 1H), 6.79 - 6.71 (m, 2H), 6.38 (dd, J = 8.8, 2.4 Hz, 1H), 6.34 (d, J = 2.3 Hz, 1H), 4.12 (s, 2H), 3.87 (s, 3H).

7-Hydroxy-3-(4-hydroxy-3-methoxyphenyl)-2-methyl-4*H*-chromen-4-one (21)

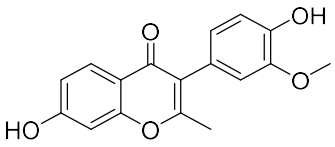

The reaction was carried out following general procedure **2** using ketone **20** (331 mg, 1.2 mmol, 1 eq.), acetic anhydride (1.1 ml, 16.8 mmol, 14 eq.), potassium carbonate (822 mg, 5.95 mmol, 4.96 eq.) and DMF (5 ml). The reaction was heated at reflux for 7.5 hours. It was purified by flash chromatography on silica gel using an ethyl acetate/hexane (1:2) mixture to afford the *title compound* **21**as a yellow solid (307 mg, 1.35 mmol, 85%).

^{1} H NMR (400 MHz, methanol-d_4): δ (ppm) 7.85 (d, J = 8.8 Hz, 1H), 6.80 - 6.77 (m, 1H), 6.75 (s, 1H), 6.73 (d, J = 1.9 Hz, 1H), 6.70 (d, J = 2.2 Hz, 1H), 6.59 (dd, J = 8.0, 1.9 Hz, 1H), 3.74 (s, 3H), 2.18 (s, 3H).

^{13}C NMR (101 MHz, methanol-d_4): δ (ppm) 177.4, 164.3, 163.0, 157.9, 147.5, 146.0, 126.9, 124.4, 123.0, 122.6, 115.7, 114.8, 114.7, 113.9, 101.7, 55.0, 18.2.

HRMS found (ESI): MH^+ 299.0925, calc for $C_{17}H_{15}O_5$ 299.0914.

IR ν_{max} (film)/cm^{-1} : 3297, 2972, 1620, 1595, 1515, 1453, 1267, 1199, 1169, 1118, 1043.

4-(4-(4-Hydroxy-3-methoxyphenyl)-5-methyl-1*H*-pyrazol-3-yl)benzene-1,3-diol (22)

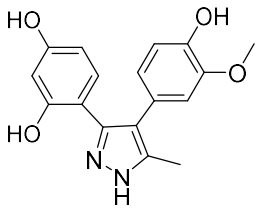

The reaction was carried out following general procedure 3 using chromone **21** (247 mg, 0.828 mmol, 1 eq.), hydrazine hydrate (5.0 ml, 100 mmol, 123 eq.) and ethanol (5 ml). The crude was purified by flash chromatography on silica gel using hexane/ethyl acetate /methanol (8:4:2) as the solvent mixture to afford the *title compound* **22** as a yellow solid (101 mg, 0.323 mmol, 39%).

^{1}H NMR (400 MHz, methanol-d_4): δ (ppm) 6.93 (d, J = 8.5 Hz, 1H), 6.84 (d, J = 8.0 Hz, 1H), 6.76 (d, J = 1.9 Hz, 1H), 6.70 (dd, J = 8.0, 1.9 Hz, 1H), 6.37 (d, J = 2.5 Hz, 1H), 6.12 (dd, J = 8.5, 2.5 Hz, 1H), 3.73 (s, 3H), 2.22 (s, 3H).

^{13}C NMR (101 MHz, methanol-d_4): δ (ppm) 157.8, 157.0, 147.6, 145.0, 129.4, 125.7, 122.6, 117.1, 115.0, 113.5, 106.0, 102.5, 55.0, 9.0.

HRMS found (ESI): MH^+ 313.1184, calc for $C_{17}H_{17}N_2O_4$ 313.1183.

IR ν_{max} (film)/cm^{-1} : 3255, 2973, 1599, 1447, 1410, 1253, 1212, 1169, 1043, 876.

1-(2,4-Dihydroxyphenyl)-2-(3,4-dihydroxyphenyl)ethan-1-one (24)

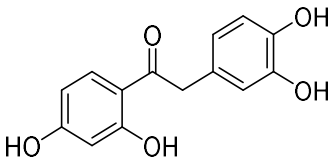

The title compound **24** was synthesised according to general procedure **1** using resorcinol **8** (330 mg, 3.0 mmol, 1.0 eq.), 2-(3,4-dihydroxyphenyl)acetic acid **23** (504 mg, 3.0 mmol, 1.0 eq.) and boron trifluoride diethyletherate (6.0 ml, 50 mmol, 17 eq.) and the crude product was purified by flash chromatography on silica gel using ethyl acetate/hexane (2:5) and then using ethyl acetate/hexane (1:2) as the solvent mixture to yield the title compound **24** as a brown solid (420 mg, 1.61 mmol, 53%).

^{1}H NMR (400 MHz, methanol-d_4): δ (ppm) 7.78 (d, J = 8.7 Hz, 1H), 6.73 (dd, J = 5.1, 3.0 Hz, 2H), 6.61 (dd, J = 8.1, 2.1 Hz, 1H), 6.36 (dd, J = 8.9, 2.4 Hz, 1H), 6.28 (d, J = 2.4 Hz, 1H), 4.03 (s, 2H).

3-(3,4-Dihydroxyphenyl)-7-hydroxy-2-methyl-4*H*-chromen-4-one (25)

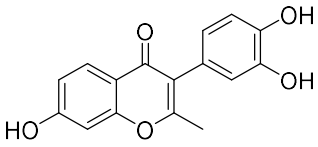

The reaction was carried out following general procedure 2 using ketone **24** (419 mg, 1.61 mmol, 1 eq.), acetic anhydride (2.10 ml, 22.2 mmol, 13.8 eq.), potassium carbonate (1.10 g, 7.98 mmol, 4.96 eq.) in DMF (5 ml) and the reaction was heated at reflux for 7 hours. It was partially purified by flash chromatography on silica gel using 7% methanol in dichloromethane. Then, the transesterification reaction was carried out according to general procedure 5 and the crude was purified by column chromatography using 5% methanol in dichloromethane to afford the *title compound* **25** as a brown solid (54 mg, 0.18 mmol, 11%).

^{1}H NMR (400 MHz, methanol-d_4): δ (ppm) 7.98 (d, J = 8.8 Hz, 1H), 6.92 (dd, J = 8.8, 2.3 Hz, 1H), 6.89 - 6.81 (m, 2H), 6.71 (d, J = 2.0 Hz, 1H), 6.61 (d, J = 2.1 Hz, 1H), 2.31 (s, 3H).

^{13}C NMR (101 MHz, methanol-d_4): δ (ppm) 177.4, 164.2, 163.1, 158.0, 145.0, 144.8, 127.0, 124.5, 122.7, 121.7, 117.3, 115.7, 115.0, 114.7, 101.6, 18.2.

HRMS found (ESI): MH^+ 285.0753, calc for $C_{16}H_{13}O_5$ 285.0757.

IR ν_{max} (film)/cm^{-1} : 3226, 2928, 2628, 1621, 1584, 1564, 1452, 1284, 1241, 1158.

4-(3-(2,4-Dihydroxyphenyl)-5-methyl-1*H*-pyrazol-4-yl)benzene-1,2-diol (26)

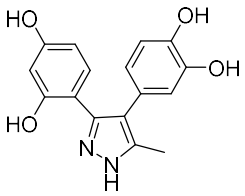

The reaction was carried out following general procedure **3** using chromone **25** (40 mg, 0.14 mmol, 1 eq.), hydrazine hydrate (1.0 ml, 20.4 mmol, 140 eq.) and ethanol (5 ml). The crude was purified by flash chromatography on silica gel by using 15% methanol in dichloromethane to afford the *title compound* **26** as a brown solid (18 mg, 0.060 mmol, 43%).

^{1}H NMR (400 MHz, methanol-d_4): δ (ppm) 6.89 - 6.75 (m, 1H), 6.70 (d, J = 8.0 Hz, 1H), 6.56 (d, J = 2.0 Hz, 1H), 6.45 (dd, J = 8.0, 2.0 Hz, 1H), 6.22 (d, J = 2.4 Hz, 1H), 5.97 (dd, J = 8.6, 2.4 Hz, 1H), 2.08 (s, 3H).

^{13}C NMR (101 MHz, methanol-d_4): δ (ppm) 179.1, 157.7, 157.0, 145.0, 144.1, 139.8, 129.1, 125.7, 121.5, 117.1, 117.0, 115.2, 109.6, 106.0, 102.5, 22.8, 8.9.

HRMS found (ESI): MH^+ 299.1020, calc for $C_{16}H_{15}N_2O_4$ 299.1026**.**

IR vmax (film)/cm^{-1}: 3202, 2957, 2923, 1531, 1405, 1245, 1191, 960.

1-(2,4-Dihydroxyphenyl)-2-(3-hydroxy-4-methoxyphenyl)ethan-1-one (28)

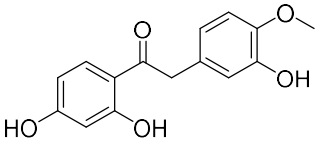

The reaction was carried out following general procedure 1 using resorcinol **8** (330 mg, 3.0 mmol, 1.0 eq.), 2-(3-hydroxy-4-methoxyphenyl)acetic acid **27** (546 mg, 3.0 mmol, 1.0 eq.)

and boron trifluoride diethyl etherate (6.0 ml, 50 mmol, 17 eq.) and the crude product was purified by flash chromatography on silica gel using ethyl acetate/hexane (35%) and then ethyl acetate/hexane (50%) as the eluent mixture to afford the title compound **28** as a yellow solid (378 mg, 1.37 mmol, 46%).

^{1}H NMR (400 MHz, chloroform-*d*): δ (ppm) 7.62 (d, J = 8.8 Hz, 1H), 6.77 - 6.68 (m, 2H), 6.64 (d, J = 2.1 Hz, 1H), 6.28 (dd, J = 8.8, 2.4 Hz, 1H), 6.24 (d, J = 2.4 Hz, 1H), 3.98 (s, 2H), 3.75 (s, 3H).

7-Hydroxy-3-(3-hydroxy-4-methoxyphenyl)-2-methyl-4*H*-chromen-4-one (29)

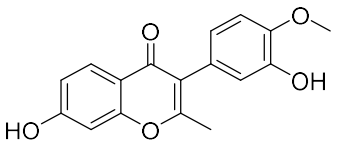

The *title compound* **29** was synthesised according to general procedure 2 using ketone **28** (378 mg, 1.37 mmol, 1.0 eq.), acetic anhydride (2.00 ml, 21.1 mmol, 15.4 eq.), potassium carbonate (944 mg, 6.83 mmol, 4.96 eq.) in DMF (5 ml). The reaction mixture was heated at reflux for 7 hours. The crude was partially purified by flash chromatography using a 70% solution of ethyl acetate in hexane. Then, the transesterification reaction was carried out according to general procedure 5 to afford the *title compound* **29** as a yellow solid (346 mg, 1.15 mmol, 84%).

^{1}H NMR (400 MHz, methanol-d_4): δ (ppm) 7.84 (d, J = 8.8 Hz, 1H), 6.88 (d, J = 8.2 Hz, 1H), 6.78 (dd, J = 8.8, 2.2 Hz, 1H), 6.70 (d, J = 2.2 Hz, 1H), 6.63 (d, J = 2.1 Hz, 1H), 6.60 (d, J = 2.1 Hz, 1H), 6.58 (d, J = 2.1 Hz, 1H), 3.78 (s, 3H), 2.17 (s, 3H).

^{13}C NMR (101 MHz, methanol-d_4): δ (ppm) 177.3, 164.0, 163.7, 158.0, 147.4, 146.2, 126.9, 126.0, 122.4, 121.7, 117.3, 115.5, 115.0, 111.4, 101.7, 55.0, 18.2.

HRMS found (ESI): MH^+ 299.0912, calc for $C_{17}H_{15}O_5$ 299.0914.

IR ν_{max} (film)/cm^{-1} : 3869, 3524, 2952, 2531, 1567, 1436, 1399, 1279, 1164, 1019, 759, 689.

4-(4-(3-Hydroxy-4-methoxyphenyl)-5-methyl-1*H*-pyrazol-3-yl)benzene-1,3-diol (30)

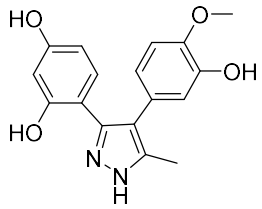

The reaction was carried out following general procedure 3 using chromone **29** (246 mg, 0.824 mmol, 1 eq.), hydrazine hydrate (5.00 ml, 107.9 mmol, 130 eq.) and ethanol (5 ml) to afford the *title compound* **30** as a yellow solid (62 mg, 0.192 mmol, 24%) without purification.

^{1}H NMR (400 MHz, methanol-d_4): δ (ppm) 6.82 (d, J = 8.5 Hz, 1H), 6.73 (d, J = 8.3 Hz, 1H), 6.58 (d, J = 2.1 Hz, 1H), 6.51 (dd, J = 8.2, 2.1 Hz, 1H), 6.26 (d, J = 2.4 Hz, 1H), 5.99 (dd, J = 8.6, 2.5 Hz, 1H), 3.68 (s, 3H), 2.04 (s, 3H).

^{13}C NMR (101 MHz, methanol-d_4): δ (ppm) 157.7, 156.9, 146.7, 146.0, 129.4, 127.0, 121.6, 117.0, 116.8, 115.6, 111.5, 109.7, 106.2, 102.6, 55.0, 9.1.

HRMS found (ESI): MH^+ 313.1184, calc for $C_{17}H_{17}N_2O_4$ 313.1183.

IR ν_{max} (film)/cm^{-1} : 3277, 2927, 1621, 1598, 1522, 1440, 1249, 1207, 1159, 1128.

2-(2,3-Dihydrobenzo[b][1,4]dioxin-6-yl)-1-(5-ethyl-2,4-dihydroxyphenyl)ethan-1-one (31)

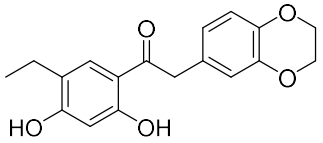

The title compound **31** was synthesised according to general procedure 1 using ethyl resorcinol **13** (413 mg, 3.0 mmol, 1.0 eq.), 2-(2,3-dihydroxybenzo[1,4]dioxin-6-yl)acetic acid **9** (582 mg, 3.0 mmol, 1.0 eq.) and boron trifluoride diethyl etherate (6.0 ml, 50 mmol, 17 eq.) and the crude product was purified by flash chromatography on silica gel by using an ethyl acetate/hexane (25%) eluent mixture to afford the title compound as a light brown solid (535 mg, 1.70 mmol, 57%).

^{1}H NMR (400 MHz, chloroform-*d*): δ (ppm) 7.57 (d, J = 0.9 Hz, 1H), 6.82 (d, J = 8.2 Hz, 1H), 6.78 (d, J = 2.1 Hz, 1H), 6.75 - 6.67 (m, 1H), 6.29 (s, 1H), 4.22 (s, 4H), 4.10 (s, 2H), 2.56 (m, 2H), 1.20 (t, J = 7.5 Hz, 3H).

3-(2,3-Dihydrobenzo[b][1,4]dioxin-6-yl)-6-ethyl-7-hydroxy-2-methyl-4*H*-chromen-4-one (32)

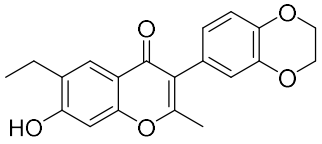

The reaction was carried out following general procedure 2 using ketone **31** (535 mg, 1.7 mmol, 1 eq.), acetic anhydride (2.5 ml, 26.4 mmol, 15.5 eq.), potassium carbonate (1.17 g, 8.45 mmol, 4.96 eq.) in DMF (5 ml). The reaction was heated at reflux for 5 hours. The crude product was purified with 35% solution of ethyl acetate in hexane to afford the title compound **32** as a light brown solid (126 mg, 0.37 mmol, 22%).

^{1}H NMR (400 MHz, chloroform-*d*): δ (ppm) 7.88 (d, J = 0.9 Hz, 1H), 6.78 (d, J = 8.2 Hz, 1H), 6.70 (d, J = 2.0 Hz, 1H), 6.69 - 6.61 (m, 2H), 4.10 - 4.01 (m, 4H), 2.59 (q, J = 7.5 Hz, 2H), 1.98 (s, 3H), 1.21 - 1.16 (m, 3H).

3-(2,3-Dihydrobenzo[b][1,4]dioxin-6-yl)-6-ethyl-7-methoxy-2-methyl-4*H*-chromen-4-one (33)

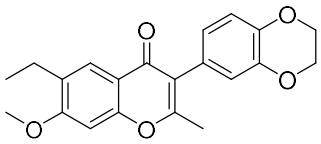

The reaction was carried out by mixing chromone **32** (26 mg, 0.077 mmol, 1.0 eq.), methyl iodide (0.050 ml, 0.077 mmol, 1.0 eq.) and DBU (0.050 ml ,0.077 mmol, 1 eq.) in DMF (2 ml) for 5 hours. The reaction mixture was quenched with water and then extracted thrice with ethyl acetate. The collected organic extracts were washed twice with water and thrice with brine,

dried over anhydrous $MgSO_4$ and the solvent was removed *in vacuo* to give the crude product which was then purified by flash chromatography using ethyl acetate/hexane (1:4) as the solvent mixture. The title compound **33** was obtained as light brown solid (6.0 mg, 0.017 mmol, 22%).

^{1}H NMR (400 MHz, chloroform-*d*): δ (ppm) 7.95 (s, 1H), 6.91 (d, *J* = 8.2 Hz, 1H), 6.79 (d, *J* = 2.0 Hz, 1H), 6.77 (s, 1H), 6.75 (d, *J* = 2.0 Hz, 1H), 6.73 (d, *J* = 2.0 Hz, 1H), 4.29 (s, 4H), 3.92 (s, 3H), 2.79 - 2.61 (m, 2H), 2.29 (s, 3H), 1.22 (t, *J* = 7.5 Hz, 4H).

^{13}C NMR (101 MHz, chloroform-*d*): δ (ppm) 176.4, 162.4, 161.9, 156.2, 143.3, 143.1, 131.2, 126.6, 125.4, 123.7, 122.8, 119.4, 117.2, 116.7, 97.7, 64.4, 64.3, 55.8, 23.0, 19.4, 14.0**.**

HRMS found (ESI): MH^+ 353.1370, calc for $C_{21}H_{21}O_5$ 353.1384.

IR ν_{max} (film)/cm^{-1} : 2922, 1628, 1609, 1581, 1452, 1391, 1282, 1257, 1195, 1095, 1066.

4-(4-(2,3-Dihydrobenzo[b][1,4]dioxin-6-yl)-5-methyl-1*H*-pyrazol-3-yl)-6-ethylbenzene-1,3-diol (34)

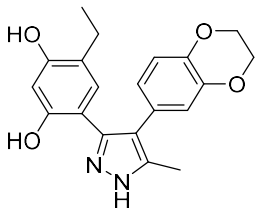

The reaction was carried out following general procedure 3 using chromone **32** (98 mg, 0.29 mmol, 1 eq.), hydrazine hydrate (2.0 ml, 41 mmol, 140 eq.) and ethanol (5 ml). The crude product was partially purified by column chromatography using toluene/DCM/methanol (8:4:2) as the eluent system. The product was again purified by preparative TLC using a toluene/ethyl acetate/methanol (8:4:1.5) mixture to afford the title compound **34** as a light brown solid (9.0 mg, 0.025 mmol, 8%).

^{1}H NMR (400 MHz, methanol-d_4): δ (ppm) 6.75 (d, *J* = 8.0 Hz, 1H), 6.70 (s, 1H), 6.64 - 6.53 (m, 2H), 6.22 (s, 1H), 4.15 (s, 4H), 2.24 - 2.16 (m, 2H), 2.11 (s, 3H), 1.02 (t, *J* = 7.5 Hz, 3H).

^{13}C NMR (101 MHz, methanol-d_4): δ (ppm) 155.3, 154.4, 143.7, 142.8, 128.5, 127.3, 123.1, 121.1, 118.8, 116.9, 116.7, 108.4, 102.1, 64.3, 21.4, 12.8, 9.0.

HRMS found (ESI): MH^+ 353.1495, calc for $C_{20}H_{21}N_2O_4$ 353.1496.

IR ν_{max} (film)/cm^{-1}: 3314, 2926, 2874, 1620, 1494, 1459, 1280, 1243, 1225, 1067, 893**.**

The observed NMR data was in accordance with what is reported in the literature.[17]

2-(4-Hydroxyphenyl)-1-(2,4,6-trihydroxyphenyl)ethan-1-one (37)

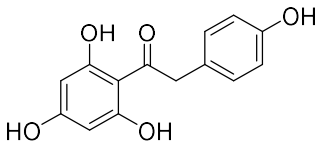

The title compound **37** was synthesised according to general procedure 1 using phloroglucinol **35** (378 mg, 3.0 mmol, 1.0 eq.), 2-(4-hydroxyphenyl) acetic acid **36** (456 mg, 3.0 mmol, 1.0 eq.) and boron trifluoride diethyletherate (6.0 ml, 50 mmol, 16.6 eq.) and the crude product was purified by flash chromatography on silica gel using a 7% solution of methanol in dichloromethane to afford the title compound **37** as a yellow solid (90 mg, 0.34 mmol, 11%).

^{1}H NMR (400 MHz, methanol-d_4): δ (ppm) 6.98 (m, J = 8.5, 0.5 Hz, 5H), 6.61 (t, J = 8.6 Hz, 4H), 5.71 (s, 2H), 4.17 (s, 2H).

5,7-Dihydroxy-3-(4-hydroxyphenyl)-2-methyl-4*H*-chromen-4-one (38)

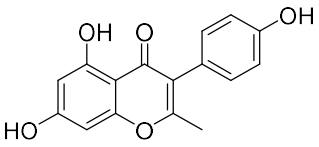

The title compound **38** was synthesised according to general procedure 2 using ketone **37** (90 mg, 0.35 mmol, 1 eq.), acetic anhydride (0.50 ml, 5.28 mmol, 15.2 eq.), potassium carbonate (237 mg, 1.70 mmol, 4.96 eq.) in DMF (5 ml) and heated at reflux for 7 hours. After this, transesterification was performed according to general procedure 5 and the crude was purified by using column chromatography using a 7% solution of methanol in dichloromethane to afford the title compound **38** as a yellow solid (6 mg, 0.021 mmol, 6%).

^{1}H NMR (400 MHz, methanol-d_4): δ (ppm) 7.06 - 6.90 (m, 2H), 6.87 - 6.70 (m, 2H), 6.22 (d, J = 2.1 Hz, 1H), 6.08 (d, J = 2.1 Hz, 1H), 2.16 (s, 3H).

^{13}C NMR (101 MHz, methanol-d_4): δ (ppm) 181.3, 164.6, 164.5, 162.1, 157.9, 157.1, 131.4, 122.8, 121.2, 114.9, 103.7, 98.4, 93.2, 18.0.

HRMS found (ESI): MH^+ 285.0761, calc for $C_{16}H_{12}O_5$ 285.0757.

(*E*)-3-(Dimethylamino)-1-(2-hydroxy-5-methoxyphenyl)prop-2-en-1-one (44)

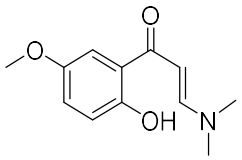

1-(2-hydroxy-5-methoxyphenyl)ethan-1-one **43** (199 mg, 1.20 mmol, 1 eq.) and *N*,*N* dimethylformide–dimethyl acetal (1.0 ml, 7.5 mmol, 6.27 eq.) was heated at 90 ℃ for 5 hours. The solvent was removed *in vacuo* and the crude material was purified by flash chromatography with a 25% solution of ethyl acetate in hexane followed by gradient elution from 30% to 50% ethyl acetate in hexane to afford the title compound **44** as a yellow solid (159 mg, 0.71 mmol, 60%).

^{1}H NMR (400 MHz, chloroform-*d*): δ (ppm) 7.88 (d, J = 12.1 Hz, 1H), 7.19 (d, J = 3.1 Hz, 1H), 7.00 (dd, J = 9.0, 3.0 Hz, 1H), 6.88 (d, J = 9.0 Hz, 1H), 5.72 (d, J = 12.1 Hz, 1H), 3.80 (s, 3H), 3.19 (s, 3H), 2.96 (s, 3H).

3-Iodo-6-methoxy-4*H*-chromen-4-one (45)

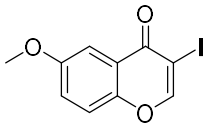

(*E*)-3-(Dimethylamino)-1-(2-hydroxy-methoxyphenyl)prop-2-en-1-one **44** (159 mg, 0.723 mmol, 1 eq.) was dissolved in chloroform (15 mL) and iodine (275 mg, 1.08 mmol, 1.5 eq.) was added into this solution. The reaction was stirred at 25 ℃ overnight. The reaction was

quenched with a saturated solution of sodium thiosulfate (25 mL) and the aqueous layer was extracted three times with chloroform and concentrated *in vacuo*. The crude was purified by flash chromatography using a 15% solution of ethyl acetate in hexane to afford the title compound **45** as a white solid (150 mg, 0.496 mmol, 69%).

^{1}H NMR (400 MHz, chloroform-*d*): δ (ppm) 8.19 (s, 1H), 7.48 (d, J = 3.1 Hz, 1H), 7.31 (dd, J = 9.2, 0.4 Hz, 1H), 7.19 (dd, J = 9.2, 3.1 Hz, 1H), 3.82 (s, 3H).

3-(3,5-Dimethoxyphenyl)-6-methoxy-4*H*-chromen-4-one (48)

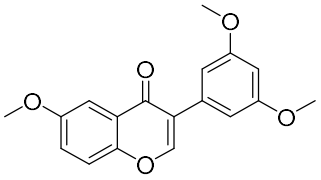

The title compound **48** was synthesised according to general procedure 4 using iodochromone **45** (50 mg, 0.165 mmol, 1.0 eq.), benzo[d][1,3]dioxol-5-ylboronic acid **47** (33 mg, 0.18 mmol, 1.1 eq.), potassium carbonate (45 mg, 0.33 mmol, 2.0 eq.) and tetrakis(triphenylphosphine)palladium(0) (19 mg, 0.017 mmol, 0.1 eq.). The crude product was purified by column chromatography using toluene/DCM/methanol (10:2:0.5) as an eluent to afford the *title compound* **48** as an off-white solid (46 mg, 0.15 mmol, 89%).

^{1}H NMR (400 MHz, chloroform-*d*): δ (ppm) 8.03 (s, 1H), 7.67 (d, J = 3.1 Hz, 1H), 7.42 (d, J = 9.1 Hz, 1H), 7.34 - 7.17 (m, 1H), 6.74 (d, J = 2.3 Hz, 2H), 6.50 (t, J = 2.3 Hz, 1H), 3.91 (s, 3H), 3.83 (s, 6H).

2-(4-(3,5-Dimethoxyphenyl)-1*H*-pyrazol-3-yl)-4-methoxyphenol (49)

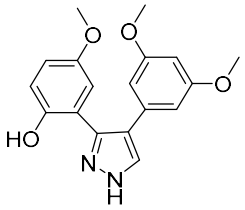

The reaction was carried out following general procedure 3 using chromone **48** (46 mg, 0.15 mmol, 1.0 eq.), hydrazine hydrate (1.0 ml, 20.5 mmol, 139 eq.) and ethanol (5 ml). The desired product was pure enough without flash chromatography. The *title compound* **49** was obtained as light brown solid (40 mg, 0.122 mol, 83%).

^{1}H NMR (400 MHz, methanol-d_4): δ (ppm) 7.67 (s, 1H), 6.73 (d, J = 8.9 Hz, 1H), 6.68 (m, J = 8.7, 2.8 Hz, 2H), 6.40 (d, J = 2.3 Hz, 2H), 6.26 (t, J = 2.1 Hz, 1H), 3.57 (s, 6H), 3.43 (s, 3H).

^{13}C NMR (101 MHz, methanol-d_4): δ (ppm) 160.9, 152.4, 149.4, 135.4, 120.2, 117.9, 116.5, 115.6, 115.4, 114.2, 106.0, 98.6, 93.7, 91.6, 54.6, 54.3.

HRMS found (ESI): MH^+ 327.1332, calc for $C_{18}H_{19}N_2O_4$ 327.1339.

IR ν_{max} (film)/cm^{-1} :3868, 3745, 3599, 3403, 1662, 1540, 1298, 1092, 975.

3-(2,3-Dihydrobenzo[b][1,4]dioxin-6-yl)-6-methoxy-4*H*-chromen-4-one (51)

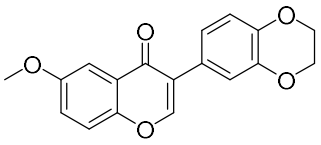

The reaction was carried out following general procedure 4 using iodochromone **45** (70 mg, 0.23 mmol, 1.0 eq.), (2,3-dihydrobenzo[b][1,4]dioxin-6-yl)boronic acid **50** (45 mg, 0.25 mmol, 1.1 eq.), potassium carbonate (64 mg, 0.463 mmol, 2 eq.) and tetrakis(triphenylphosphine)-palladium(0) (26 mg, 0.023 mmol, 0.1 eq.). The crude was purified by flash chromatography on silica gel by using toluene/DCM/methanol (10:2:0.5) as an eluent system to afford the title compound **51** as a light brown solid (14 mg, 0.045mmol, 19%).

^{1}H NMR (400 MHz, chloroform-*d*): δ (ppm) 7.90 (s, 1H), 7.60 (d, *J* = 3.1 Hz, 1H), 7.34 (d, *J* = 9.1 Hz, 1H), 7.21 (d, *J* = 3.1 Hz, 1H), 7.05 (d, *J* = 2.1 Hz, 1H), 6.98 (dd, *J* = 8.3, 2.1 Hz, 1H), 6.86 (d, *J* = 8.4 Hz, 1H), 4.22 (s, 4H), 3.84 (s, 3H).

2-(4-(2,3-Dihydrobenzo[b][1,4]dioxin-6-yl)-1*H*-pyrazol-3-yl)-4-methoxyphenol (52)

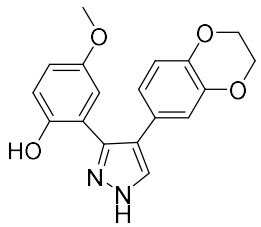

The *title compound* **52** was synthesised according to general procedure 3 using chromone **51** (14 mg, 0.047 mmol, 1.0 eq.), hydrazine hydrate (0.50 ml, 10.2 mmol, 218 eq.) and ethanol (3 ml). The crude product was purified by flash chromatography by using ethyl acetate/petroleum ether (5:5) as eluent to afford the *title compound* **52** as a light brown solid (5 mg, 0.015 mmol, 35%).

^{1}H NMR (400 MHz, chloroform-*d*): δ (ppm) 7.59 (s, 1H), 6.94 (d, *J* = 8.9 Hz, 1H), 6.91 (t, *J* = 1.9 Hz, 1H), 6.88 (s, 1H), 6.87 - 6.83 (m, 2H), 6.76 (dd, *J* = 8.8, 3.1 Hz, 1H), 4.28 (d, *J* = 1.0 Hz, 4H), 3.47 (s, 3H).

^{13}C NMR (101 MHz, chloroform-*d*): δ (ppm) 152.0, 149.8, 146.9, 143.5, 143.1, 129.3, 126.3, 123.0, 120.3, 118.5, 117.6, 117.4, 116.6, 116.3, 112.4, 64.5, 64.4, 55.4.

HRMS found (ESI): MH^+ 325.1177, calc for $C_{18}H_{17}N_2O_4$ 325.1183.

IR ν_{max} (film)/cm^{-1} : 2930, 1582, 1463, 1434, 1280, 1244, 1067, 1036, 930, 852.

3-(Benzo[d][1,3]dioxol-5-yl)-6-methoxy-4*H*-chromen-4-one (54)

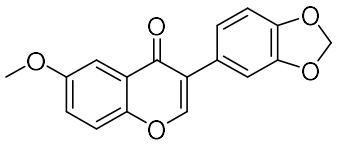

The reaction was carried out following general procedure 4 using iodochromone **45** (50 mg, 0.17 mmol, 1 eq.), benzo[d][1,3]dioxol-5-ylboronic acid **53** (30 mg, 0.18 mmol, 1.1 eq.), potassium carbonate (45 mg, 0.33 mmol, 2 eq.) and tetrakis(triphenylphosphine)palladium(0) (19 mg, 0.017 mmol, 0.1 eq.). The crude was purified by column chromatography by using toluene/DCM/methanol (10:2:0.5) as an eluent system to afford the *title compound* **54** as a light brown solid (23 mg, 0.077 mmol, 46%).

^{1}H NMR (400 MHz, chloroform-*d*): δ (ppm) 7.97 (s, 1H), 7.66 (d, J = 3.1 Hz, 1H), 7.41 (d, J = 9.1 Hz, 1H), 7.34 - 7.18 (m, 1H), 7.11 (dd, J = 1.7, 0.4 Hz, 1H), 6.99 (dd, J = 8.0, 1.7 Hz, 1H), 6.88 (dd, J = 8.1, 0.4 Hz, 1H), 6.00 (s, 2H), 3.91 (s, 3H).

2-(4-(Benzo[d][1,3]dioxol-5-yl)-1*H*-pyrazol-3-yl)-4-methoxyphenol (55)

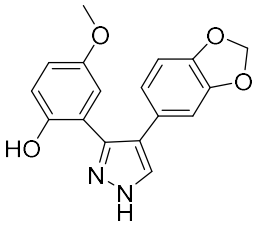

The reaction was carried out following general procedure 3 using chromone **54** (23 mg, 0.077 mmol, 1 eq.), hydrazine hydrate (1.0 ml, 9.58 mmol, 123 eq.) and ethanol (3 ml). The *title compound* **55** (16 mg, 0.051 mmol, 66%) was enough pure without further purification by flash chromatography.

^{1}H NMR (400 MHz, chloroform-*d*): δ (ppm) 7.50 (s, 1H), 6.87 (d, J = 8.9 Hz, 1H), 6.78 (d, J = 8.9 Hz, 4H), 6.72 – 6.64 (m, 1H), 5.89 (d, J = 17.4 Hz, 2H), 3.40 (s, 3H).

^{13}C NMR (101 MHz, chloroform-*d*): δ (ppm) 151.0, 148.7, 146.7, 146.0, 145.5, 128.5, 125.7, 122.1, 119.4, 116.6, 115.6, 115.1, 111.5, 109.2, 107.5, 100.1, 54.4.

HRMS found (ESI): MH^+ 311.1020, calc for $C_{17}H_{15}N_{2}{}^{15}O_4$ 311.1026.

IR ν_{max} (film)/cm^{-1} : 3252, 2999, 2925, 2855, 1467, 1434, 1224, 1176.42, 1034, 807.

References :

1. Aminov, R. I., A brief history of the antibiotic era: lessons learned and challenges for the future. *Front. Microbiol.* **2010**, *1* 134.
2. Etebu, E.; Arikekpar, I., Antibiotics: Classification and mechanisms of action with emphasis on molecular perspectives. *Int. J. Appl. Microbiol. Biotechnol. Res* **2016**, *4* 90-101.
3. Alanis, A. J., Resistance to antibiotics: are we in the post-antibiotic era? *Arch. Med. Res.* **2005**, *36* 697-705.
4. Davies, J.; Davies, D., Origins and Evolution of Antibiotic Resistance. *Microbiol. Mol. Biol. Rev.* **2010**, *74* 417.
5. Aslam, B.; Wang, W.; Arshad, M. I.; Khurshid, M.; Muzammil, S.; Rasool, M. H.; Nisar, M. A.; Alvi, R. F.; Aslam, M. A.; Qamar, M. U., Antibiotic resistance: a rundown of a global crisis. *Infect. Drug. Resist.* **2018**, *11* 1645.
6. Kapoor, G.; Saigal, S.; Elongavan, A., Action and resistance mechanisms of antibiotics: A guide for clinicians. *J. Anaesthesiol. Clin. Pharmacol.* **2017**, *33* 300.
7. Falagas, M. E.; Kasiakou, S. K., Toxicity of polymyxins: a systematic review of the evidence from old and recent studies. *Crit. Care* **2006**, *10* R27.
8. Velkov, T.; Roberts, K. D.; Nation, R. L.; Thompson, P. E.; Li, J., Pharmacology of polymyxins: new insights into an 'old' class of antibiotics. *Future microbiol.* **2013**, *8* 711-724.
9. Halaby, T.; Al Naiemi, N.; Kluytmans, J.; van der Palen, J.; Vandenbroucke-Grauls, C. M., Emergence of colistin resistance in Enterobacteriaceae after the introduction of selective digestive tract decontamination in an intensive care unit. *Antimicrob. Agents Chemother.* **2013**, *57* 3224-3229.
10. Son, S. J.; Huang, R.; Squire, C. J.; Leung, I. K., MCR-1: a promising target for structure-based design of inhibitors to tackle polymyxin resistance. *Drug Discov. Today* **2018**.
11. Stojanoski, V.; Sankaran, B.; Prasad, B. V.; Poirel, L.; Nordmann, P.; Palzkill, T., Structure of the catalytic domain of the colistin resistance enzyme MCR-1. *BMC Biol.* **2016**, *14* 81.
12. Nordmann, P.; Poirel, L., Plasmid-mediated colistin resistance: an additional antibiotic resistance menace. *Clin. Microbiol. Infect.* **2016**, *22* 398-400.
13. Liu, Y.-Y.; Wang, Y.; Walsh, T. R.; Yi, L.-X.; Zhang, R.; Spencer, J.; Doi, Y.; Tian, G.; Dong, B.; Huang, X., Emergence of plasmid-mediated colistin resistance mechanism

MCR-1 in animals and human beings in China: a microbiological and molecular biological study. *Lancet Infect. Dis.* **2016**, *16* 161-168.

14. Hinchliffe, P.; Yang, Q. E.; Portal, E.; Young, T.; Li, H.; Tooke, C. L.; Carvalho, M. J.; Paterson, N. G.; Brem, J.; Niumsup, P. R., Insights into the mechanistic basis of plasmid-mediated colistin resistance from crystal structures of the catalytic domain of MCR-1. *Sci. Rep.* **2017**, *7* 39392.
15. Wei, P.; Song, G.; Shi, M.; Zhou, Y.; Liu, Y.; Lei, J.; Chen, P.; Yin, L., Substrate analog interaction with MCR-1 offers insight into the rising threat of the plasmid-mediated transferable colistin resistance. *FASEB J.* **2017**, *32* 1085-1098.
16. Liu, Z.-X.; Han, Z.; Yu, X.-L.; Wen, G.; Zeng, C., Crystal Structure of the Catalytic Domain of MCR-1 (cMCR-1) in Complex with d-Xylose. *Crystals* **2018**, *8* 172.
17. Cheung, K.-M. J.; Matthews, T. P.; James, K.; Rowlands, M. G.; Boxall, K. J.; Sharp, S. Y.; Maloney, A.; Roe, S. M.; Prodromou, C.; Pearl, L. H., The identification, synthesis, protein crystal structure and in vitro biochemical evaluation of a new 3, 4-diarylpyrazole class of Hsp90 inhibitors. *Bioorgaic Med. Chem. Lett.* **2005**, *15* 3338-3343.
18. Vo, C. D.; Shebert, H. L.; Zikovich, S.; Dryer, R. A.; Huang, T. P.; Moran, L. J.; Cho, J.; Wassarman, D. R.; Falahee, B. E.; Young, P. D., Repurposing Hsp90 inhibitors as antibiotics targeting histidine kinases. *Bioorganic Med. Chem. Lett.* **2017**, *27* 5235-5244.
19. Jonathan, C., Organic Chemistry. Jonathan Clayden, Nick Geeves, Stuart Warren. *Paperback, 2nd Edition.–2012.–1234 p* **2012**.
20. Kurti, L.; Czakó, B., *Strategic applications of named reactions in organic synthesis*. Elsevier: 2005.
21. Nakajima, M.; Fukami, H.; Konishi, K.; Oda, J., Synthesis of Aromatic Carbonyl Compounds by Friedel-Crafts Reaction Using BF3 Catalyst. *Agri. Biol. Chem.* **1963**, *27* 700-705.
22. Effenberger, F.; Epple, G., Catalytic Friedel-Crafts Acylation of Aromatic Compounds. *Angew. Chem. Int. Ed.* **1972**, *11* 300-301.
23. P. Ellis, G., Chemistry of Heterocyclic Compounds: Chromenes, Chromanones, and Chromones, Volume 31. 2008; pp 581-631.
24. Gaspar, A.; Matos, M. J.; Garrido, J.; Uriarte, E.; Borges, F., Chromone: A Valid Scaffold in Medicinal Chemistry. *Chemical Reviews* **2014**, *114* 4960-4992.
25. Wang, H., Comprehensive Organic Name Reactions. **2010**.

26. Li, J. J., *Name Reactions: A Collection of Detailed Mechanisms and Synthetic Applications Fifth Edition*. Springer Science & Business Media: 2014.
27. Rulev, A. Y., Aza-Michael reaction: achievements and prospects. *Russ. Chem. Rev.* **2011**, *80* 197-218.
28. Bruckner, R., *Advanced organic chemistry: reaction mechanisms*. Elsevier: 2001.
29. Yadav, S. K., Process for the Preparation of Chromones, Isoflavones and Homoisoflavones Using Vilsmeier Reagent Generated from Phthaloyl Dichloride and DMF. *Int. J. Org. Chem.* **2014**, *Vol.04No.04* 11.
30. Bhat, M.; Belagali, S., Synthesis of Azo-Bridged Benzothiazole-Phenyl Ester Derivatives via Steglich Esterification. *Int. J. Curr. Eng. Technol* **2014**, *4* 2711-2714.
31. Neises, B.; Steglich, W., Simple Method for the Esterification of Carboxylic Acids. *Angew. Chem. Int. Ed. Engl.* **1978**, *17* 522-524.
32. Lutjen, A. B.; Quirk, M. A.; Barbera, A. M.; Kolonko, E. M., Synthesis of (E)-cinnamyl ester derivatives via a greener Steglich esterification. *Bioorganic Med. Chem. Lett.* **2018**, *26* 5291-5298.
33. March, J., *Advanced organic chemistry: reactions, mechanisms, and structure*. John Wiley & Sons: 1992.
34. Suzuki, A., Recent advances in the cross-coupling reactions of organoboron derivatives with organic electrophiles, 1995–1998. *J. Organomet. Chem.* **1999**, *576* 147-168.
35. Miyaura, N.; Suzuki, A., Palladium-Catalyzed Cross-Coupling Reactions of Organoboron Compounds. *Chem.Rev.* **1995**, *95* 2457-2483.
36. Miyaura, N.; Suzuki, A., Stereoselective synthesis of arylated (E)-alkenes by the reaction of alk-1-enylboranes with aryl halides in the presence of palladium catalyst. *J. Chem. Soc. Chem. Commun.* **1979**, 866-867.
37. Miyaura, N.; Yanagi, T.; Suzuki, A., The palladium-catalyzed cross-coupling reaction of phenylboronic acid with haloarenes in the presence of bases. *Synth. Commun.* **1981**, *11* 513-519.
38. Amatore, C.; Jutand, A.; Le Duc, G., Kinetic Data for the Transmetalation/Reductive Elimination in Palladium-Catalyzed Suzuki–Miyaura Reactions: Unexpected Triple Role of Hydroxide Ions Used as Base. *Chem. Eur. J.* **2011**, *17* 2492-2503.
39. Matos, K.; Soderquist, J. A., Alkylboranes in the Suzuki− Miyaura coupling: Stereochemical and mechanistic studies. *J. Org. Chem.* **1998**, *63* 461-470.
40. Carrow, B. P.; Hartwig, J. F., Distinguishing Between Pathways for Transmetalation in Suzuki− Miyaura Reactions. *J. Am. Chem. Soc* **2011**, *133* 2116-2119.

41. Vasselin, D. A.; Westwell, A. D.; Matthews, C. S.; Bradshaw, T. D.; Stevens, M. F., Structural studies on bioactive compounds. 40. Synthesis and biological properties of fluoro-, methoxyl-, and amino-substituted 3-phenyl-4 H-1-benzopyran-4-ones and a comparison of their antitumor activities with the activities of related 2-phenylbenzothiazoles. *J. Med. Chem.* **2006**, *49* 3973-3981.
42. Dong, H.; Li, K.; Zheng, C.; Liu, J.; Lv, Z.; Li, T.; Liu, C., Synthesis and antitumor activity of novel 3-(substituted amino)-chromone derivatives. *Acta Chim. Sin* **2009**, *67* 819-824.

Appendices:

4-(4-(2,3-Dihydrobenzo[b][1,4]dioxin-6-yl)-5-methyl-1*H*-pyrazol-3-yl)benzene-1,3-diol (12)

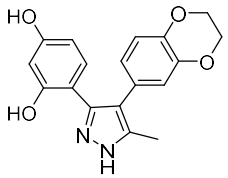

^{1}H NMR (400 MHz, methanol-d_4)

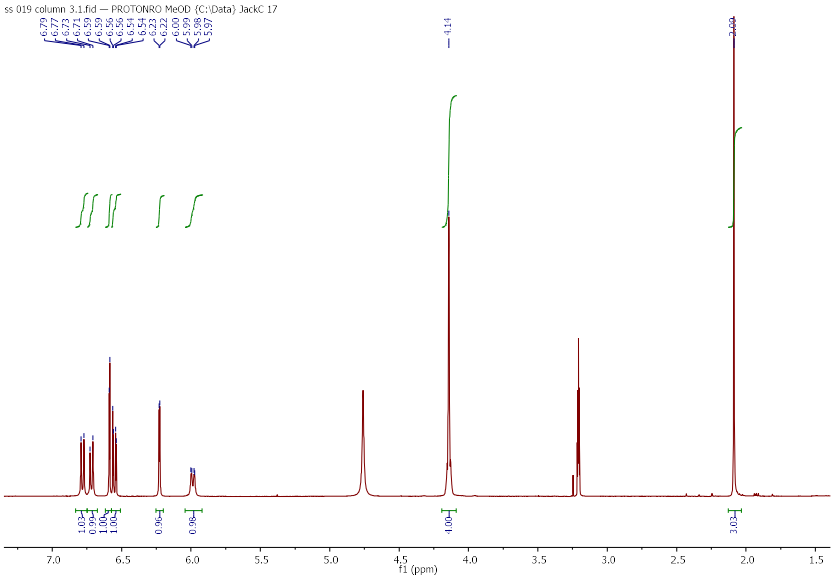

^{13}C NMR (101 MHz, methanol-d_4)

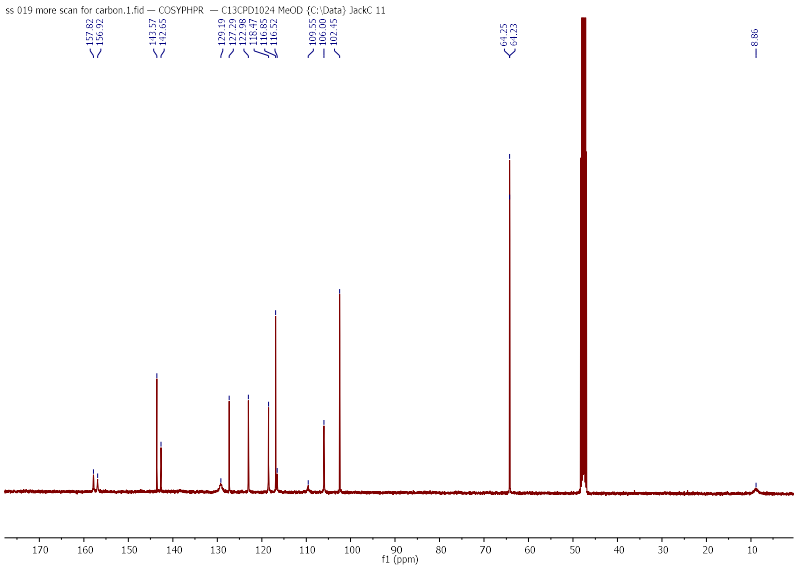

4-Ethyl-6-(4-(4-methoxyphenyl)-5-methyl-1*H*-pyrazol-3-yl)benzene-1,3-diol (17)

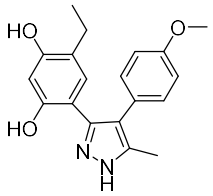

^{1}H NMR (400 MHz, chloroform-*d*)

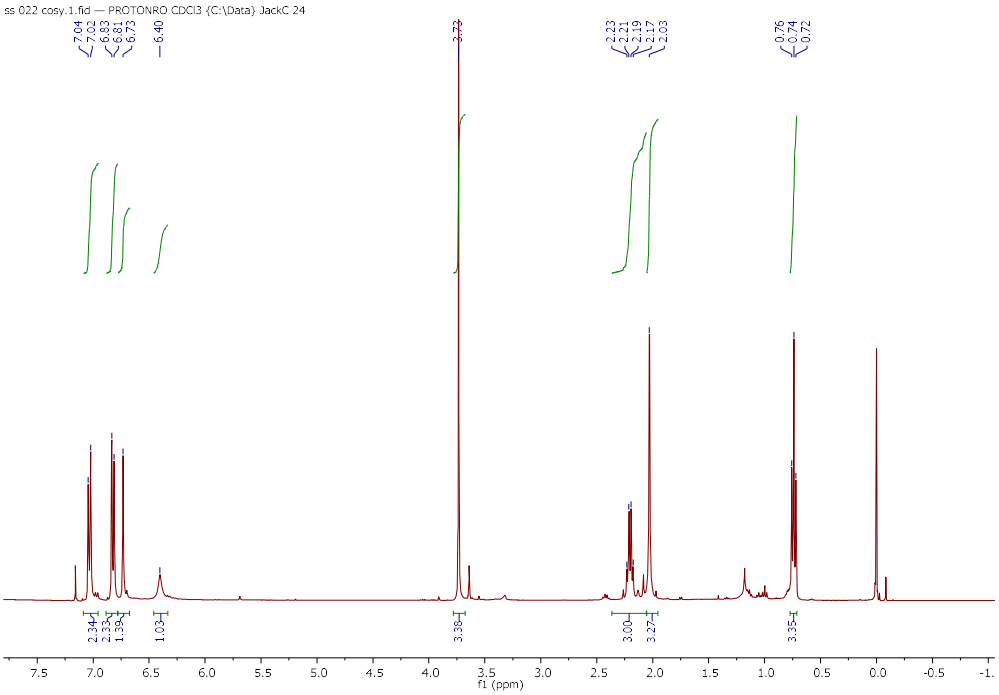

^{13}C NMR (101 MHz, chloroform-*d*)

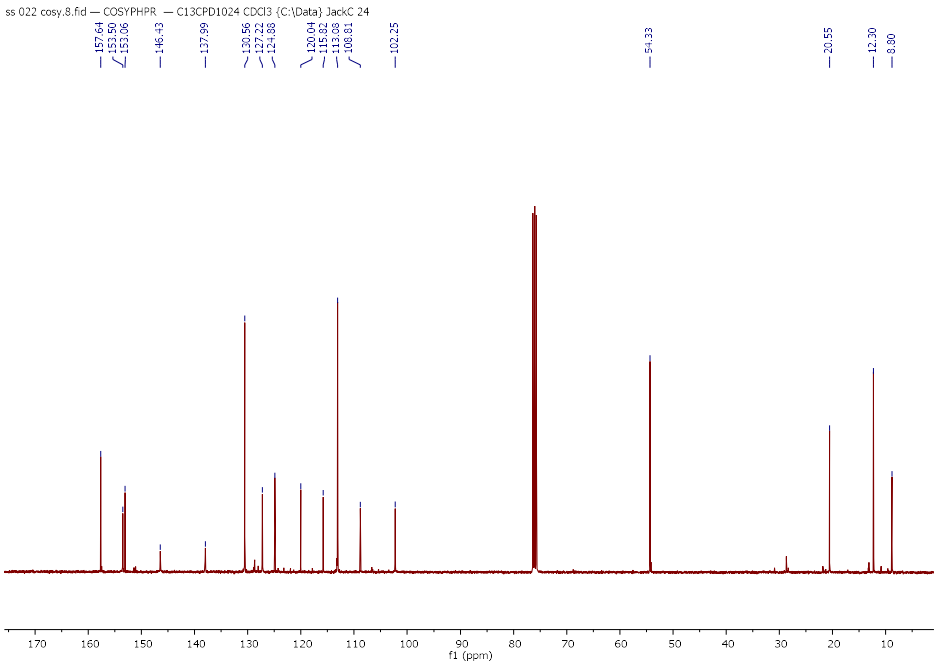

4-Ethyl-6-(4-(4-methoxyphenyl)-1,5-dimethyl-1*H*-pyrazol-3-yl)benzene-1,3-diol (18)

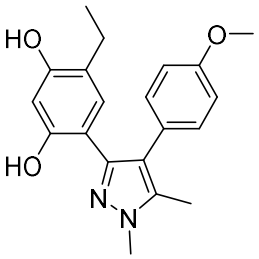

^{1}H NMR (400 MHz, chloroform-*d*)

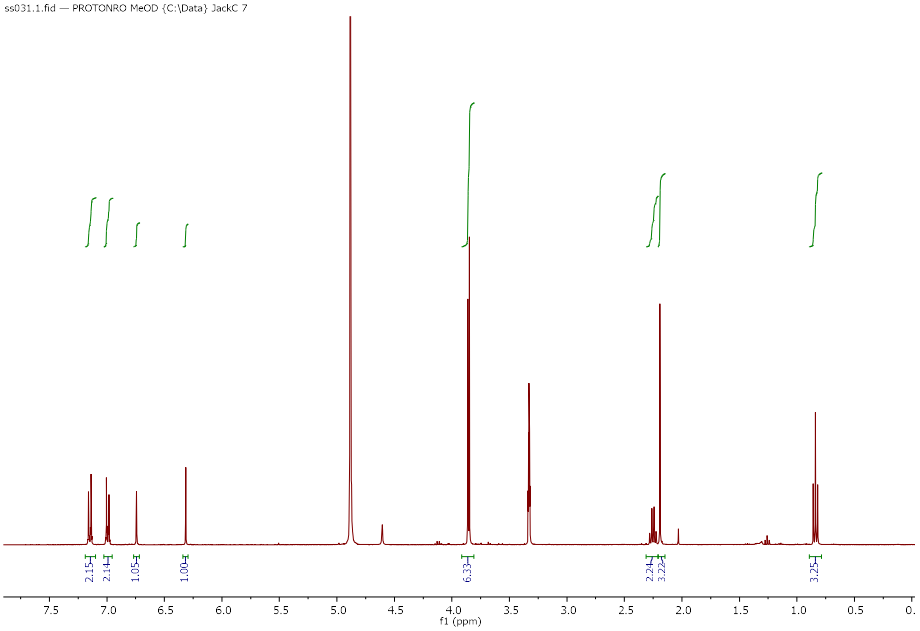

^{13}C NMR (101 MHz, chloroform-*d*)

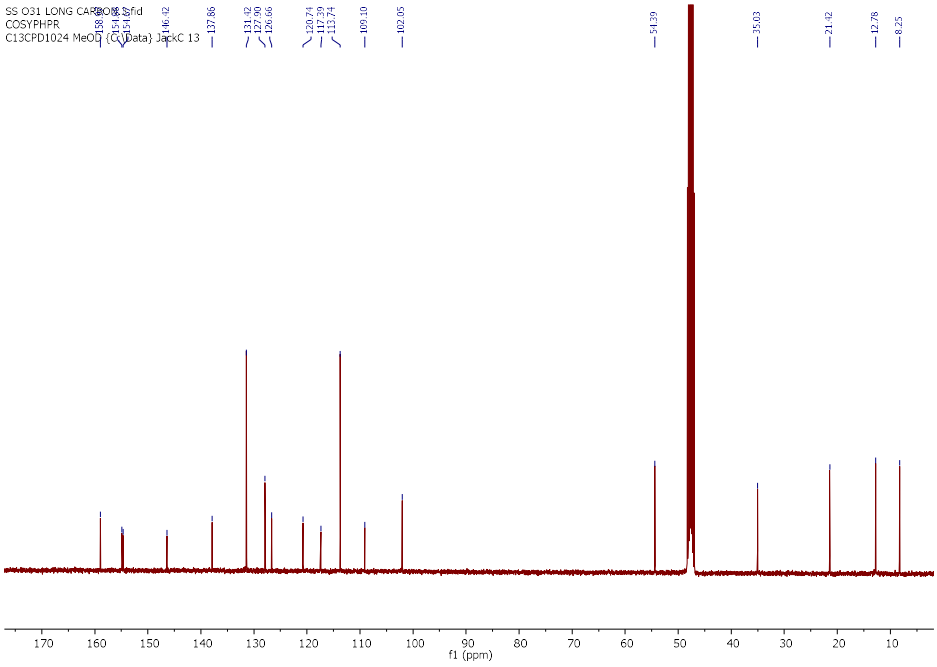

7-Hydroxy-3-(4-hydroxy-3-methoxyphenyl)-2-methyl-4*H*-chromen-4-one (21)

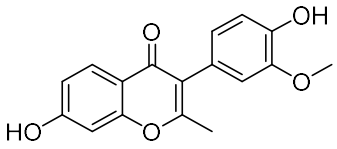

^{1}H NMR (400 MHz, methanol-d_4)

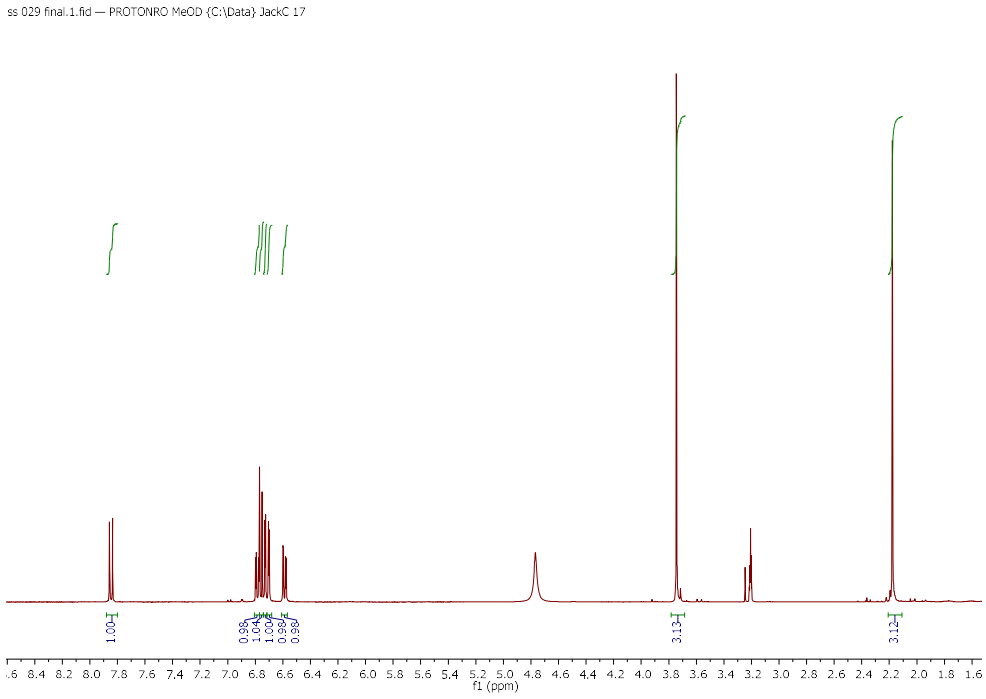

^{13}C NMR (101 MHz, methanol-d_4)

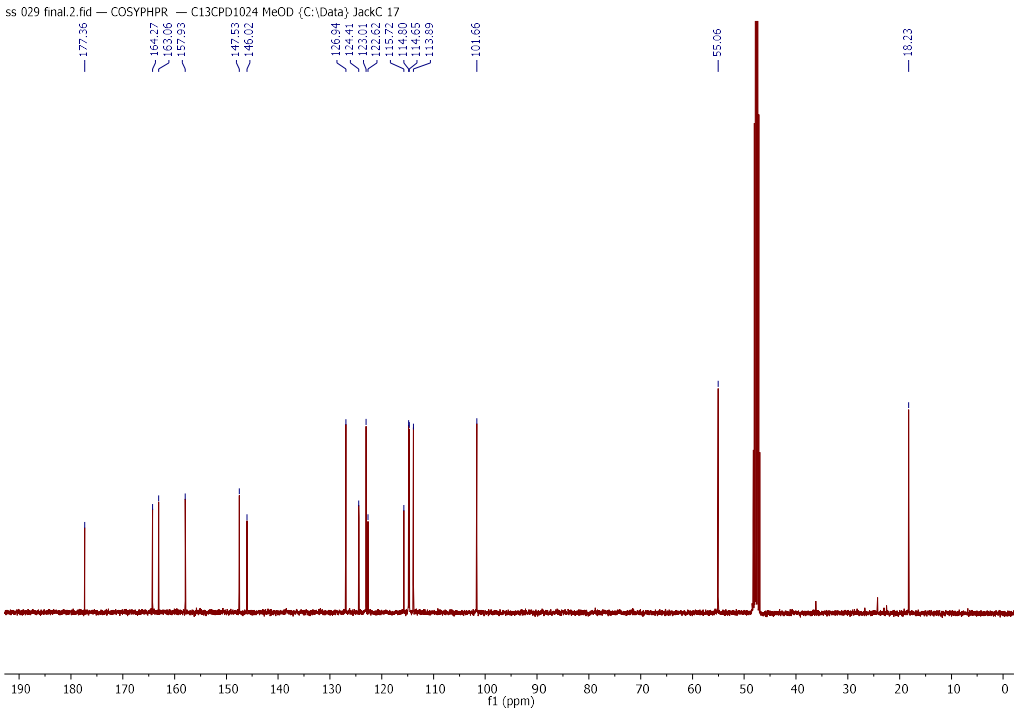

4-(4-(4-Hydroxy-3-methoxyphenyl)-5-methyl-1*H*-pyrazol-3-yl)benzene-1,3-diol (22)

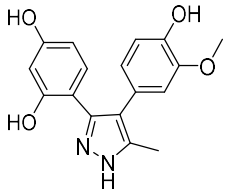

^{1}H NMR (400 MHz, methanol-d_4)

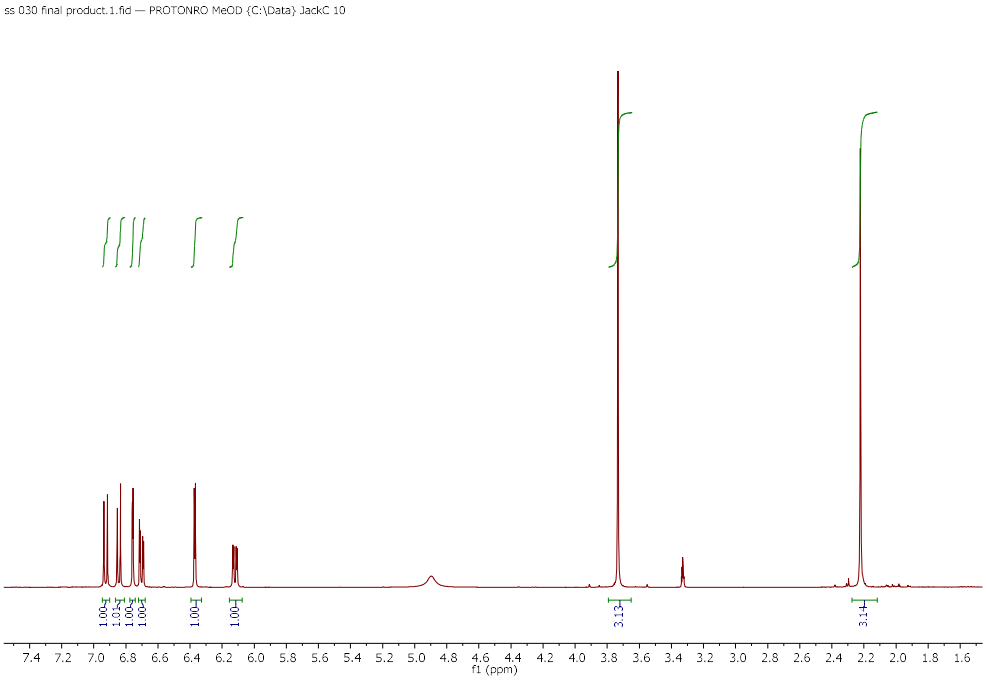

^{13}C NMR (101 MHz, methanol-d_4)

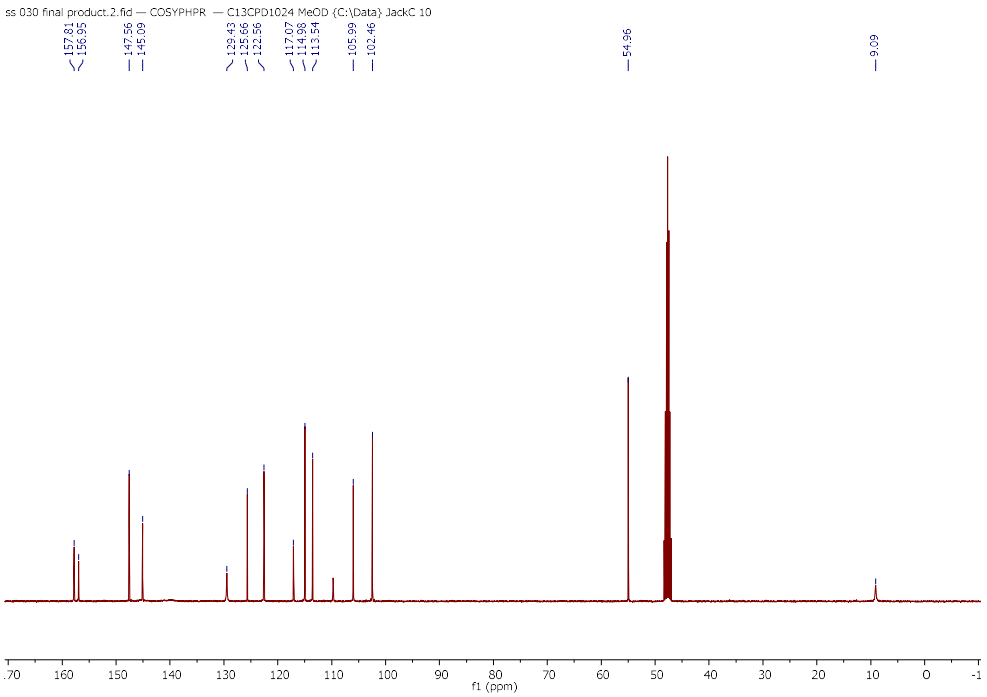

3-(3,4-Dihydroxyphenyl)-7-hydroxy-2-methyl-4*H*-chromen-4-one (25)

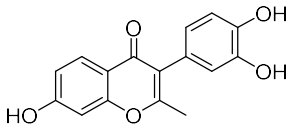

^{1}H NMR (400 MHz, methanol-d_4)

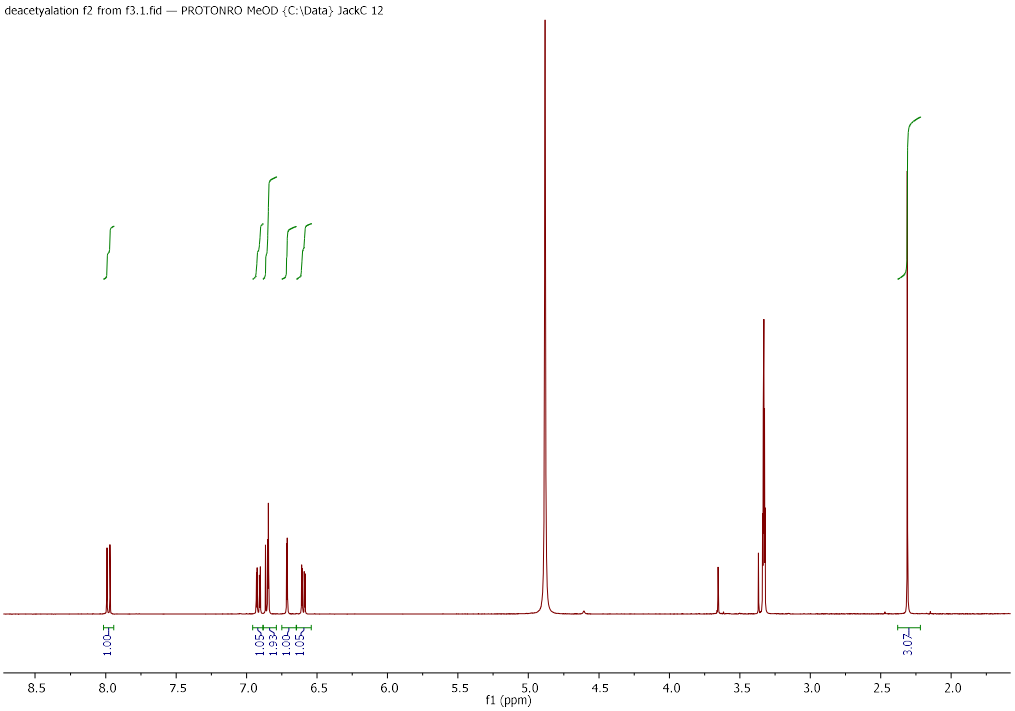

^{13}C NMR (101 MHz, methanol-d_4)

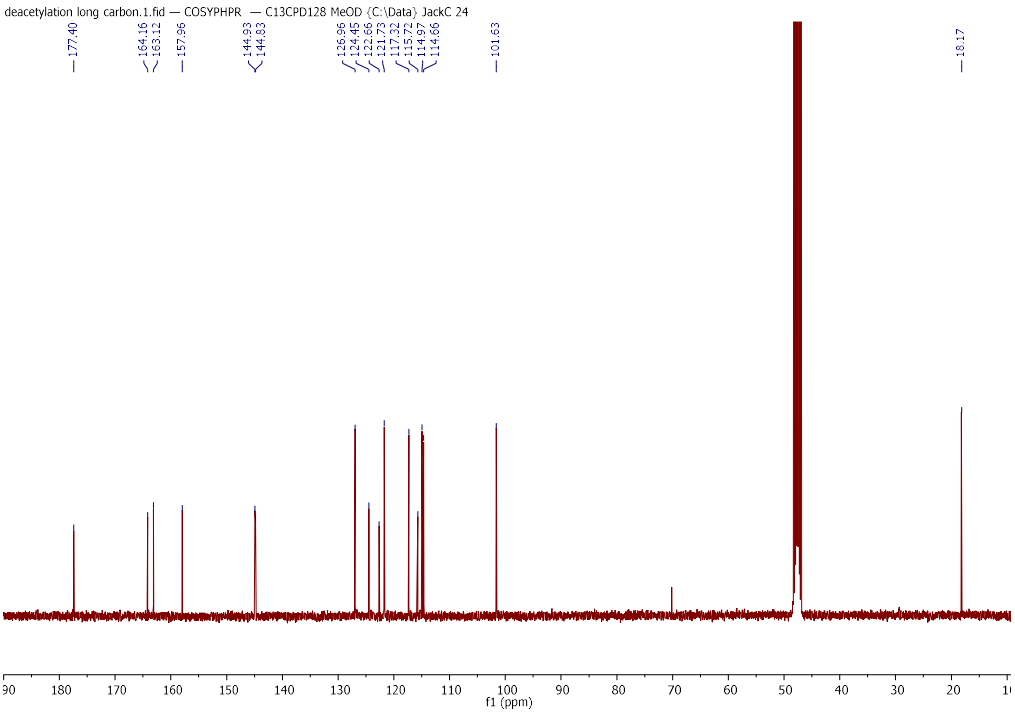

4-(3-(2,4-Dihydroxyphenyl)-5-methyl-1*H*-pyrazol-4-yl)benzene-1,2-diol(26)

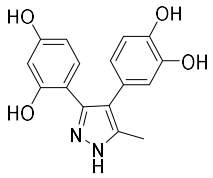

^{1}H NMR (400 MHz, methanol-d_4)

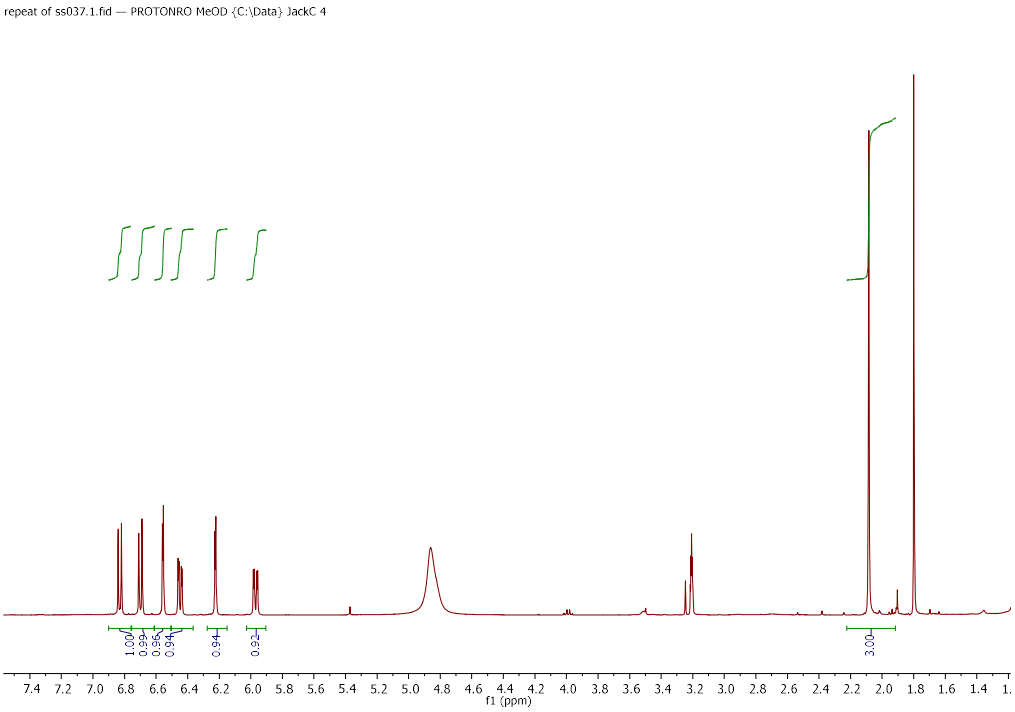

^{13}C NMR (101 MHz, methanol-d_4)

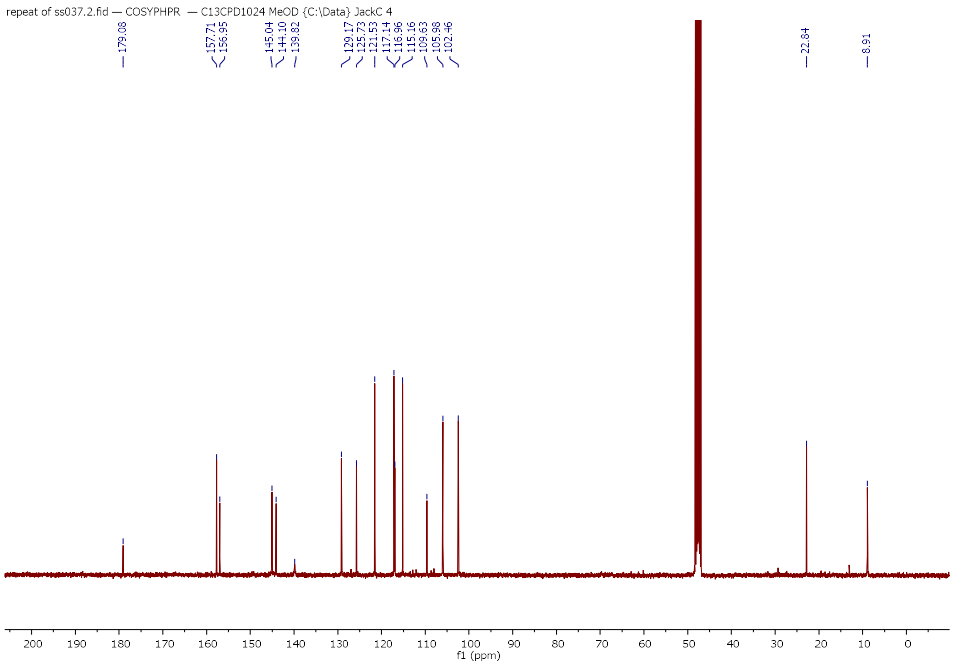

7-Hydroxy-3-(3-hydroxy-4-methoxyphenyl)-2-methyl-4*H*-chromen-4-one (29)

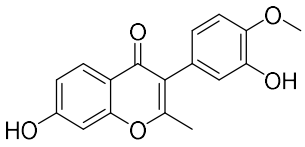

^{1}H NMR (400 MHz, methanol-d_4)

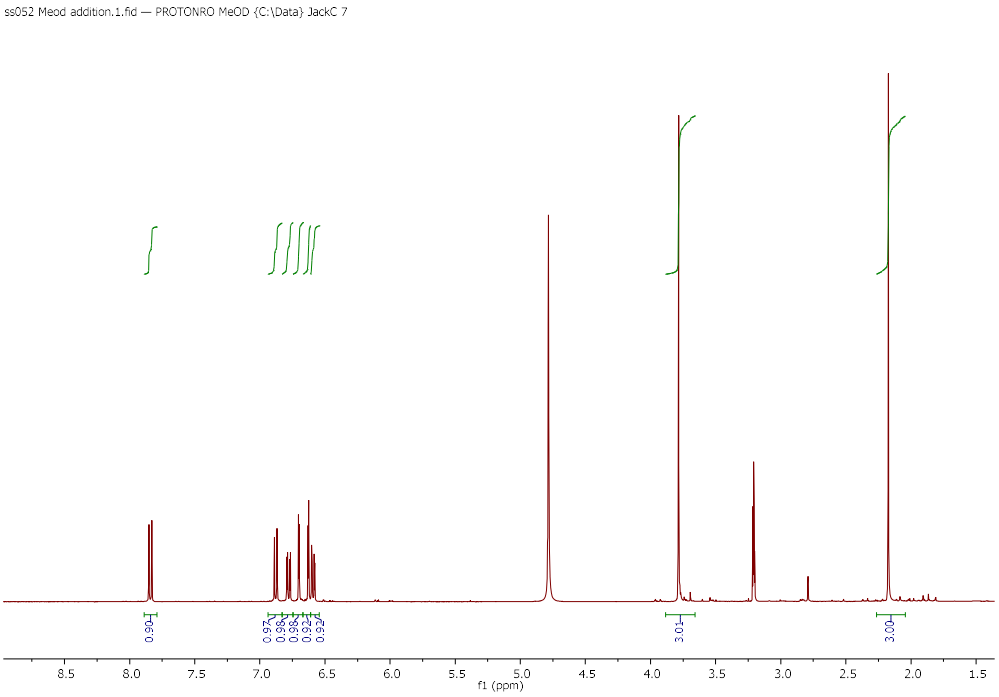

^{13}C NMR (101 MHz, methanol-d_4)

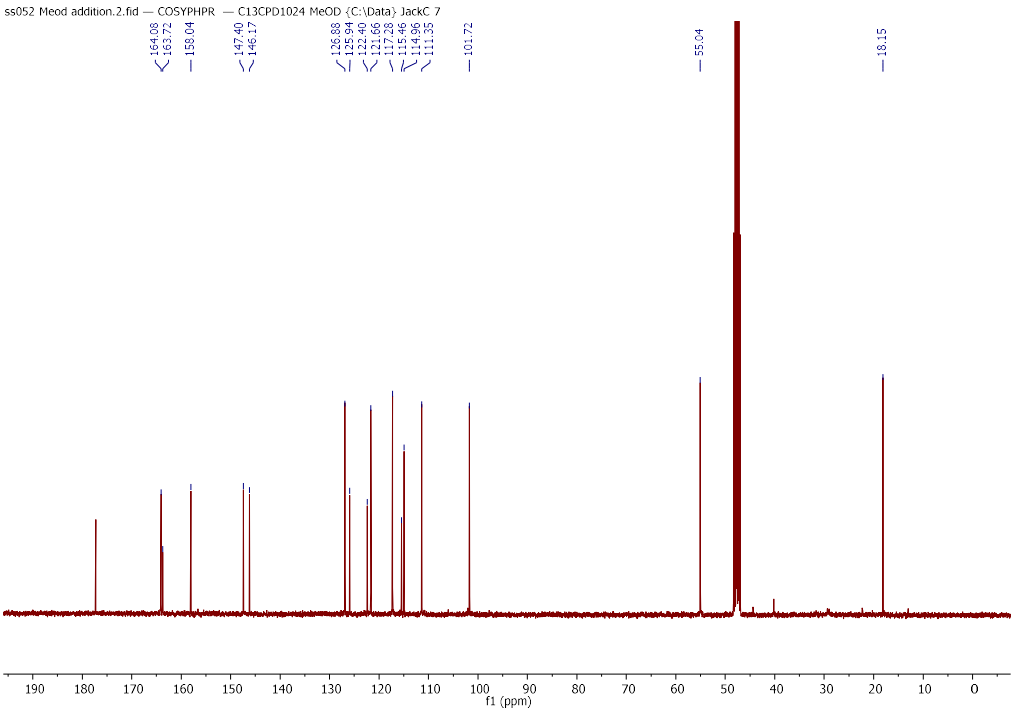

4-(4-(3-Hydroxy-4-methoxyphenyl)-5-methyl-1*H*-pyrazol-3-yl)benzene-1,3-diol (30)

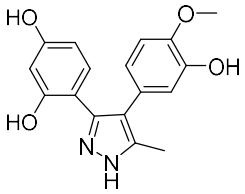

^{1}H NMR (400 MHz, methanol-d_4)

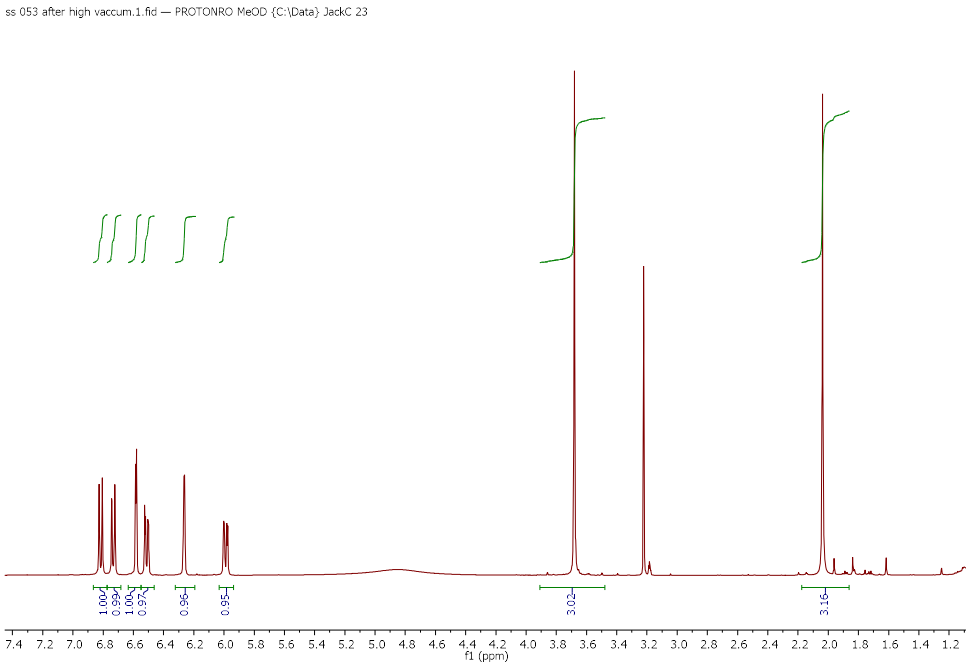

^{13}C NMR (101 MHz, methanol-d_4)

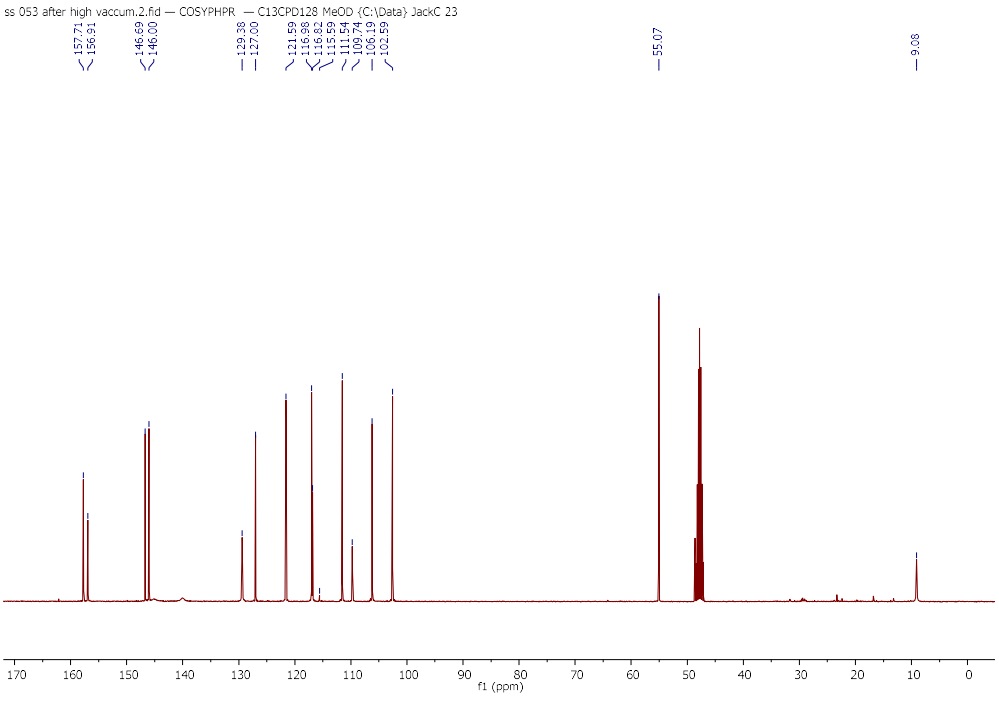

3-(2,3-Dihydrobenzo[b][1,4]dioxin-6-yl)-6-ethyl-7-methoxy-2-methyl-4*H*-chromen-4-one (33)

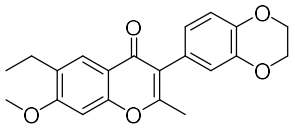

^{1}H NMR (400 MHz, chloroform-*d*)

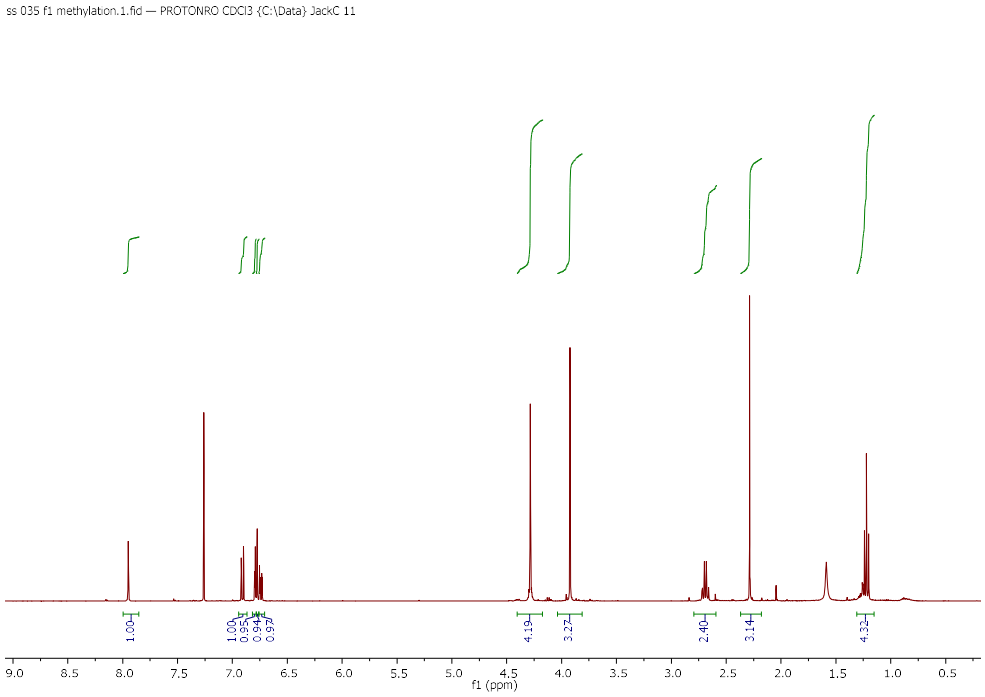

^{13}C NMR (100 MHz, chloroform-*d*)

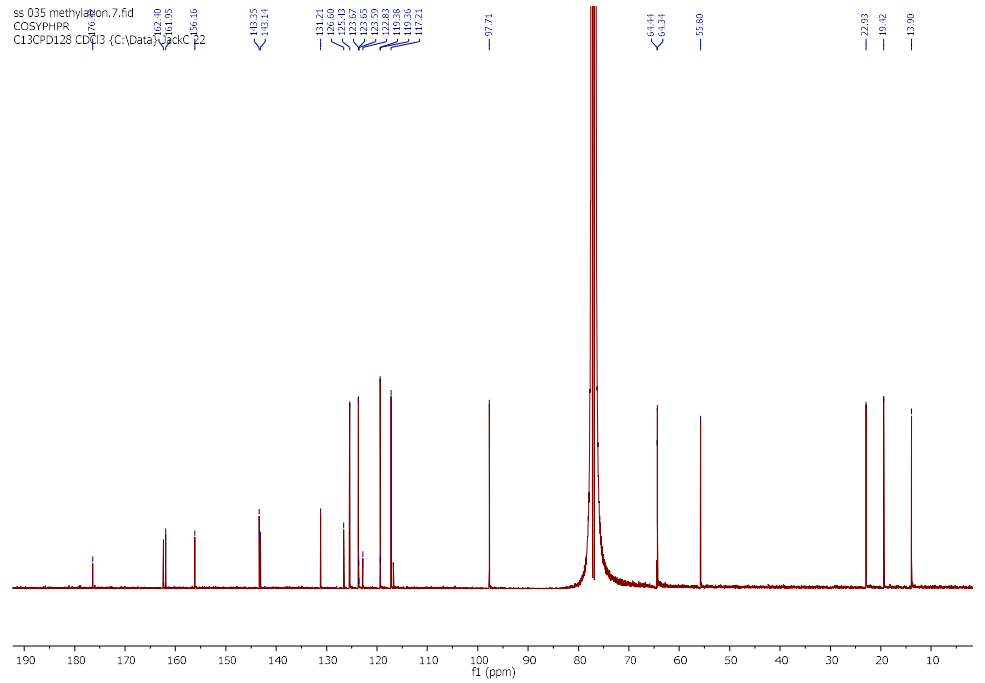

4-(4-(2,3-Dihydrobenzo[b][1,4]dioxin-6-yl)-5-methyl-1*H*-pyrazol-3-yl)-6-ethylbenzene-1,3-diol (34)

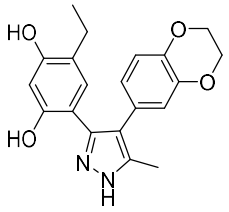

^{1}H NMR (400 MHz, methanol-d_4)

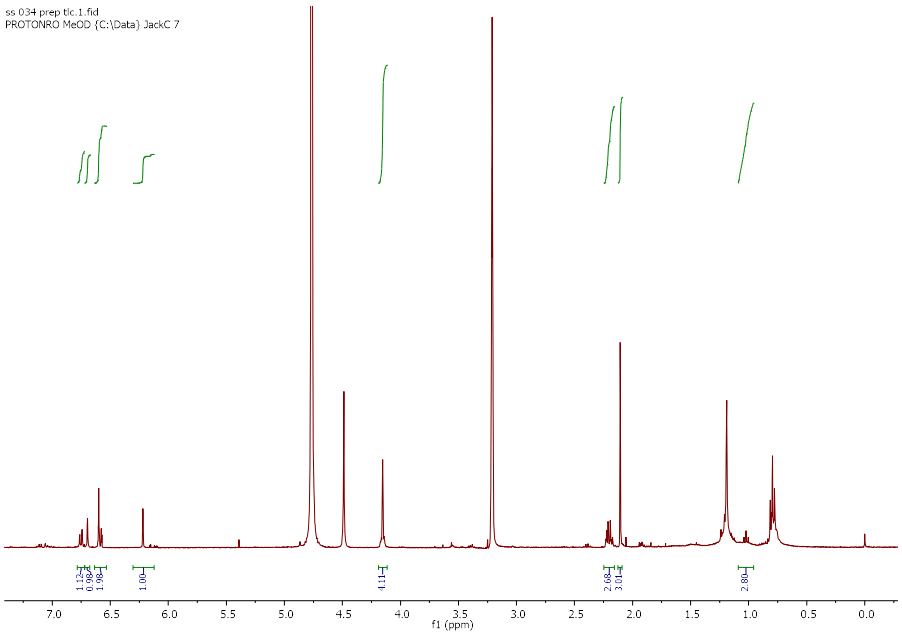

^{13}C NMR (101 MHz, methanol-d_4)

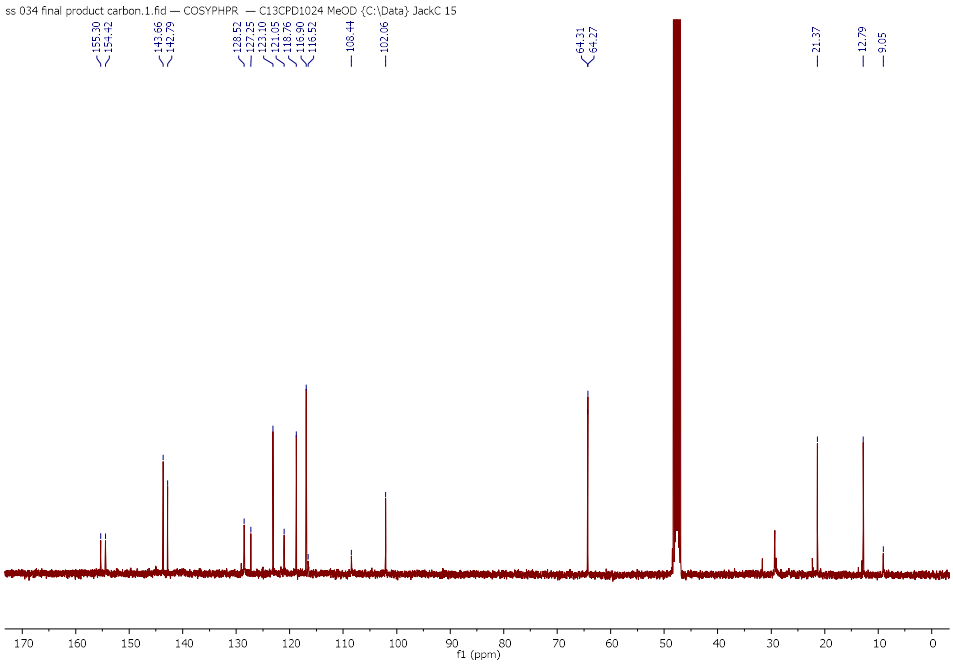

5,7-Dihydroxy-3-(4-hydroxyphenyl)-2-methyl-4*H*-chromen-4-one (38)

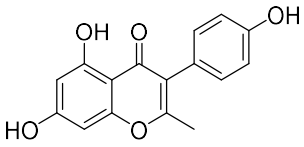

^{1}H NMR (400 MHz, methanol-d_4)

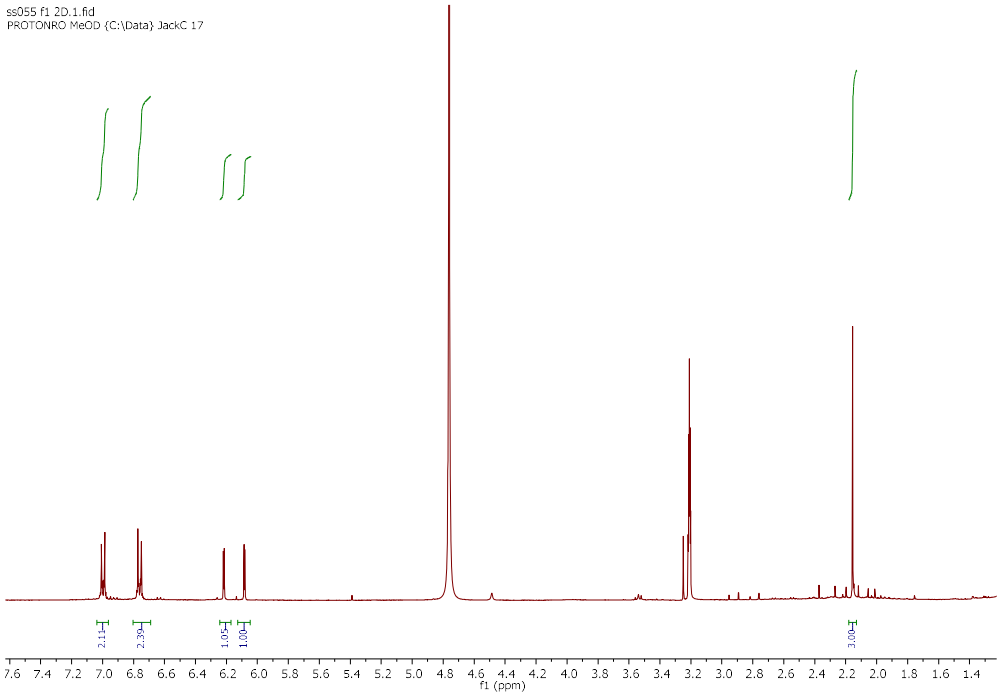

^{13}C NMR (101 MHz, methanol-d_4)

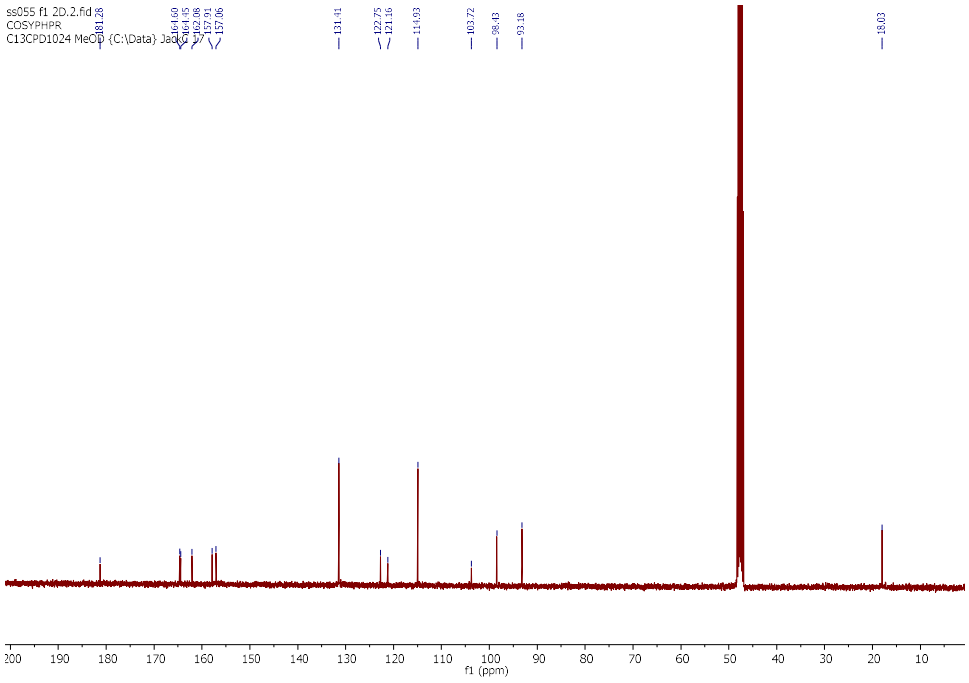

2-(4-(3,5-Dimethoxyphenyl)-1*H*-pyrazol-3-yl)-4-methoxyphenol (49)

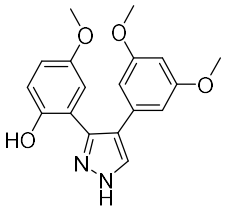

^{1}H NMR (400 MHz, methanol-d_4)

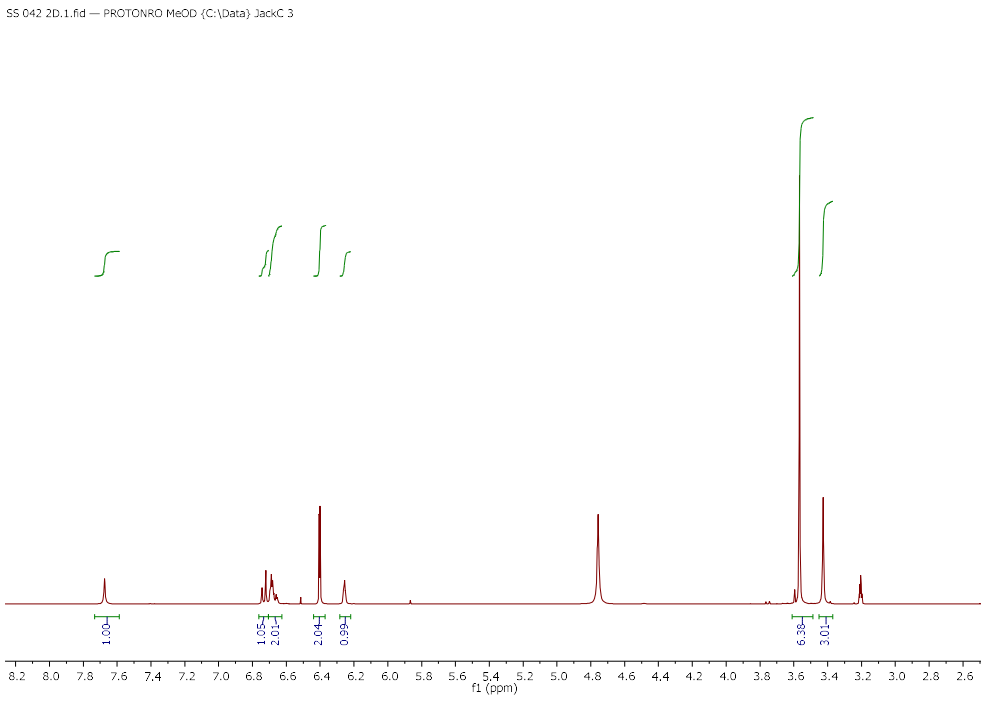

^{13}C NMR (101 MHz, methanol-d_4)

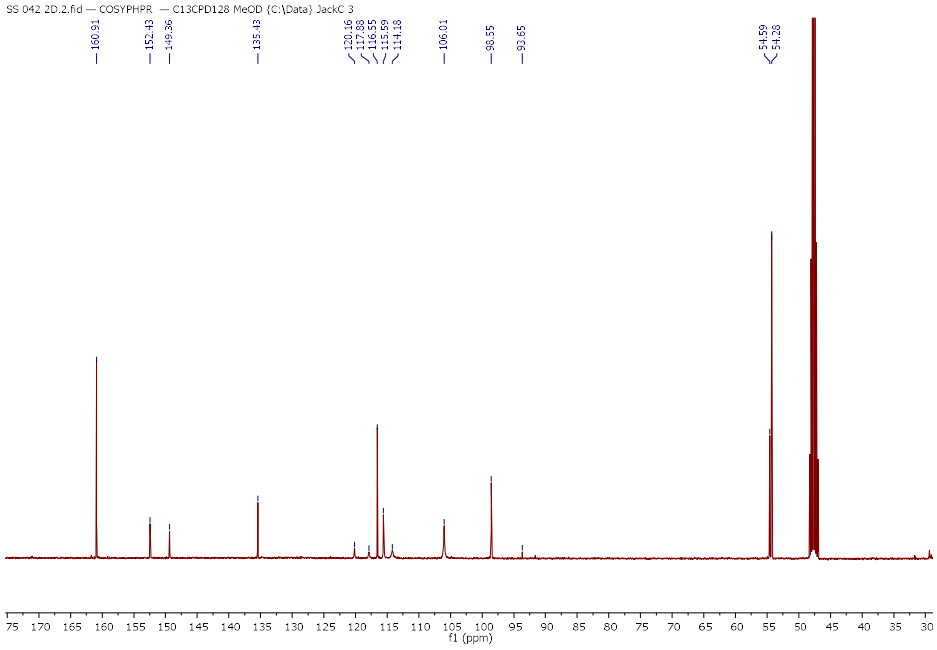

2-(4-(2,3-Dihydrobenzo[b][1,4]dioxin-6-yl)-1*H*-pyrazol-3-yl)-4-methoxyphenol (52)

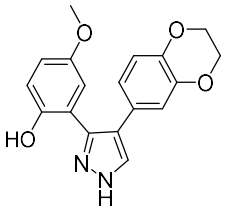

^{1}H NMR (400 MHz, chloroform-*d*)

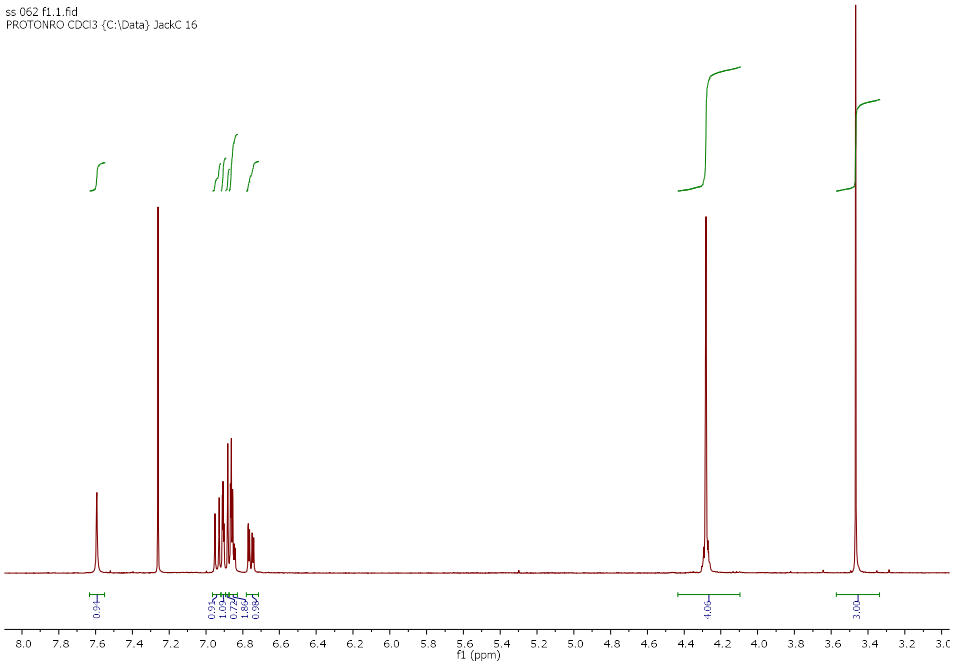

^{13}C NMR (100 MHz, chloroform-*d*)

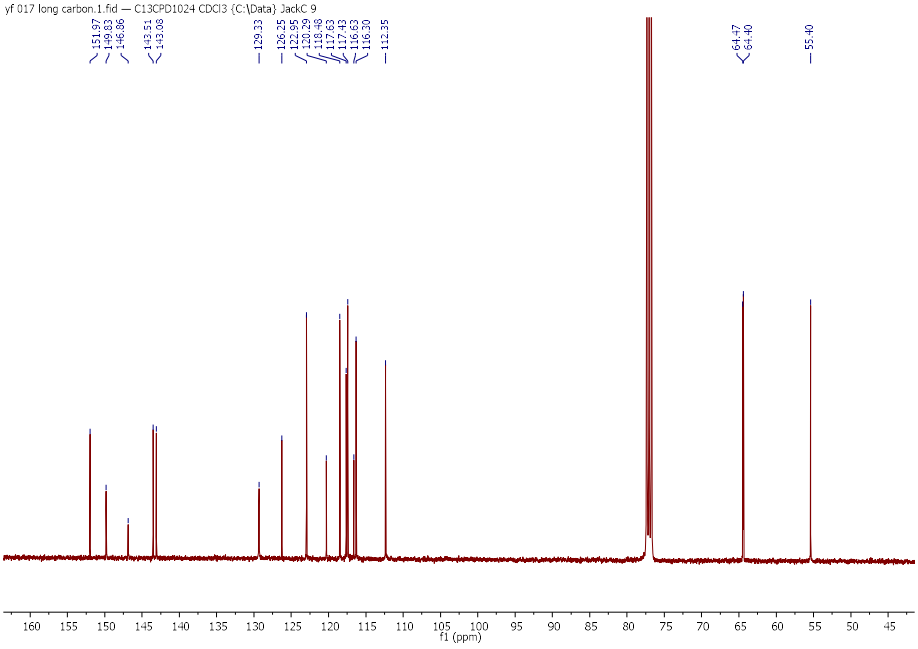

2-(4-(Benzo[d][1,3]dioxol-5-yl)-1*H*-pyrazol-3-yl)-4-methoxyphenol (55)

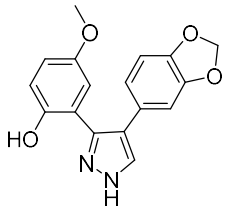

^{1}H NMR (400 MHz, chloroform-*d*)

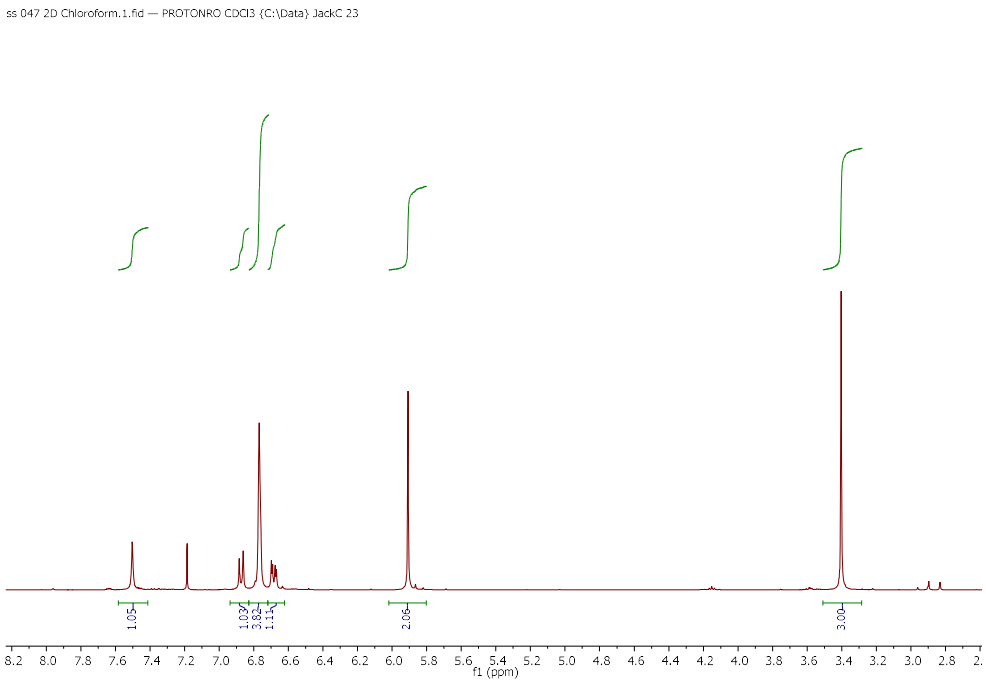

^{13}C NMR (100 MHz, chloroform-*d*)